PHD

The 2-oxoacid dehydrogenase complex of Haloferax volcanii

Al-Mailem, Dina Musaed

Award date:
2006

Awarding institution:
University of Bath

The 2-Oxoacid Dehydrogenase Complex of *Haloferax volcanii*

Dina Musaed Al-Mailem

A thesis submitted for the degree of Doctor of Philosophy
University of Bath
Department of Biology and Biochemistry

2006

COPYRIGHT

ProQuest LLC
789 East Eisenhower Parkway
P.O. Box 1346
Ann Arbor, MI 48106-1346

The 2-Oxoacid Dehydrogenase Complex of *Haloferax volcanii*

By Dina Musaed Al-Mailem

ACKNOWLEDGEMENTS

I HAVE LOOKED FORWARD TO WRITE THIS PAGE AS IT MAKES THE END OF MY THESIS AND MANY PEOPLE DESERVE THANKS. FIRST AND FOREMOST, I WOULD LIKE TO EXPRESS MY SINCERE GRATITUDE TO MY SUPERVISORS PROF. MICHAEL DANSON AND DR. DAVID HOUGH FOR THEIR HELP AND SUPPORT GIVEN ME DURING MY WORK. I PARTICULARLY APPRECIATE THEIR VALUABLE GUIDANCE AND SUPERVISION.

I WOULD ALSO LIKE TO THANK DR. THORSTEN ALLERS (UNIVERSITY OF NOTTINGHAM) FOR PROVIDING ME WITH VECTORS, EXPRESSION STRAIN AND FOR HIS COOPERATION. ALSO, PAUL WILKINSON (UNIVERSITY OF BATH) FOR SEQUENCING AND ALAN MAJERNICK FOR HIS HELP WITH ANAEROBIC GROWTH STUDIES. ALSO, MY PROJECT STUDENTS MARIA KEAYS AND DANIEL NICHOLSON.

MANY THANKS EXTEND TO ALL PRESENT AND PAST MEMBERS OF LAB 1.33 NATHALIE WERY, URSULA GERIKE, AMINATA KANU, TINA ST-JOHN, MIKKI KOO, HANS-CHRISTIAN AASS, HARYATI JAMALUDDIN, TRACEY GOULT, VICKY MOORE, CAROLINE EMPTAGE, CAROLINE HEATH AND HENRY LAMBLE FOR THEIR FRIENDSHIP, CONTINUOUS HELP AND SUPPORT.

THANKS ARE ALSO DUE TO ALL MEMBERS OF CENTRE FOR EXTREMOPHILE RESEARCH AND MY ASSESSOR DR.ALEX JEFFRIES FOR THEIR HELP AND ADVICE. ALSO, FOR UNIVERSITY OF BATH GIVING ME THE CHANCE TO DO MY PHD.

ALSO, I WOULD LIKE TO THANK ALL MY FRIENDS WHO MADE MY TIME IN BATH MOST ENJOYABLE.

I AM PARTICULARLY GRATEFUL FOR MY MUM AND DAD, MY BROTHERS AND MY SISTER NOURA FOR ENDLESS SUPPORT AND ENCOURAGEMENT. ALSO, ALL MY FAMILY AND FRIENDS BACK HOME FOR THEIR SUPPORT IN DIFFERENT WAYS.

FINALLY, I WOULD LIKE TO THANK MY HUSBAND AHMAD FOR HIS CONTINUOUS SUPPORT, PATIENCE, AND UNDERSTANDING, AND MY SON MUSAED WHO PROVIDED ME WITH LOTS OF LOVE, HUMOR AND HOPE DURING THIS WORK.

SPECIAL THANKS ARE DUE TO KUWAIT UNIVERSITY FOR FUNDING.
HOPEFULLY, I HAVE NOT FORGOTTEN ANYBODY FROM MY ACKNOWLEDGEMENT.

ABOVE ALL, I THANK GOD FOR PROVIDING ME WITH POTENTIAL, PATIENCE AND MOTIVATION NEEDED TO COMPLETE THIS WORK.

List of Contents

List of Figures

Abbreviations

bp	Base pair
BCOADHC	Branched-chain 2-oxoacid dehydrogenase complex
BSA	Bovine serum albumin
CDTA	Diaminocyclohexane tetraacetic acid
CoA	Coenzyme A
CS	Citrate synthase
DCPIP	2,6-dichlorophenol-indophenol
DEPC	Diethyl pyrocarbonate
dH_2O	Distilled water
DMSO	Dimethyl sulphoxide
DNA	Deoxyribonucleic acid
DNase	Deoxyribonuclease
dNTP	Deoxynucleoside triphosphate
DSMZ	Deutsche Sammlung von Mikroorganismen und Zellkulturen GmbH Braunschweig, Germany (German collection of Microorganisms and Cell Culture)
DTNB	5,5'-dithio bis-2-nitrobenzonate
DTT	Dithiothreitol
E1	2-Oxoacid decarboxylase
E2	Dihydrolipoyl acyl-transferase
E3 (DHlipDH)	Dihydrolipoamide dehydrogenase
EDTA	Ethylenediamine tetraacetic acid, (disodium)
FAD	Flavin adenine dinucleotide
Fd	Ferredoxin
Fd promoter	Ferredoxin promoter
GDH	Glucose dehydrogenase
GSH	Reduced glutathione
GSSG	Oxidised glutathione
Hfx. volcanii	*Haloferax volcanii*
H98	*Hfx. volcanii* H98 expression strain (ΔpyrE2 Δ hdrB)
Hv-YPC	Complete medium for H98 **(30% SW + 10x YPC: Yeast extract (Y), peptone (P) and Casamino Acids(C)**
Hmg-CoA	3-Hydroxy-3-methylglutaryl Coenzyme A
IPTG	Isopropyl β-D-thiogalactopyranoside

Kb	Kilo base
LB	Luria-Bertani
MGM1	Modified growth medium (used for wild type *Hfx. volcanii*)
MGM2	Modified growth medium (used for anaerobic growth *Hfx. volcanii*)
M_r	Relative molecular mass
mRNA	Messenger ribonucleic acid
NAD^+	Nicotinamide adenine dinucleotide
NADH	Nicotinamide adenine dinucleotide (reduced)
OGDHC	2-Oxoglutarate dehydrognase complex
OADHCs	2-Oxoacid dehydrogenase multienzyme complexes
OFORs	2-Oxoacid ferredoxin oxidoreductases
ORF	Open-reading frame
PAGE	Polyacrylamide gel electrophoresis
PCR	Polymerase chain reaction
PDHC	Pyruvate dehydrogenase complex
PEG	Polyethylene glycol
RNA	Ribonucleic acid
RNase	Ribonuclease
RNaseOut	Recombinant Ribonuclease Inhibitor
RNase H	Ribonuclease H
rRNA	Ribosomal RNA
rpm	Revolutions per minute
RT-PCR	Reverse transcription and Polymerase chain reaction
SDS	Sodium dodecyl sulphate
SW	Salt water
TAE	Tris-acetate EDTA
TCA	Trichloroacetic acid
TEMED	N, N, N', N'-tetramethylethylene diamine
X-Gal	5-bromo-4-chloro-3-indoyl β-D-galactopyranoside
TPP	Thiamine pyrophosphate

Abstract

In aerobic bacteria and eukaryotes, a family of 2-oxoacid dehydrogenase multienzyme complexes (OADHCs) functions in the pathways of central metabolism for the oxidative decarboxylation of 2-oxoacids yielding acyl-CoA and NADH. The complexes comprise multiple copies of three enzymes: 2-oxoacid decarboxylase (E1), dihydrolipoyl acyl-transferase (E2) and dihydrolipoamide dehydrogenase (DHlipDH; E3). No OADHC activity has ever been found in Archaea; instead, the oxidation of 2-oxoacids is catalysed by an unrelated and structurally more simple family of 2-oxoacid ferredoxin oxidoreductases that are found throughout the Archaea and in anaerobic bacteria. Therefore, the detection of both E3 activity and its substrate, lipoic acid, in the halophilic archaea, and gene sequences corresponding to a 2-oxoacid dehydrogenase multienzyme complex operon in halophilic archaea and in a number of aerobic archaeal genomes, was unexpected. Given that genome analyses argue against the presence of non-functional ORFs in prokaryotes, it is important to elucidate the function of this putative OADHC in Archaea, and this forms the basis of the work reported in this study.

Therefore, the project was designed to investigate the expression and function of these putative OADHC multienzyme complexes in *Hfx. volcanii*. *Hfx. volcanii* is a halophilic archaeon that grows optimally at 42°C, in an optimum salt concentration of 18% (w/v) and at pH 7.

Starting with an *in vivo* investigation of transcription of the whole operon and/or individual genes by using RT-PCR, it was proved that all four genes of the complex are transcribed as an operon. Secondly, in growth studies of *Hfx. volcanii* on a variety of substrates and growth conditions it was found that there was no change in the level of DHlipDH expression, except with growth on branched-chain amino acids. However, neither complex nor E1 activity could be detected with pyruvate, 2-oxoglutarate or with any of branched-chain 2-oxoacid as substrates. Thirdly, homologous expression of the E1α and β genes in *Hfx. volcanii* resulted in the

production of recombinant E1 enzyme with a very low activity with branched-chain 2-oxoacids and pyruvate, but no activity could be detected with 2-oxoglutarate. Finally, heterologous expression of E1 in *Escherichia. coli*, resulted in the enzyme being expressed as inclusion bodies. This E1 was purified, solubilized using 8 M urea and refolded by specific refolding buffer ending with highly expressed E1. However, no E1 activity could be detected due to the presence of a substance in the refolding buffer that interacts with assay content.

The findings are discussed in the context of parallel studies in the research group on the putative OADHC operon in other archaea.

Introduction

1.1 Archaea: phylogenetic considerations

Owing to its considerable degree of conservation across all organisms, the gene that encodes the small subunit ribosomal RNA (SSU rRNA) has been extensively used for the classification of microorganisms and has allowed the recognition of the Archaea as a third distinct domain of the tree of life (Woese and Fox, 1977). rRNA sequence analyses indicated that all organisms fall within one of the three evolutionarily distinct domains: the Bacteria, the Archaea (previously known as archaebacteria) and the Eukarya (Woese *et al.*, 1990). Both Archaea and Bacteria diverged at a very early stage in the evolution of life on earth. It is thought that the Archaea and Eukarya share a common stem on the tree, with the root lying between them and the Bacteria (Doolittle and Brown, 1994). From the phylogenetic tree (Figure 1.1), the hyperthermophilic archaea, and a few thermophilic bacteria, represent the shortest lineages and are close to the root, indicating that they have undergone the least change and therefore they may be the most primitive of extant organisms.

Many Archaea grow in extreme environments, which could be indicative of their ancestral evolutionary divergence. They can be found in habitats that define the physical limits for biological systems, such as geothermal hot or acidic springs, hypersaline lakes and deep-sea hydrothermal vents. At present the archaeal domain is organized into two major lineages based on 16S rRNA sequence comparisons: the Euryarchaeota and the Crenarchaeota (Forterre *et al.*, 2002). The Euryarchaeota include methanogens, the extreme halophiles, and some hyperthermophiles. Only hyperthermophilic organisms have been cultivated from Crenarchaeota. The genera belonging to Crenarchaeota are: *Sulfolobus*, *Aeropyrum*, *Acidainus*, *Pyrolobus*, *Pyrodictium*, *Desulforococcus*, *Staphylothermus*, *Thermoproteus* and *Thermofilum.* Moreover, two additional phyla have been discovered recently. Firstly, the so called phylum Korarchaeota has been postulated on the basis of PCR amplification of 16S rRNA genes from environmental DNA, but has not confirmed by the cultivation of any organisms (Barns *et al.*, 1996). Secondly, the novel phylum Nanoarchaeota is

represented by the hyperthermophilic, anaerobic, nano-sized coccus *Nanoarchaeum equitans*; it grows only in co-culture with new chemolithoautotrophic *Ignicoccus* species (Huber *et al.*, 2002; Huber *et al.*, 2003).

As more complete genomes are sequenced, phylogenetic analysis is entering a new era: that of phylogenomics. One branch of this expanding field aims to reconstruct the evolutionary history of organisms on the basis of the analysis of their genomes (Delsuc *et al.*, 2005). The availability of complete genome sequences from cultivated archaeal species [the 45 species genome completed or are near completion are listed in Allers and Mevarech (2005)] has stimulated the research in this area and served as an important framework for tracking genomes of uncultivated archaea in complex communities.

However, while, archaeal genome diversity reflects both phylogeny and physiological adaptations to a wide range of growth conditions, it is complicated by frequent gene acquisition by horizontal gene transfer (Makarova and Koonin, 2003).

Finally, Archaea possess a characteristic of Eukaryotes and Bacteria in that they could be infected with viruses. Generally, more than 5000 viruses have been described but only about 39 of them infect archaeal hosts. The majority of these attack thermophilic archaea belonging to the phylum Crenarchaeota (Prangishvili, 2003; Prangishvili *et al.*, 2001; Rice *et al.*, 2004). About 18 viruses of methanogenic and extremely halophilic archaea have been described (Porter *et al.*, 2005). The first virus infecting a halophilic archaeon was discovered in 1974 (Torsvik and Dundas, 1974). Currently about 15 haloarchaeal viruses (haloviruses) have been reported (Dyall-Smith *et al.*, 2003).

To conclude, the Archaea are a diverse group of organisms comprising a distinct evolutionary lineage in addition to that of the Bacteria and Eukarya. Whilst much of the fascination in the Archaea comes from their adaptation to growth in extreme environmental conditions, PCR amplification of environmental DNA indicates that there may be numerous mesophilic archaea. Indeed greater archaeal diversity is expected to be recognized through improved molecular ecological searches and more sophisticated cultivation techniques

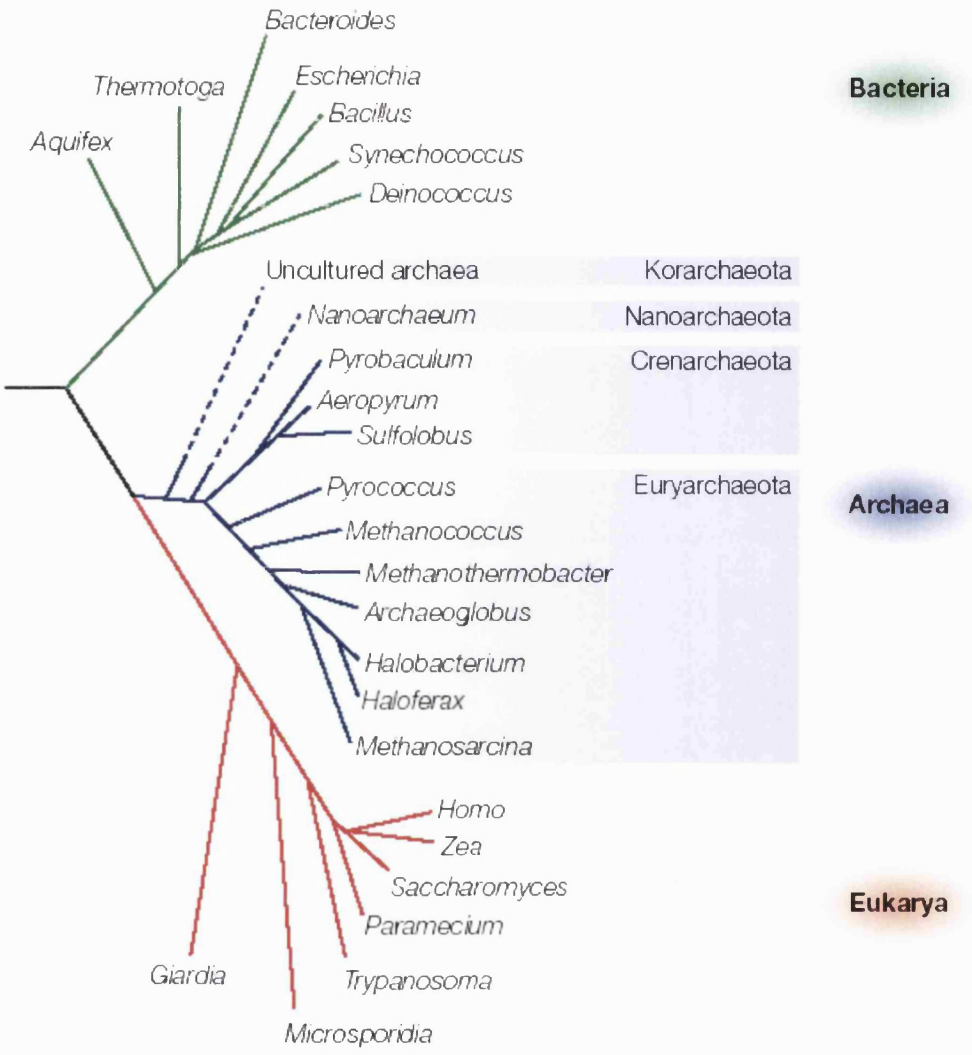

Figure 1.1: The universal tree of life.
This phylogenetic tree was constructed using ribosomal RNA sequences and illustrates the tripartite view of evolutionary divergence. Owing to the paucity of identified species, the positions of the phyla Korarchaeota and Nanoarchaeota on the rRNA tree are uncertain (indicated by dashed branches). Reproduced from Allers and Mevarech (2005).

1.2 Extremophiles

Microorganisms that require extreme environments to grow are called extremophiles and the enzymes they produce are called extremozymes. MacElory first used the term extremophiles three decades ago (MacElroy, 1974). Extremophiles are peculiar microorganisms that can grow and thrive in extreme environments, which were previously considered incompatible with biological materials and too hostile to support life. The majority of extremophiles are members of the Archaea (Woese *et al.*, 1990); however, extremophilic bacteria have also been identified. The extreme environment is a relative term, as the environments that are extreme for one organism are crucial for the survival of the other. Extremophiles include those organisms adapted to high temperatures (thermophiles) which can generally be classified into moderate thermophiles (growth optimum 50 to 60°C), extreme thermophiles (growth optimum 60 to 80°C), and hyperthermophiles (growth optimum 80 to 110°C or even up to 121°C), low temperatures (-2 to 20°C) (psychrophiles), high salinity (2 - 5 M NaCl) (halophiles) and high alkalinity (pH > 8) (alkalophiles) or high acidity (pH < 4) (acidophiles) (Rothschild and Mancinelli, 2001; Madigan and Marrs, 1997). There are also several extremophiles adapted to high pressure (piezophiles), high level of radiations (radiophiles) or toxic compounds or high metal concentration (metallophiles) or any conditions that may be considered unusual. Also, some extremophiles are subjected to multiple stress conditions such as high temperatures and low pH (thermoacidophiles).

The research group, in which the work of this thesis was carried out, has a research interest in the biotechnological applications of extremozymes. It is recognized that the majority of enzymes used in biotechnology to date have been isolated from mesophilic organisms; however, their application is still restricted by their limited stability to extreme conditions. The discovery of new extremophilic species, and their genome sequence determination, provide a path to the discovery of new enzymes, with the possibility that these may lead to novel applications. Due to their extreme stability, extremozymes offer new opportunities for biocatalysis and biotransformation. Examples of potentially useful extremozymes include cellulases, amylases, xylanases, proteases, pectinases, keratinases, lipases, esterases, catalases, peroxidases and

phytases, all of which have great potential for application in various biotechnological processes (Gomes and Steiner, 2004).

However, the renewed interest that is currently emerging as a result of new developments in the cultivation and production of extremophiles, and the success in the cloning and expression of their genes in mesophilic hosts, will increase the biocatalytic applications of extremozymes (Gomes and Steiner, 2004). Moreover, the novel metabolic pathways found in the Archaea may further increase the diversity of the enzymes available.

1.3 Halophilic archaea

Haloarchaea is the common name applied to members of the Class Halobacteria (Order Halobacteriales), and consists of the extremely halophilic archaea. Halobacteriales now includes about 18 genera (Grant *et al.*, 2001; Dyall-Smith, 2004). Halophilic archaea can be differentiated from halophilic bacteria on the basis of their archaeal characteristics, in particular the presence of ether-linked lipids (Ross *et al.*, 1981). It was believed that high salinities are dominated by Archaea, Bacteria and one eukaryotic species, the alga *Dunaliella salina*, but recently melanized fungi have been isolated from Adriatic salterns, and can be considered as a new group of eukaryotic halophiles (Butinar *et al.*, 2005).

Hypersaline environments include naturally-occurring salt and soda lakes such as the Great Salt Lakes (USA), the Dead Sea (Israel) and soda lakes in Africa, Europe and USA, plus manufactured salterns. The halophilic archaea maintain an osmotic balance by accumulating intracellular concentrations of salt (mainly KCl) that are isotonic with the exterior (mainly NaCl) (Kushner, 1988). However, a recent study has reported the isolation of the first examples of haloarchaea that are able to grow at sea water salinity (Purdy *et al.*, 2004).

The halophilic archaea are strict aerobes or facultatively anaerobic, chemoorganotrophs that are found ubiquitously in nature in hypersaline brines (Oren and Gurevich, 1994; Rodriguez-Valera, 1988). Some can even grow anaerobically, either using nitrate as an alternative electron acceptor (Wanner and Soppa, 1999) or by arginine fermentation (Ruepp and Soppa, 1996). Some of these halophilic archaea

grow at near neutral pH (pH 7.2-7.5), while the alkalophilic haloarchaea have growth optima between pH 8.5-10. The optimum salt concentration for growth varies among different halophilic archaea, ranging between 15% - 25% although most will grow at 23% salt (sea water is ~ 3.5%). Usually, strains with low salt optima can grow at higher salt concentrations, but strains with high salt optima will not grow below 20% salt. Despite living in natural waters all around the world, most strains grow best between 30 and 45°C and many are slightly thermophilic (e.g. 50°C for *Halorubrum saccharovorum*); even the Antarctic isolate, *Halorubrum lacusprofundi*, grows optimally at about 30°C (Dyall-Smith, 2004). Oxygen solubility is known to decrease with increasing temperature and salinity. This is offset by the relatively slow growth rates of haloarchaea, and their efficient terminal oxidase. Also, it has been found that halophilic archaea have relatively long generation times compared to *E. coli* (e.g. 3-4 h for *Hfx. volcanii*; 8-12 h for *Halobacterium* spp.). Nevertheless, it has been found that the hypersaline environment in which halophiles flourish is a fundamental factor for their resistance to desiccation, damaging radiation and high vacuum (Kottemann *et al.*, 2005).

A unique feature of halophiles is the purple membrane, a specialized region of the cell membrane that contains bacteriorhodopsin. Bacteriorhodopsin acts as a light-dependent transmembrane proton pump that can be used to drive ATP synthesis and support a period of phototrophic growth. It is induced by high light intensity and low oxygen tension (Krebs and Khorana, 1993). Halophilic archaea are pigmented and can be easily identifiable by their red colour, mainly caused by carotenoid pigments. These have been shown to be necessary for stimulating an active photorepair system to repair thymine dimers resulting from ultra violet radiation (Joo and Kim, 2005); as a result, halophiles come to predominate at higher salt concentrations. The carotenoid content of the cells was shown to decrease dramatically when the salt concentration of the growth medium increased (Rodriguez-Valera *et al.*, 1983). However, in other extreme halophiles it was found that their pigmentation increased at higher salt concentration (Kushwaha *et al.*, 1982). Moreover, halophiles produce buoyant gas vesicles, like many aquatic bacteria, to enable the cells to float to more oxygen rich surface layers

because they are primarily aerobic and live in concentrated brines in which oxygen solubility is low, especially at high temperatures.

Haloarchaea are prokaryotes and except for halococci, they lack a rigid cell wall; instead, they have a single layer of a glycoprotein that is called the surface layer or S-layer. The subunits of the S-layer are held together by divalent cations, and can be completely removed by treating the cells with EDTA. Cell shapes vary (Figure 1.2), with many being rod shaped. *Haloarcula* spp. are often geometrically shaped with square or triangular forms. *Haloferax* spp. are often a thin, cup-shape, recently described as like a 'potato chip'. The cell shape can vary depending on the growth conditions (Dyall-Smith, 2004).

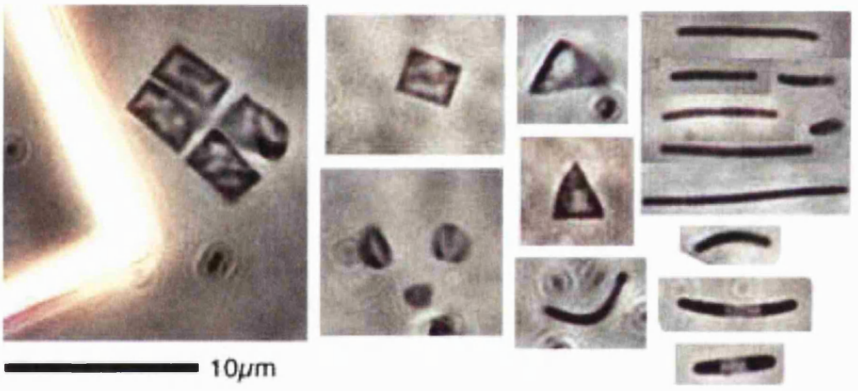

Figure 1.2: Different shape of halophilic archaea found in salt lake water.
The figure shows square, discs, triangles and rod shape halophiles (left to right). Reproduced from Dyall-Smith (2004).

25 years ago, a square halophilic archaeon was described (Walsby, 1980). This archaeon is of specific interest due to its unique shape and its abundance in hypersaline ecosystems. Recent studies report the isolation and cultivation of the square archaeon, the proposed name for which is *Haloquadratum walsbyi* (Bolhuis *et al.*, 2004; Burns *et al.*, 2004; Walsby, 2005) (Figure 1.3).

Halophilic genomes have a high GC content, which can be as high as 70%; in addition, some genera of halophilic archaea contain a considerable amount of highly

repetitive DNA, the function of which unknown. Moreover, halophilic archaea are insensitive to most of the antibiotics used in bacterial vector-host systems. But later it was reported that mevinolin, an inhibitor of eukaryotic 3-hydroxy-3-methylglutaryl coenzyme A reductase (Hmg-CoA), also strongly inhibits this enzyme in haloarchaeal extracts and prevents cell growth in liquid media (Cabrera *et al.*, 1986; Lam and Doolittle, 1989). They also have sensitivity to novobiocin, which inhibits DNA gyrase by blocking binding of ATP (Holmes and Dyallsmith, 1990; Holmes *et al.*, 1994), and they are trimethoprim sensitive (Zusman *et al.*, 1989). So, a number of plasmids had been constructed containing antibiotic resistance genes and even nutritional requirement genes (Allers *et al.*, 2004). These plasmids are available and their development has enabled transformant selection, and this will facilitate the homologous expression of halophilic proteins in their native, high-salinity environments.

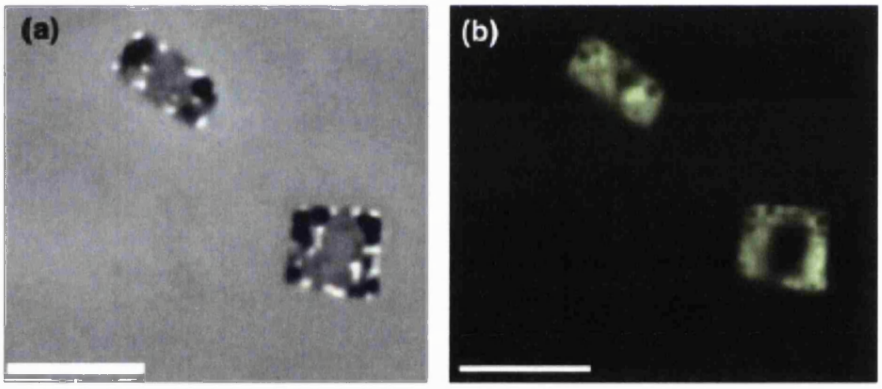

Figure 1.3: Walsby's square halophilic archaeon.
(a) Cells examined by phase contrast microscopy; (b) the same field viewed by epifluorescence microscopy after acridine orange staining. Reproduced from Burns *et al.* (2004).

1.4 *Haloferax volcanii*

Hfx. volcanii was first isolated from the Dead Sea in 1975 (Mullakhanbhai and Larsen, 1975). It is a salt-loving archaeon belonging to the family Halobacteriaceae. *Hfx. volcanii* is an obligate halophile (Mullakhanbhai and Larsen, 1975). It has disk shaped cells and shows involuted forms in the presence of salt. *Hfx. volcanii* is a

chemoorgantroph, and grows aerobically in both complex and minimal media (Mevarech and Werczberger, 1985). Optimum growth conditions are NaCl concentrations between 1.5-2.5 M at 37°C to 42°C with higher Mg^{2+} requirements (0.2 M) compared to other halophiles. *Hfx. volcanii* has a relatively long generation time of 3-4 hours, and produces a pink pigment. Overall, the organism can be easily cultivated in the laboratory.

The use of *Hfx. volcanii* for molecular biological studies has the advantage over many of halophiles in that the genome is relatively stable. Also, *Hfx. volcanii* has some of the best manipulated genetic tools among Archaea, including reporter genes (Holmes and Dyall-Smith, 2000), a transformation system (Cline *et al.*, 1989), an auxotrophic mutant, and shuttle vectors with selectable markers in each host by display of two types of antibiotic resistance or antibiotic resistance and nutritional requirements (Allers *et al.*, 2004; Holmes *et al.*, 1991; Holmes *et al.*, 1994; Lam and Doolittle, 1989). Moreover, there is a gene knockout system developed recently based on *pyr*E2 gene, which encodes the orotate phosphoribosyl transferase involved in uracil biosynthesis (Bitan-Banin *et al.*, 2003). In addition, a recent study was able to construct highly-reproducible two-dimensional (2-D) gel electrophoresis proteome maps of *Hfx. volcanii* proteins, which will improve the ability to rapidly analyze any changes that may occur in the protein expression profile between different samples (Karadzic and Maupin-Furlow, 2005). These developments have established the organism as the species of choice for genetic-level studies of halophilic archaea.

1.5 Halophilic enzymes

Halophilic enzymes utilize different adaptation mechanisms to withstand high salt concentrations in their environments. Therefore, enzymes from halophilic archaea must function in near saturating concentrations of KCl or NaCl and generally they are only stable in solvents of very high salt concentrations (Eisenberg and Wachtel, 1987), under which most proteins from non-halophilic organisms are likely to unfold or precipitate. Consequently, expression of halophilic genes in *E.coli* can result in soluble but inactive enzymes that may be reactivated by the addition of high salt concentration [e.g. *Hfx. volcanii* citrate synthase (Connaris *et al.*, 1999)]. More often, however, the

recombinant enzyme is produced as inclusion bodies that then need to be resolubilsed by unfolding with a chaotropic agent, and subsequently refolded in high salt concentrations [e.g. *Hfx. volcanii* dihydrolipoamide dehydrogenase (Connaris *et al.*, 1999)].

Protein folding under high-salt conditions is crucial for the survival of halophilic archaea. It has been shown that a chaperone supports correct protein folding in the cytoplasm of halophilic archaea (Franzetti *et al.*, 2001). Once properly folded, halophilic proteins are stabilized by the same intramolecular forces as their non-halophilic counterparts (Frolow *et al.*, 1996). In addition, aggregation is prevented by minimalization of hydrophobicity and accumulation of negative charges on the protein surface (Madern *et al.*, 2000; Mevarech *et al.*, 2000; Scandurra *et al.*, 2000), such as having an excess of acidic amino acids (i.e. glutamate and aspartate) on their surface (Danson and Hough, 1997). In addition, genome sequences now reveal the unusual abundance of surface exposed acidic residues is a general feature of halophilic proteins and most likely prevents their aggregation or salting out at high ionic strength (Fukuchi *et al.*, 2003). As both NaCl and KCl are salting-out agents, acting to remove water from the protein surface, these negative charges play a role in binding hydrate ions, so retaining a surface hydration layer; also, the reduction of their surface hydrophobicity reduces the tendency to aggregate at high salt concentration.

However, it has been found that such a high proportion of acidic amino acids is not present in the amylase from the thermophilic halophilic bacteria *Halothermothrix orenii* (Mijts and Patel, 2002).

1.6 Biotechnological potential of halophiles and their components

Halophilic archaea provide the main source of extreme halophilic enzymes. The proteins of halophilic archaea have been adapted to be active in the hypersaline conditions. Therefore, the unique properties of these biocatalysts have resulted in different novel applications in industrial processes. Several proteins from halophiles with biocatalytic applications had been reported, such as xylanases, amylases, proteases and lipases (Gomes and Steiner, 2004).

Halophilic macromolecules other than enzymes also have potential uses. For example, liposomes may have applications in cosmetics and medicines for the transport of compounds to specific sites in the body. Ether-linked lipids from archaeal halophiles have a high chemical stability and more resistance against esterases than liposomes based on fatty acids derivatives (Gambacorta *et al.*, 1995). Novel ether lipids have been obtained from *Halobacterium salinarum.* Also, biosurfactants and halophilic exopolysaccharides may enhance the remediation of oil-contaminated soil and water; many cases of successful bioremediation of hydrocarbons have been reported using halophiles from different environments such as marine, Arctic, and Antarctic environments (Delille *et al.*, 1998; Margesin and Schinner, 1999). Compatible solutes have gained in interest as biomolecular stabilizers and whole cell or stress-protective agents. For example, ectoin from *Halomonas elongata* can act as a stabilizer in the polymerase chain reaction (PCR) (Sauer and Galinski, 1998). Other examples are betaine used to improve osmotic tolerance of important crops such as rice, potato and tomato, trehalose as a cryoprotectant for freeze-drying of biomolecules, and diglycerol phosphate as a general protein stabilizer (Lamosa *et al.*, 2000). Halogenated organic compounds are of environmental concern due to their toxicity and persistency; halophilic archaea, especially those belonging to the genera *Haloarcula*, *Halobacterium* and *Haloferax* are adapted to high concentrarions (up to 1mM) of these compounds and can metabolise, for example, trichlorophenols, or the insecticides lindane and DTT (Joo and Kim, 2005).

It is likely that the biotechnological applications of halophiles and their components will increase as more genomes are sequenced and their proteins are characterised by proteomic and genomic analyses.

1.7 Central metabolism in Halophiles

Living organisms catabolise their nutrients both to supply the precursors of all cell components and to generate the energy necessary for biosynthesis (anabolism) and other endergonic processes. The metabolic links between catabolism and anabolism are the pathways of central metabolism, which serve as the major route of energy production. Considering growth on carbohydrates, central metabolism can be divided

into the conversion of sugars to pyruvate, and then the metabolic fate of pyruvate, either to organic end products or to CO_2 by complete oxidation via the citric acid cycle.

Halophilic archaea are chemo-organotrophs and many use amino acids and protein as sole sources of carbon. However, a number of carbohydrate-utilizers among the halophilic archaea have been isolated (Tomlinson and Hochstein, 1972a; Tomlinson and Hochstein, 1972b). One example is *Halobacterium saccharovorum*, which utilises glucose via a modified Entner-Doudoroff pathway (Tomlinson *et al.*, 1974). Glucose is oxidized to gluconate and then dehydrated to 2-keto-3-deoxygluconate, which in turn is phosphorylated to 2-keto-3-deoxy-6-phosphogluconate (Figure 1.4). Aldol cleavage produces equimolar amounts of pyruvate and glyceraldehyde 3-phosphate, the later being further metabolized via the common normal Entner-Doudoroff pathways found in Eukaryotes and Bacteria (Danson, 1993). The modified Entner-Doudoroff pathway has been found in other species of *Halobacterium* and in species of *Haloferax* and *Halococcus* (Pimenov *et al.*, 1987; Rawal *et al.*, 1988; Severina and Pimenov, 1988), and it may be common to all halophilic archaea. It has not been found in thermophilic or methanogenic archaea but has been found in a few bacterial genera. No route for glucose metabolism other than the Entner-Doudoroff pathway has been found in halophiles. On the other hand, it has been found that halophiles such as *Haloarcula vallismortis* can catabolise hexoses other than glucose, such as fructose via the Embden-Meyerhof pathway (Altekar and Rangaswamy, 1990; Altekar and Rangaswamy, 1991).

The metabolic fate of pyruvate (a 2-oxoacid) is considered in the next section in the context of the 2-oxoacid dehydrogenase complexes and the 2-oxoacid ferredoxin oxidoreducatases, as it is these enzymes in particular with which the work of this thesis is concerned.

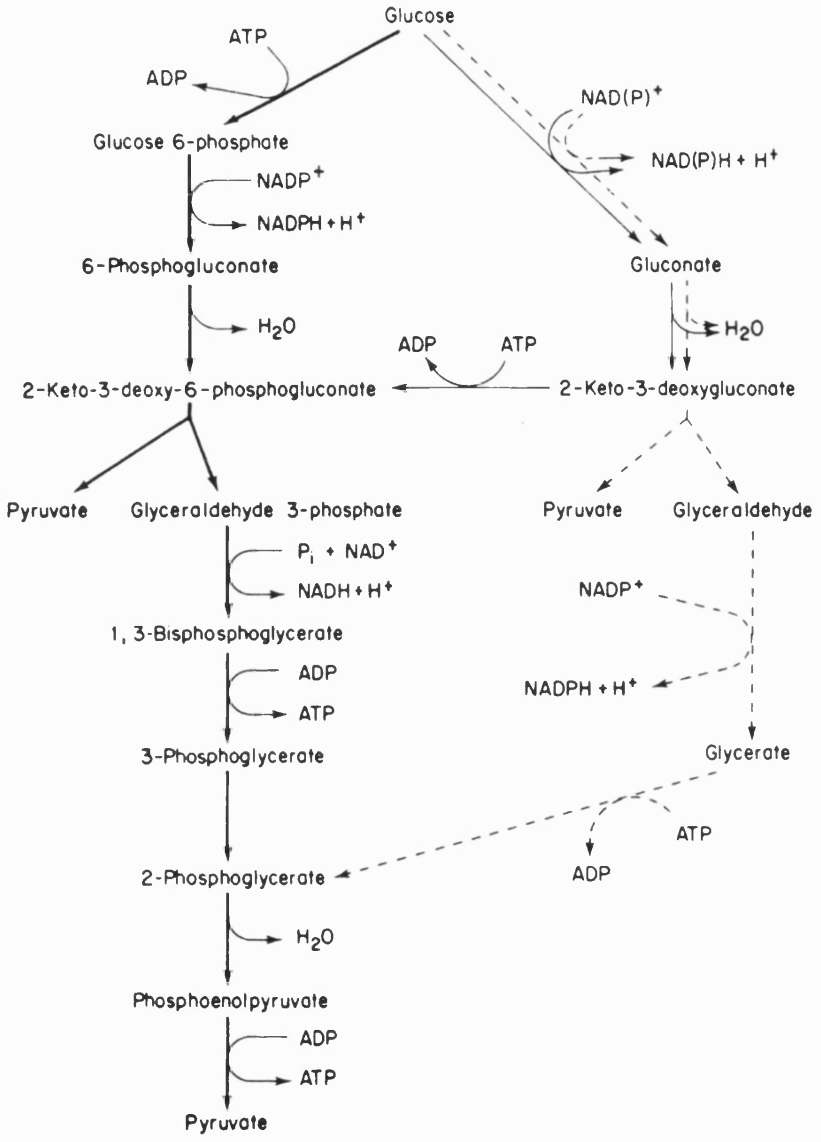

Figure 1.4: Pathways of glucose metabolism in halophilic and thermophilic archaea.

The modified Entner-Doudoroff pathway of halophiles (light solid lines) and the semi-phosphorylated and the non-phosphorylated Entner-Doudoroff pathway of *Sulfolobus solfataricus* and *Thermoplasma acidophilum* (dashed lines) are shown in comparison with the classical Entner-Doudoroff pathway of Bacteria (heavy solid lines). Reproduced from Danson (1993).

1.8 The 2-Oxoacid dehydrogenase multienzyme complex (OADHC)

Aerobic bacteria and eukaryotes posses a non-covalent assembly of protein subunits that catalyse the successive steps of a multistep chemical reaction. The 2-oxoacid dehydrogenase complexes constitute a family of related enzymes that includes the pyruvate dehydrogenase complex (PDHC), the 2-oxoglutarate dehydrogenase complex (OGDHC) and the branched- chain 2-oxoacid dehydrogenase complexes (BCOADHCs). They catalyse the oxidative decarboxylation of the relevant 2-oxoacid, transferring the resultant acyl group to CoA with reduction of NAD^+ and the generation of acyl-SCoA, CO_2, and NADH. The net reaction is shown below:

$$\textbf{2-oxoacid} + NAD^+ + \textbf{CoASH} \longrightarrow \textbf{acyl-SCoA} + CO_2 + \textbf{NADH} + H^+$$

The complexes comprise multiple copies of three enzymes, 2-oxoacid decarboxylase (E1), dihydrolipoyl acyl-transferase (E2) and dihydrolipoamide dehydrogenase (E3). The E1 catalyses the thiamine pyrophosphate (TPP)-dependent oxidative decarboxylation of the 2-oxoacid and the transfer of the resultant acyl group to the lipoic acid of E2. Then E2 transfers the acyl-group to CoA. Finally, E3 reoxidizes the dihydrolipoamide, by the reduction of the non-covalently bound cofactor FAD, in conjunction with a protein disulfide bond and an amino acid base, which are themselves then reoxidized by NAD^+, forming NADH (Perham, 2000). The steps of the catalytic mechanism are summarized in Figure 1.5.

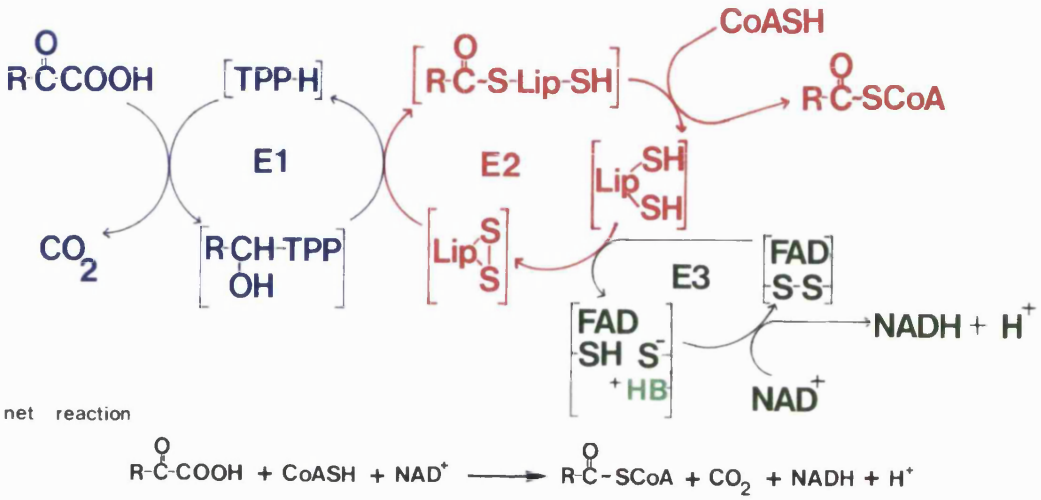

Figure 1.5 The general reaction mechanism catalysed by OADHCs.
The diagram shows the three enzyme components: E1, E2 and E3. Symbols; B: a histidine base on E3; TPP-H: thiamine pyrophosphate; Lip: enzyme-bound lipoic acid; FAD: flavin adenine dinucleotide; NAD^+: nicotinamide adenine dinucleotide. Modified from Perham (2000).

E1 is either a homodimer (α_2) as found in the PDHC of *E.coli*, *Pseudomonas aeruginosa* and *Pseudomonas putida* (Hester *et al.*, 1995) or as $\alpha_2\beta_2$ heterotetramer as in E1 of the eukaryotic PDHC and BCOADHC, and in PDHC of *Bacillus stearothermophilus* (Hawkins *et al.*, 1990) and BCOADHC of *P. putida* (Burns *et al.*, 1988).

E2 forms the catalytic core of the complex and contains the cofactor lipoic acid, which is bound covalently by an amide linkage to the amino group of a conserved lysine residue of the lipoyl domain, resulting in a long swinging arm that shuttles between the required active sites. In the primary sequence, next to the lipoyl domain is the E2 binding domain where both E1 and E3 are bound tightly (Reed, 1974), followed by the catalytic core of E2 enzyme. E2 forms the structural core of the 2-oxoacid dehydrogenase complexes, to which copies of E1 and E3 are non-covalently bound. The number of copies of each component can vary between the different complexes

and between phylogenetic groups of any one system. For example, in the PDHC from Gram-negative bacteria there are 24 polypeptide chains of the E2 component in each core molecule, whereas in the complex from Gram-positive bacteria and eukaryotes there are 60 E2 chains. Most OGDHCs and BCOADHCs have 24 E2 chains in their core structures (Izard *et al.*, 1999; Perham, 1991; Perham, 2000; Reed, 1974; Reed and Hackert, 1990). As an example Figure 1.6 illustrates the structure of the *E. coli* PDHC.

In any organism, the E3 component is a homodimer and it is the same gene product that serves the different complexes, its role in each being to reoxidise dihydrolipoamide. The E1 and E2 components of the complexes display specificity for the substrate of the overall reaction, whereas E3 can be shared by several different OADHCs, except in the case of *P. putida* which has specific three different E3 (Hester *et al.*, 1995).

The different multienzyme complexes catalyse very similar and practically irreversible steps in central metabolism. The pyruvate dehydrogenase complex, which catalyses the conversion of pyruvate to acetyl-CoA, and so links glycolysis and the citric acid cycle; the 2-oxoglutarate dehydrogenase complex, that catalyses the conversion of 2-oxoglutarate to succinyl-CoA, a step within the citric acid cycle; and the branched-chain 2-oxoacid dehydrogenase complex, which oxidatively decarboxylates the branched-chain 2-oxoacids produced by the transamination of leucine, isoleucine and valine, and which is involved in amino acid degradation (Huang and Chuang, 1996; Reed, 1974). The intact complexes are thus of giant size, with molecular masses of (5-10) x 10^6 and diameters of up to 50 nm, which is significantly bigger than a ribosome (Perham *et al.*, 2002). The number of E1 and E3 chains in each complex varies dependent on the symmetry and source.

Additional components are found in some multienzyme systems in higher organisms. For example, the mammalian PDHC contains a protein kinase and phosphatase, which control the activity of the complex through (de) phosphorylation of serine residues of E1 (Davie *et al.*, 1995; Patel and Roche, 1990). However, although bacterial PDHCs contain amino acid sequences similar to the eukaryotic phosphorylation sites, the bacterial complexes are not phosphorylated (Hester *et al.*, 1995); this may be true in Archaea.

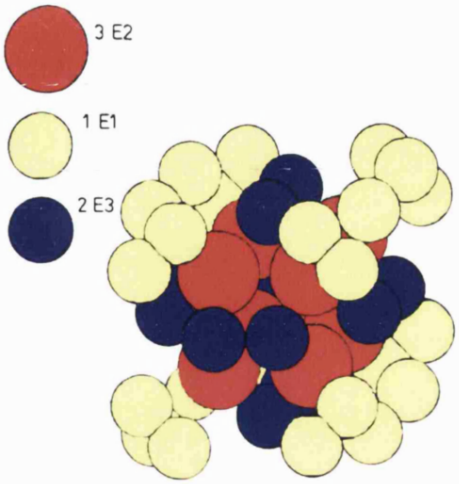

E1 (2-Oxoacid decarboxylase)
E2 (Dihydrolipoyl acyl-transferase)
E3 (Dihydrolipoamide dehydrogenase)

Figure 1.6: This is a schematic diagram of the *E. coli* PDHC showing 24 E1: 24 E2: 24 E3.

1.9 The 2-Oxoacid ferredoxin oxidoreducatases (OFORs)

No 2-oxoacid dehydrogenase complex activity has ever been found in Archaea (Danson, 1993). Instead, the oxidation of 2-oxoacids is catalysed by an unrelated and structurally simpler family of 2-oxoacid ferredoxin oxidoreductases (OFORs) (Figure 1.6). The catalytic mechanism of FOR does not involve the participation of a lipoic acid moiety or NAD^+; instead, the acyl-moiety formed on decarboxylation of the 2-oxoacid is transferred directly to CoA, and the reducing equivalents are passed via an iron sulphur center to ferredoxin. (Kerscher and Oesterhelt, 1981b).

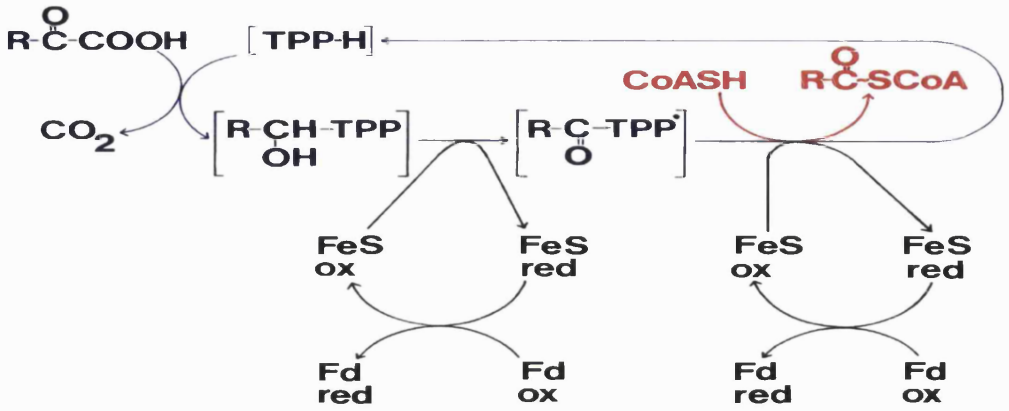

Figure 1.7: The catalytic mechanism of the 2-oxoacid ferredoxin oxidoreducatase of the halophilic archaea.

[It should be noted that in the methagenic archaeon, *Methanosarcina barkerii*, the iron-sulphur centres of both the enzyme and the ferredoxin are only reduced in the presence of both substrates, pyruvate and CoA (Bock *et al.*, 1997), and that a similar mechanism may occur in the halophilic enzyme.] Symbols; Fd: ferredoxin; FeS: an enzyme-bound iron-sulphur cluster. Reproduced from Danson *et al.* (2004).

These oxidoreductases consist of the pyruvate FOR, the 2-oxoglutarate FOR and the branched chain 2-oxoacid FOR that catabolise pyruvate, 2-oxoglutarate and the branched-chain 2-oxoacids, respectively (Kerscher and Oesterhelt, 1981b; Kerscher and Oesterhelt, 1982; Schut *et al.*, 2001). The halophilic archaeaon *Halobacterium salinarum* possesses a pyruvate and 2-oxoglutarate FOR, which have an $\alpha_2\beta_2$ subunit structure (Kerscher and Oesterhelt, 1981a; Plaga *et al.*, 1992). However, OFORs in the thermophilic archaea generally consist of four subunits as an octamer ($\alpha_2\beta_2\gamma_2\delta_2$) (Schut *et al.*, 2001). On the other hand, the thermophilic archaeon *Sulfolobus* OFOR comprises a heterodimer, and is able to react with both pyruvate and 2-oxoglutarate (Fukuda *et al.*, 2001; Fukuda and Wakagi, 2002; Zhang *et al.*, 1996). In addition, a recent study reported the expression and characterisation of two sets of genes possibly encoding putative heterodimeric OFORs from the aerobic and hyperthermophilic Crenarchaeon *Aeropyrum pernix* K1 (Nishizawa *et al.*, 2005). Active branched chain

2-oxoacid FOR has been purified under anaerobic conditions from the hyperthermophilic archaeon, *Thermococcus profundus*; it is a hetero-octamer ($\alpha_2\beta_2\gamma_2\delta_2$) consisting of four types of subunit (Ozawa *et al.*, 2005).

These oxidoreductases are found throughout the Archaea, both aerobes and anaerobes, whereas in Bacteria it is only in the anaerobic members that oxidoreductases replace the dehydrogenase complexes. However, facultatively anaerobic bacteria such as *E. coli* posses low levels of pyruvate ferrodoxin oxidoreductase in addition to higher catalytic activities of the pyruvate dehydrogenase multienzyme complex (Blaschkowski *et al.*, 1982).

Despite the obvious structural differences between OFORs and OADHCs, there are distinct mechanistic similarities between them. The net result of both complexes is the formation of an acyl-CoA via a TPP-dependent decarboxylation process, in which a hydroxyl-TPP is formed as an intermediate. The main difference is the direct transfer of the acyl-moiety from TPP to CoA in Archaea, whereas the OADHCs utilize an enzyme-bound lipoic acid as a carrier. Also, an extra enzyme activity, DHlipDH, is required within the dehydrogenases to reoxidized the lipoic acid and transfer the reducing equivalents to NAD^+. Thus it has been shown that archaeal oxidoreductases lack lipoic acid (Kerscher and Oesterhelt, 1981a) and the reducing equivalents are transferred via proteins iron-sulphur centre to ferredoxin.

1.10 Dihydrolipoamide dehydrogenase (DHlipDH)

The dihydrolipoamide dehydrogenase is the third enzyme component of the OADHCs and it catalyses the NAD-dependent oxidation of dihydrolipoamide through a catalytic mechanism involving oxidation and reduction of an intrachain disulphide bond and a base on the enzyme. It has a non-covalently but tightly bound FAD cofactor that contributes in the transfer of electrons from dihydrolipoamide to NAD^+.

The net reaction of DHlipDH is:

Dihydrolipoamide + NAD^+ ⟶ lipoamide + NADH + H^+

Despite the absence of detectable OADHC activity in the Archaea, DHlipDH has been detected in a number of aerobic members. It was first discovered in the

halophilic archaea (Danson *et al.*, 1984). The halophilic DHlipDH exists as a homodimer, has a molecular mass (M_r) of 112000-120000 and is extremely thermostable, showing no detectable loss of activity after 15 min incubation at 95°C, whereas other halophilic enzymes are inactivated at much lower temperatures (Danson *et al.*, 1984). DHlipDH is shown to be inactive when assayed in the absence of salt as with many other halophilic enzymes. However, readdition of 2 M NaCl to the inactive enzyme results in complete restoration of activity almost immediately, even after storage for 24 h at 4 °C in the absence of salt (Danson *et al.*, 1984).

The presence of DHlipDH in Archaea, Bacteria and Eukarya initially suggested that it might be an ancient enzyme that evolved before the divergence from the common ancestor (Danson, 1988). It was further proposed that it might have retained its function in Archaea, but in the aerobic bacteria and eukarya it had been sequestered to function as a an integral part of the OADHCs. Moreover, the existence of the archaeal enzyme in absence of the complexes of which it is normally a component suggests that DHlipDH may have another physiological substance than dihydrolipoamide or may fulfill an additional cellular role that not previously revealed.

However, as discussed below, it turns out that the presence of DHlipDH in the Archaea does infact signal the presence of a putative OADHC in these organisms.

1.11 Archaeal OADHCs

Further investigations led to the detection of lipoic acid in *Halobacterium salinarum*, suggesting that this might indeed be the physiological substrate of DHlipDH (Danson *et al.*, 1984; Pratt *et al.*, 1989). The gene encoding DHlipDH in *Hfx. volcanii* was then cloned and sequenced (Vettakkorumakankav *et al.*, 1992) and sequence alignments showed that it is clearly related to the DHlipDHs from bacterial and eukaryal OADHCs. Further sequencing upstream of the DHlipDH gene led to the discovery of an operon in *Hfx. volcanii* containing four genes whose predicted protein sequences show significant identity to the OADHC components E1α, E1β, E2 and E3 of both Bacteria and Eukaryotes (Figure 1.8) (Jolley *et al.*, 2000). Despite the lack of a detectable dysfunction in a E3 knock-out mutant (Jolley *et al.*, 1996b), the presence of a high percentage of acidic amino acids in all the proteins from the operon suggested

that they were functionally adapted to a high-salt environment and, therefore the genes have not arrived in *Hfx. volcanii* by recent horizontal gene transfer. E3 activity was also detected in the cell extracts of *Thermoplasma acidophilum* (Smith *et al.*, 1987).

The functional importance of the *Hfx. volcanii* operon would be supported if the same or similar operons were present in other archaeal species. Recently, genes encoding the components of a putative OADHC from a number of aerobic archaea have been identified from genome sequences (Figure 1.9). However, none of the sequenced anaerobic archaea possesses the operon structure characteristic of the OADHCs, although two methanogenic organisms may possess remnants of the individual components. Yet, unlike the bacterial and eukaryal situations, only one single complex operon appears to be present in each archaeal species analysed (Danson *et al.*, 2004).

The situation in the halophilic archaea may be even more complicated in that, in addition to the 4-gene OADHC operon (figure 1.8) a partial operon encoding an E1α and E1β but devoid of the genes for a complete E2 and E3 has been detected in *Hfx. volcanii*; an "unattached" lipoyl domain is also present. Mutation experiments suggest that the genes are functional during anaerobic growth on Casamino Acids and nitrate (Wanner and Soppa, 2002). It should be noted also that expression of a gene encoding an E1 subunit of OADHC was induced in *Hfx. volcanii* in a glucose medium (Zaigler *et al.*, 2003). This E1 gene differs from the E1 genes of the operon previously detected and also the E1 genes in the second partial operon mentioned above (Jolley *et al.*, 2000; Wanner and Soppa, 2002). Thus *Hfx. volcanii* appears to possess at least three different E1 proteins. However, due to the absence of a complete genome sequence of *Hfx. volcanii*, further conclusions are not possible.

Our research group has recently achieved the expression of E1α and E1β from *Tp. acidophilum* in *E. coli*. They demonstrated that the protein products form an $\alpha_2\beta_2$ heterotetramer possessing decarboxylase catalytic activity with the three branched-chain 2-oxoacids and pyruvate, but no activity with 2-oxoglutarate. This represents the first report of the catalytic function of these putative archaeal multienzyme complexes (Heath *et al.*, 2004).

The question of why no OADHC activity can be detected in halophilic and other archaea remains unresolved. It could be that the complex is transcribed but only E3 is expressed, or that whole complex is produced but it is unstable or it is not assembled into an active complex. Also, it may be that the true 2-oxoacid substrate has not yet been found and thus no activity is being detected, although the data from *Tp. acidophilum* would suggest that this is not the case, at least in this archaeon. Furthermore, do all these complexes from the various Archaea have the same substrate specificity; is that specific activity is affected by the corresponding OFOR, and how are the two enzyme systems coordinately regulated?

All these findings add more questions about the nature of the OADHCs in Archaea and in halophilic archaea specifically; this then forms the basis of the research carried out in this PhD project.

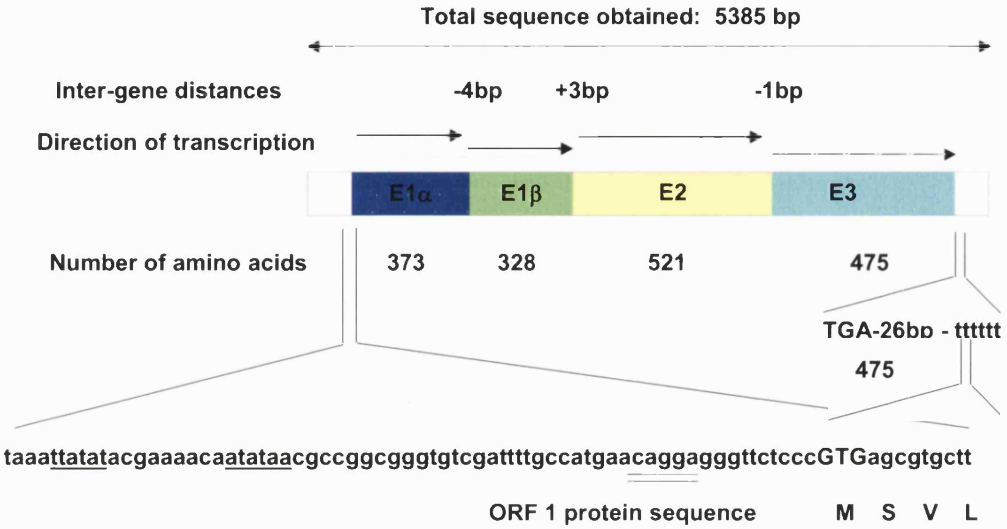

Figure 1.8: The putative OADHC operon of *Hfx. volcanii*.
The figure shows the arrangement, inter-gene distances (bp) and proposed direction of transcription of the four genes constituting the proposed *Hfx. volcanii* operon. The corresponding numbers of amino acids of the protein products are given. The DNA sequence at the 5′ end of E1, plus the upstream region, are shown to illustrate the proposed promoter sequences (underlined), the Shine-Delgarno sequence (doubly underlined) and the GTG start codon. The proposed transcriptional stop signal is also shown. Reproduced from Danson *et al.* (2004).

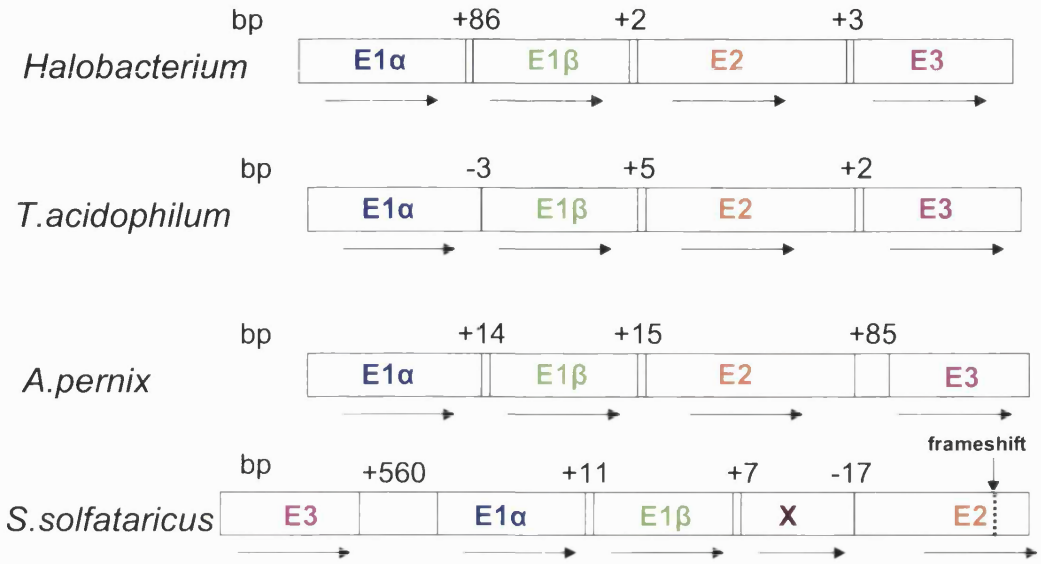

Figure 1.9: Putative OADHC operons of four aerobic archaea.
The figure shows the arrangement, inter-gene distances (bp) and proposed directions of transcription of the open-reading frames (ORFs) constituting the E1α, E1β, E2 and E3 genes of the proposed 2-oxoacid dehydrogenase complex operons of *Halobacterium* NRC-1, *Thermoplasma acidophilum*, *Aeropyrum pernix* and *Sulfolobus solfotaricus*. The *S. solfotaricus* operon posses an unknown gene X between E1β and E2, and there is a frameshift within the E2 gene. Reproduced from Danson *et al.* (2004).

1.12 Project aims

Of particular interest are the genes that apparently encode the components of a 2-oxoacid dehydrogenase complex, which our research group has discovered to be present in the genome of the *Hfx. volcanii*, in addition to the presence of an active E3 and its substrate lipoic acid, but in the absence of any whole complex activity. So the aims of the project were to detect if these genes are transcribed and translated into an active protein, to study their level of expression and to determine the substrate specificity of the whole complex.

These objectives are approached by:

1- An investigation of the *in vivo* transcription of the whole operon and/or individual genes by the reverse transcription-polymerase chain reaction (RT-PCR).

2- Growth studies of *Hfx. volcanii* under different metabolic conditions to determine conditions in which the OADHC operon might be expressed.

3- Homologous expression of the OADHC genes in *Hfx. volcanii*.

4- Heterologous expression of the E1 α and β genes in *E. coli*.

Materials and Methods

2.1 Materials

Cell culture: *Haloferax volcanii* (DSM No. 3757) was obtained from DSMZ the Deutsche Sammlung von Mikroorganismen und Zellkulturen GmbH Braunschweig, Germany (German collection of Microorganisms and Cell Culture). Yeast extract, peptone and branched-chain amino acids were supplied by Fisher Scientific, Loughborough, UK, while agar, tryptone and carbencillin disodium salt were from Sigma-Aldrich, Gillingham, UK. Bacto™ Yeast Extract, Bacto™ Casamino Acids and Bacto™Agar were obtained from BD-Biosciences, Oxford, UK, whereas Bacteriological peptone was from Oxoid. Basingstoke, UK. Unless mentioned otherwise, the rest of chemicals were supplied from Sigma-Aldrich, Gillingham, UK, with high commercial purity.

Enzyme assays: DL-6,8-Thioctic acid amide (DL-lipoamide) 99-100%, DL-6,8 Thioctic acid (± α lipoic acid), oxaloacetic acid, β-NAD, coenzyme A ,thiamine pyrophosphate TPP (cocarboxylases) and 2-oxoacid substrates were provided by Sigma-Aldrich Gillingham, UK. Bio-Rad Protein assay Dye reagent concentrate was obtained from Bio-Rad Laboratories Hemel Hempstead, UK, and Albumin Standard was from Pierce, USA.

Molecular biological studies: Oligonucleotide primers were obtained from MWG-Biotech AG, Germany. dNTP was obtained from Bioline, London, UK, Vent® DNA polymerase was from New England Biolabs, Hitchin Herts, UK. Agarose was obtained from Helena Biosciences Europe, Sunderland, UK, while ethidium bromide was from Sigma-Aldrich, Gillingham, UK, whereas blue/orange 6x loading dye was supplied by Promega, Southampton, UK. 1kb, 100 bp and low DNA mass ladder were from Invitrogen, Paisley, UK.

2.2 Methods

2.2.1 Strains and Culture Conditions

Hfx. volcanii was grown in 18% (w/v) salt-water modified growth medium (MGM1) consisting of 14.4% (w/v) NaCl, 1.8% (w/v) $MgCl_2.6H_2O$, 2.1% (w/v) $MgSO_4.7H_2O$, 0.42% (w/v) KCl, 0.5% (w/v) peptone, 0.1% (w/v) yeast extract, pH 7.2, at 42°C with shaking at 200 rpm (Mevarech and Werczberger, 1985).

Minimal medium was used for growth experiments and consisted of the same salts as modified growth medium with 0.5% (v/v) glycerol, 0.05% (w/v) sodium succinate (other carbon or energy source can be used), 5 mM NH_4Cl, 1mM K_2HPO_4 buffer, 20 mM Tris-HCl (pH 7.5), and 0.1% (v/v) trace elements solution. The trace elements solution consisted of 0.36 mg/ml $MnCl_2.4H_2O$, 0.44 mg/ml $ZnSO_4.7H_2O$, 2.3 mg/ml $FeSO_4.7H_2O$ and 0.05 mg/ml $CuSO_4.5H_2O$, prepared in pure water and filter sterilized (Dyall-Smith, 2004). Growth was routinely monitored by measuring optical density at λ 600 nm.

Where required, the medium was solidified by the addition of 1.5% (w/v) agar. Agar plates were prepared thick to a depth of around 7-10 mm (in contrast to normal 4 mm) and incubated at 42°C wrapped in a plastic bag or in an airtight containers to avoid desiccation and salt crystal formation (DasSarma and Fleischmann, 1995). Cultures were stored on the bench or in the refrigerator in well-sealed glass bottles or flasks, or on plates sealed in plastic. Frozen stocks were maintained at –80°C (maximum of 2 years) or in liquid nitrogen (maximum of 15 years) in the same medium containing 20% (v/v) and 15% (v/v) glycerol respectively (Dyall-Smith, 2004).

E. coli strains were routinely grown in Luria-Bertani (LB) broth (1% (w/v) NaCl, 1% (w/v) tryptone and 5% (w/v) yeast extract) at 37°C with shaking at 200 rpm or on agar plates containing LB medium supplemented with 1.5% (w/v) agar at 37°C for the time required. The medium was supplemented with carbencillin (50μg/ml) or Kanamycin (30 μg/ml) as required. Strains were stored at -80°C in LB with 20% (v/v) glycerol or on plates sealed in plastic in the fridge.

2.2.2 Biochemical Technique and Activity Studies

2.2.2.1 Preparation of cell extracts

Hfx. volcanii cells were harvested by centrifugation at 11,000 x g for 15 min at 4°C using rotor JA 25.15 (Beckman Avanti J25, Beckman Coulter, UK). Cell paste was resuspended at 0.2 g/ml in extracting buffer consisted of 2 M KCl or NaCl, 50 mM Tris-HCl (pH 8.0), 1 mM EDTA (0.2g in 1ml buffer). The extract was then subjected to three 30 s bursts (amplitude = 14micron) of sonication in a bath of ice with a 60 second cooling time between each burst using a 150-W Ultrasonic Disintegrator (MSE Scientific Instruments); cell debris was removed by centrifugation at 16,000 x g for 10 min and the supernatant was used in enzyme assays.

E. coli extracts were prepared in a similar manner with the exception that cells were resuspended in 0.1 M KCl or NaCl, 50 mM Tris-HCl (pH 8.0), 1 mM EDTA.

2.2.2.2 Enzyme assay

Generally, assays were carried out at 37°C, 42°C or 45°C when assaying *E. coli*, *Hfx. volcanii* or recombinant *Hfx. volcanii* enzymes respectively. Buffers were prepared with 2 M salts (KCl or NaCl) in the case of *Hfx. volcanii* assay and 0.1 M for *E.coli*. The pH was adjusted after the addition of salts using KOH or NaOH to the pH recommended.

2-oxoacid substrates: either pyruvate, 2-oxoglutarate or deaminated branched-chain amino acids such as 4-methyl-2-oxopentanoate (leucine), 3-methyl-2-oxopentanoate (isoleucine) or 3-methyl-2-oxobutanoate (valine).

Kinetic parameters of the assays were determined by the direct linear method of Eisenthal and Cornish-Bowden (1974).

2.2.2.3 DHLipDH enzyme assay

Hfx. volcanii DHlipDH assays were carried out in 2 M KCl or NaCl, 50 mM Tris-HCl (pH 8.0), 1 mM EDTA buffer, 1 mM NAD^+ and 0.4 mM dihydrolipoamide, in a final volume of 1 ml (Jolley *et al.*, 1996b). 1 unit of enzyme activity is defined as the

amount required to produce 1 μmol of product per minute. The same conditions were used for *E.coli* cell extracts except assay buffer contained 0.1 M KCl or NaCl.

Catalytic activity was assayed spectrophotormetrically using a Cary 300 Bio UV- visible spectrophotometer (Varian, UK). The reaction reduces NAD^+ to NADH, which has an absorption maximum at 340 nm and a molar extinction coefficient of 6,200 M^{-1} cm^{-1}. Initial rates were calculated using the Cary Kinetics programme.

2.2.2.4 Preparation of dihydrolipoamide

DL-dihydrolipoamide was prepared by the reduction of DL-lipoamide with $NaBH_4$ (Reed *et al.*, 1958). 800 mg DL-lipoamide was dissolved in 20 ml ethanol: water (4:1) over ice. 800 mg $NaBH_4$ was added in 4 ml cold distilled water, and the mixture stirred over ice for 2 h. The solution was acidified with 1 M HCl until effervescence stopped. The product was then extracted three times with 50 ml chloroform, transferred to a round-bottomed flask and rotary evaporated to dryness. The resulting crystals were dissolved in 40 ml toluene with gentle warming. 16 ml hexane was added and the precipitate collected by vacuum filtration, followed by drying in a desiccator.

The purity was determined spectophotometrically by reaction with 5,5'-dithiobis-2-nitrobenzoate (DTNB). 0.2 mM DTNB was reacted with 0.05 mM dihydrolipoamide (0.1 mM thiol groups) in a volume of 1 ml Tris-HCl buffer. For 100% purity the expected absorbance at 412 nm was 1.36 (E_m= 13,600 M^{-1} cm^{-1}). The preparation was shown to be over 98% pure.

2.2.2.5 Citrate synthase assay

Hfx. volcanii assays were carried out in 2 M KCl or NaCl, 50 mM Tris-HCl (pH 8.0), 1 mM EDTA, 0.2 mM oxaloacetate, 0.14 mM acetyl CoA and 0.1 mM DTNB, in a final volume of 1 ml. The same procedure was used for *E. coli* extracts except the assay buffer contained 0.1M KCl or NaCl.

Activity was assayed spectrophotometrically in a Cary 300 Bio UV- visible spectrophotometer, (Varian, UK) by the method of Srere *et al.* (1963). Free coenzyme A reacts with DTNB, releasing thionitrobenzoate. This has an absorption maximum at 412 nm and a molar extinction coefficient of 13,600 M^{-1} cm^{-1}. One unit (U) of enzymic

activity is 1μmol CoASH produced per minute. Initial rates were calculated using the Cary Kinetics programme.

2.2.2.6 Acetylation of coenzyme A

Coenzyme A was acetylated by dissolving 10 mg in 1 ml water, cooling on ice and adding 0.2 ml of 1 M $KHCO_3$, followed by 0.1 ml of 1 M acetic anhydride freshly-diluted with water. After incubation on ice for 10 min, acetylation was checked by addition of 20 μl of the reaction mixture to 1 ml of assay buffer containing 100 μM DTNB.

A yellow colour indicated incomplete acetylation and more acetic anhydride was added after the addition of $KHCO_3$ to maintain the pH. The final concentration of acetyl-CoA was ~7.5 mM.

2.2.2.7 2-Oxoacid dehydrogenase assay (E1)

Hfx. volcanii assays were carried out in a buffer consisting of 20 mM potassium phosphate (pH 7.0), 2 mM $MgCl_2$, 0.2 mM TPP and 2 M KCl or NaCl in a final volume of 1 ml. Buffer and cell extract were pre-incubated for 10 min at a specific temperature depending on the source of cell extract (Fries *et al.*, 2003b); 50μM 2,6-dichlorophenolindophenol (DCPIP) was then added and the assay started by the addition of the 2-oxoacid substrate for 10 min using double beam or single beam. The same conditions were used for *E .coli* cell extracts except assay buffer contained 0.1 M KCl or NaCl.

E1 enzymic activity was assayed spectrophotometrically at 595 nm in a Cary 300 Bio UV- visible spectrophotometer, (Varian, UK) by following the 2-oxoacid dependent reduction of the artificial electron acceptor DCPIP (Lessard and Perham, 1994) and a molar extinction coefficient of 22,000 M^{-1} cm^{-1}.

2.2.2.8 2-Oxoacid dehydrogenase complex assay (OADHC)

Hfx. volcanii complex assays were performed in a final volume of 1ml of 50mM potassium phosphate buffer (pH 8.0) containing 0.2 mM TPP, 2.5 mM NAD^+, 1 mM $MgCl_2$, 2 M KCl or NaCl, 2.6 mM cysteine HCl, 0.13 CoA and 2mM of complex

substrate (Reed and Mukherjee, 1969). Buffer and cell extract were pre-incubated for 10 min at a specific temperature depending on the source of cell extract then the assay was started by the addition of 2-oxoacid substrate (Fries *et al.*, 2003a) and its progress monitored by the increase in A_{340nm} for 10 min. The same procedure was used for *E. coli* extracts except the assay buffer contained 0.1M KCl or NaCl.

The complex assay measures the rate of formation of NADH at 340 nm and a molar extinction coefficient of 6,200 M^{-1} cm^{-1}.

2.2.3 Protein methods

2.2.3.1 Determination of protein concentration

Protein concentrations were determined by the method of Bradford (1976) using 20 µl of sample mixed with 200 µl Bio-Rad protein assay dye reagent concentrate (0.1 mg/ml Coomassie Brilliant Blue G-250, 10% (v/v) phosphoric acid, 5% (v/v) ethanol) in a final volume of 1ml with water. This was incubated at room temperature for approximately 15 min. The absorbance at 595 nm was determined and the protein concentrations interpreted using a calibration curve constructed from known standards. The standard used was bovine serum albumin over a range of concentrations from 0 to 100 µg/ml.

2.2.4 Molecular Biology Methods

2.2.4.1 *Hfx.volcanii* genome sequence

The putative OADHC operon was identified in the *Hfx. volcanii* DSM 3757 genome from the ENTREZ Nucleotide database (http://www3.ncbi.nlm.nih.gov) and the remainder of the operon sequence, upstream the dihydrolipoamide dehydrogenase (E3) was obtained from PhD thesis Jolley (1996a), (Appendix).

2.2.4.2 Primers design

Oligonucleotide primers were designed by using the Primerselect programme from a genetic analysis computer package (Primer Premier, version 4.04, Premier Biosoft International, Palo Alto, CA, USA). By using the identified OADHC sequence of *Hfx.*

volcanii as mention above, forward primers **(F)** of each gene of the complex were designed to start at, or a few bases downstream from, the start codon (5' end), and the reverse oligonucleotide primers **(R)** were designed to start at, or a few bases upstream of, the stop codon (3' end) of the open reading frame. Also, primer pair melting points were within 5°C of each other. The primers were resuspended in sterile MilliQ water to a final concentration of 100 pmol/µl and stored at –20°C.

2.2.4.3 Polymerase chain reaction (PCR) amplification of DNA

Reactions contained approximately 100 ng target DNA, 100 pmol of each primer, 2 mM dNTP, 5µl 10x ThermoPol reaction buffer, 4 µl dimethyl sulphoxide (DMSO), 1 µl Vent® DNA polymerase and sterile Milli-Q water to 50 µl. *Hfx. volcanii* genomic DNA was prepared by vigorously resuspending a colony in 100 µl sterile Milli-Q water and vortexing, followed by centrifugation at 15,800 x g for 5 min; the supernatant was used as template. PCR reactions were set up in 0.5 ml thin-walled tubes on ice and started by the addition of water, dNTP, 10x buffer, DMSO, primers, template mix, and lastly, polymerase enzyme. A control PCR tube that lacked DNA template was used to detect the validity and sterility of the reaction. The tubes were placed directly in a preheated (96°C) Mastercycler thermal cycler (Eppendorf). Temperature cycling was carried out as follows:

Cycle 1	96°C	5 min	
Cycle 2	96°C	1 min 30 s	**Denaturation**
Cycle 3	56°C	1 min 15 s	**Annealing**
Cycle 4	72°C	3 min	**Extension***
Go to cycle 2 and repeat 30 cycles			
Cycle 5	72°C	10 min	**Final Extension**
Cycle 6	4°C		**Hold**

*Time determined by size of expected product; this is usually 1 min per kilobase, but with *Hfx. volcanii* 3 min was always used.

A 5, 10 or 15 µl sample of the reaction mixture was visualized on a 0.8% or 1% or 1.3% (w/v) agarose gel.

2.2.4.4 Agarose gel electrophoresis

DNA fragments were routinely analysed and separated by horizontal agarose gel electrophoresis, to resolve DNA fragments between approximately 100 bp and 10,000 bp, using 0.8% to 1.3% (w/v) gels. These were made by dissolving agarose in the desired volume of 1x TAE buffer (40 mM Tris-acetate, 1 mM EDTA) (Sambrook and Russel, 2001) by heating in a microwave oven. The solution was allowed to cool before the addition of ethidium bromide (0.05µl/ml) and then the warm agarose was poured into a perspex gel mould, with a comb in place to form wells, and allowed to set either at room temperature or at 4°C. Once set the comb was removed and the gel placed in an electrophoresis tank and covered with 1x TAE buffer. DNA samples were mixed with blue/orange 6x loading dye in a 5:1 ratio and loaded onto the gel with appropriate DNA standards. Generally, a 1kb ladder was used for DNA samples > 1kb and a 100 bp ladder for samples < 1kb (ladder stock of 10 µl ladder, 90 µl dH_2O and 20 µl 6x loading dye). Electrophoresis was carried out at a constant voltage of 75-90 V for 90 min or until full separation of the bands. The stained gel was visualized and photographed using a UV light of MultiImage™ light cabinet-filter position and AlphaImager™ 3400 software (Alpha Innotech corporation).

2.2.4.5 SDS-PAGE

Cell extracts and cell debris were examined by SDS-PAGE on a 10% (w/v) polyacrylamide gel (Laemmli, 1970) with standard buffers (Sambrook and Russel, 2001). Proteins were visualized with Coomassie Brilliant Blue R 250 and molecular weights were calibrated with broad range markers (BioRad), containing myosin (M_r 210 kDa), β-galactosidase (116.3), phosphorylase b (97.4), bovine serum albumin (66.2), ovalbumin (45.0), carbonic anhydrase (31.0) and trypsin inhibitor (21.5).

In vivo transcription of the complex

3.1 Introduction

Aerobic bacteria and eukarya posses a family of 2-oxoacid dehydrogenase multienzyme complexes (OADHC), which function in the pathways of central metabolism for the oxidative decarboxylation of 2-oxoacids yielding acyl-CoA and NADH. The complexes consist of multiple copies of three enzymes (E1, E2 and E3). In contrast, no 2-oxoacid dehydrogenase complex activity has ever been found in the Archaea; alternative 2-oxoacid ferredoxin oxidoreductases are found throughout the Archaea and in anaerobic bacteria. Therefore, it was a surprise to detect both DHlipDH (E3) activity and its substrate, lipoic acid, in the halophilic archaea (Danson *et al.*, 1984; Pratt *et al.*, 1989) and gene sequences corresponding to a 2-oxoacid dehydrogenase multienzyme complex operon with no known functional significance. Additionally, Northern analysis of *Haloferax volcanii* RNA identified a 5.2-Kb RNA species (Jolley *et al.*, 2000) which is close to the length of the predicted operon 5.4 Kb and suggests that the whole operon is transcribed as a single message.

In order to determine whether the OADHC is functional in *Hfx. volcanii*, the transcription of the whole operon and/or individual gene transcription was investigated by the reverse transcription-polymerase chain reaction (RT-PCR).

3.2 Materials

Oligonucleotide primers were obtained from MWG-Biotech AG, Germany. Access RT-PCR system and random primers were supplied by Promega, Southampton, UK. DeoxyribonucleaseI (Amplification Grade), SuperScript™ II Reverse Transcriptase, RNaseOut™ and RNaseH were provided by Invitrogen, Paisley, UK. Turbo™ DNase was from Ambion, Huntingdon, UK. Unless mentioned otherwise, the rest of chemicals were supplied from Sigma-Aldrich, Gillingham, UK, with high commercial purity.

3.3 Methods

3.3.1 Oligonucleotide primer sequence design

3.3.1.1 Complex primers

Oligonucleotide primers were designed by using the Primerselect programme from a genetic analysis computer package (Primer Premier, version 4.04, Premier Biosoft International, Palo Alto, CA, USA). By using the identified OADHC sequence of *Hfx. volcanii* as mention in Chapter 2 (Section 2.2.4.1) long message primers of each gene of the complex were designed as forward primers **(F)**, starting a few bases downstream from starting codon, and the reverse oligonucleotide primers **(R)** were designed to start a few bases upstream of the stop codon of the open reading frame. The primers are shown below with site of attachment to the gene:

FE1α: 5' - **CTTCAACGCGACCCGCAG** - 3' **(from 10 down to 28bp)**

RE1α: 5' - **CTGAGGAATCCTTCGTCGCC** - 3' **(from 1100 up to 1081 bp)**

FE1β: 5' - **CAGAACCTCACCATCGTGCAG** - 3' **(from 10 down to 31 bp)**

RE1β: 5' - **CACCGCCTCACGAATACCTTC** - 3' **(from 975 up to 955 bp)**

FE2: 5' - **GAATTCAAACTCCCCGACGTC** - 3' **(from 13 down to 34 bp)**

RE2: 5' - **CACCAGCAGTTTGGGGTCTTC** - 3' **(from 1556 up to 1536 bp)**

FE3: 5' - **GAGACATCGCAACCGGAACC** - 3' **(from 11 down to 31 bp)**

RE3: 5' - **AGGGTGTGAATCGCCTGTCC** - 3' **(from 1418 up to 1399 bp)**

These primers resulted in long transcript messages of E1α: 1091bp, E1β: 966bp, E2: 1544 bp, E3: 1408bp and αβ of 2057bp.

On the other hand, short-message oligonucleotide primers for both the forward primer and the reverse one were designed within the open reading frame of each gene of the complex as described below:

F2E1α: 5' - **GGTGAGTCTCCAGCGACAGGG** -3' **(from 150 down to 170 bp)**

F3E1α: 5' - **CATCGAGGCGGTCCAGTACC** - 3' **(from 756 down to 775 bp)**

R1E1α: 5' - **TCTCGTTGCCCTTCTCGTGG** - 3' **(from 352 up to 333bp)**

R1E1β: 5' - **GACTCCGAGTGCGACTCGG** - 3' **(from 401 up to 383 bp)**

R1E2: 5' - **AACGTCGCCTTCGGTCACG** - 3' **(from 460 up to 441 bp)**

R1E3: 5' - **GAACTCGATGGTCTCCGAGCC** - 3' **(from 428 up to 408 bp)**

These primers resulted in short or long transcript messages, where the length varies according to the combination of primers that were used.

3.3.1.2 House-keeping Primers (control primers)

Glucose dehydrogenase (GDH) was chosen to act as a positive control in the RT-PCR reaction. Since the genome sequence of *Hfx. volcanii* is not yet published, the GDH sequence was identified using the GDH sequence of *Haloferax mediterranei* from the ENTREZ Nucleotide database (http://www3.ncbi.nlm.nih.gov). Blast searches against the *Hfx. volcanii* sequence, resulted in contig with 88% identity to the *Hfx. mediterranei* GDH. Accordingly, the oligonucleotide primers were designed as shown below:

FGDH: 5' - **CGGTCGTCATCGAGAAGCC** - 3' **(from 38 down to 56 bp)**

R1GDH: 5' - **ACTCGGACATGAAGCCGTGC** - 3' **(from 352 up to 333 bp)**

R2GDH: 5' - **GGTGTCGTCGTCTTCGAATGC** - 3'**(from 1037 up to 1017 bp)**

These primers resulted in long GDH message and short message, length of 1002 bp and 342 bp respectively.

3.3.2 RNA isolation

Total RNA was isolated by growing *Hfx. volcanii* aerobically on MGM1 as described in Chapter 2 (Section 2.2). At mid-exponential phase (OD_{550nm} ~ 0.5-0.8), a 1 ml sample was quickly removed to a pre-chilled 1.5 ml microcentrifuge tube and the cells were pelleted by centrifugation (11,000 x g, 1 min, 4°C). The tubes were returned to the ice and the supernatant carefully removed using a micropipette; the pellets were resuspend and lysed in 80 µl lysis solution[1] by pipetting up and down but avoiding formation of air bubbles. After incubation at 37°C for 15 min, the tubes were placed on ice for 2 min and then 30 µl of ice-cold 3 M sodium acetate pH 5.3 (Sambrook and Russel, 2001) was added and the solution vortexed for a few seconds. The lysate was centrifuged (11,000 x g, 1 min, 4°C) to remove precipitated protein and the supernatant was removed to a fresh tube. The RNA was precipitated from the supernatant by adding 2 volumes of pre-cooled absolute ethanol, and the subsequent RNA pellet (11,000 x g, 1 min, 4°C) was washed twice with pre-cooled 70% ethanol. The pellets were air-dried for 20-30 min, at 25°C under a slight vacuum. Finally, they were dissolved in 60 µl diethyl pycarbonate (DEPC[2])-treated water and were stored at -80°C (Dyall-Smith, 2004; Karunakaran and Kuramitsu, 1996).

[1]**Lysis solution:** 1 ml lysis solution consists of 25 mM NaOH, 5 µM diaminocyclohexane tetraacetic acid (CDTA), 5 mM EDTA, 8% (w/v) sucrose, 664 µl DEPC-treated water and 0.5 % (w/v) sodium dodecyl sulphate (SDS). The reagents were added in the order mentioned, and the solution was then autoclaved.

[2]**DEPC-treated water** was prepared by the addition of 0.1 ml DEPC to 100 ml water. After vigorous shaking, it was then incubated overnight at 37°C with shaking at 150-200 rpm. Finally, the solution was autoclaved (DasSarma and Fleischmann, 1995).

Generally, inactivation of nucleases is essential because of the sensitivity of the RNA and the widespread distribution of RNase; enzymatic degradation of RNA is probably the greatest single source of loss of RNA encountered during RNA isolation. Due to that, experiments were conducted in a sterile area cleaned with 70% ethanol in DEPC-treated water. In addition, all plastic ware and glassware were autoclaved twice,

and then the glassware were baked in an oven at 200-250°C for 2 h, and stored separately with the plastic ware in an oven at 60°C. Moreover, all solutions were prepared in 0.1% DEPC-treated water to inactivate nucleases.

3.3.2.1 Analysis of isolated RNA

Firstly, the concentration of total RNA isolated was determined by measuring the A_{260nm} using the formula $1A_{260} \equiv 40$ µg/ml. Secondly, the quality was determined by measuring the ratio of A_{260}/A_{280}. Thirdly, total RNA was electrophoresed on a 1% (w/v) agarose gel as described in Chapter 2 (Section 2.2.4.4) with the one exception that the samples with the loading dye were denatured at 65°C for 5-10 min before loading (Kevil *et al.*, 1997).

3.3.2.2 Purification of isolated RNA

Two reagents were used to purify the isolated RNA from contaminating DNA.

First method: The reaction was performed in an RNase-free, 0.5 ml microcentrifuge tube on ice containing 10 µl RNA sample (1 µg), 1 µl 10x DNase I reaction buffer, 1 µl DNase I (1 U/µl) and DEPC-treated water to 10 µl; the tube was incubated at room temperature for 15 min and then 1 µl of 25 mM EDTA was added. Finally, the reaction tube was heated for 10 min at 65°C.

Second method: total RNA was also purified using Turbo™ DNase. The reaction was conducted in an RNase-free 0.5 ml microcentrifuge tube; the reaction volume was 50 µl and consisted of 10 µl RNA sample (1 µg), 0.1 volume 10x Turbo DNase buffer (1:1 buffer: RNA sample), 2 µl Turbo DNase I (1:5 Turbo DNase: sample) and nuclease-free water to the volume recommended. The tube was then incubated at 37°C for 30 min. At the end of the incubation period, 10 µl DNase inactivation reagent was added (1:1 reagent: RNA) and incubated for 2 min at room temperature with occasional mixing. Finally, the reaction tube was centrifuged at 10,000 x g for 1.5 min at room temperature and the supernatant was then carefully transferred to a new tube to be used in RT-PCR.

3.3.3 RT-PCR

RT-PCR was performed using the two methods described below.

3.3.3.1 One-step Access RT-PCR system

The Access RT-PCR System is a one-tube with two-enzyme system. It was supplied with 5 units/µl AMV Reverse Transcriptase, 5 u/µl Tfl DNA polymerase, AMV/Tfl 5x reaction buffer, 25 mM $MgSO_4$, 10 mM dNTP mixture, positive control RNA with carrier, 15 µM upstream and downstream control primers, and nuclease-free water.

The reaction was performed in a 0.5 ml thin-wall sterile tube by adding components to a final concentration of 1x reaction buffer, 0.2 mM dNTP, 1 µM of control primers or gene specific primers, 1 mM $MgSO_4$, 0.1 u/µl of both AMV Reverse Transcriptase and Tfl DNA polymerase, and nuclease-free water to a final volume of 50 µl. The reagents were added in the sequence mentioned above, mixed and after that both enzymes were added and gently vortexed. The reaction was initiated by adding 10 µl of Turbo DNase-treated RNA or control RNA. Each time the reaction was performed a negative control was carried out in parallel where AMV Reverse Transcriptase was omitted.

Temperature cycling was carried out as follows:

First strand cDNA synthesis

Cycle 1	48°C	45 min	Reverse transcription
Cycle 2	92°C	2 min	AMV RT inactivation and RNA/cDNA/primer denaturation

Second strand synthesis and PCR amplification

Cycle 3	94°C	30 s	Denaturation
Cycle 4	60°C	1 min	Annealing
Cycle 5	68°C	2 min	Extension

39 cycles

Cycle 5	68°C	7 min	Final Extension
Cycle 6	4°C		Hold

Initially, RT-PCR was attempted using conditions recommended by the supplier (as mention above); these are the temperatures that were used with control RNA. However, in case of *Hfx. volcanii* RNA, a series of changes were made to optimise the PCR step, using PCR cycles mentioned in Chapter 2 (Section 2.2.4.3). At the end, 10 µl of the reaction product was analyzed on a 1.3% (w/v) agarose gel as described in Chapter Two (Section 2.2.4.4). The remainder of the reaction was stored at -20°C.

3.3.3.2 Two step RT-PCR

This method consist of two steps; the first step is the first strand cDNA synthesis using SuperScript™ II Reverse Transcriptase, and the second step is the amplification of cDNA in a PCR reaction, using a cycle length and temperature that are suitable for the high GC content of *Hfx. volcanii* DNA.

The reagents supplied with SuperScript™ II Reverse Transcriptase are 5x first strand reaction buffer and 0.1 M DTT. A 20 µl reaction volume was used by the addition of the following components to a nuclease-free microcentrifuge 0.5 ml thin walled tube: 1 µl of (50ng/µl) random primers, 10 µl of Turbo DNase treated RNA and 1 µl of 10 mM dNTP. The mixture was heated to 65°C for 5min and was rapidly chilled on ice. Then the contents of the tube were collected by a brief centrifugation followed by the addition of 4 µl 5x first strand buffer, 2 µl 0.1M DTT and 1 µl of (40 units/µl) RNaseOUT™ (RNase inhibitor). The tube contents were then gently mixed and incubated at 25°C for 2 min. Subsequently, 1 µl (200units) of SuperScript™ II Reverse Transcriptase was added, mixed gently, and then incubated at 25°C for 10 min. Two tubes were used for each sample, one as test tube, and the second as control tube lacking SuperScript™ II Reverse Transcriptase.

Finally, the RT step was carried on by incubating the tube at 42°C for 50 min, after which the reaction was inactivated by heating at 70°C for 15 min. Moreover, complementary RNA to cDNA was removed by the addition of 1 µl (2 units) of RNase H (an endoribonuclease that specifically degrades the RNA strand during second strand cDNA synthesis) and incubation at 37°C for 20 min. At this stage the sample is ready to be used in the PCR step as described in Chapter 2 (Section 2.2.4.3) by using 10% of the first strand reaction and gene specific primers. At the end of the PCR step, 10µl of

reaction product was visualized on a 1.3% (w/v) agarose gel as described in Chapter 2 (Section 2.2.4.4).

3.4 Results

3.4.1 Oligonucleotide primer design and quality

Using primers designed with homology upstream and downstream of the open reading frame, the complex genes (E1α, E1β, E2, E3 and αβ) and the GDH gene were successfully PCR-amplified from genomic DNA of *Hfx. volcanii*. The amplification was confirmed by bands of the expected size visualized on a 1% (w/v) agarose gel.

3.4.2 RNA isolation

RNA isolation by most methods may be divided into four general phases: cell lysis, inactivation of nucleases, extraction of RNA from cellular components, and purification. The crucial phases in any RNA isolation methods are the lysis and nuclease inactivation steps, and the most important differences between reported methods are in these two steps. Efficient lysis of the target microorganism is required for intracellular RNA to be released, and a high degree of efficiency is necessary to prevent bias due to preferential release of mRNA species. Most RNA isolation procedures incorporate at least some protein denaturants during lysis to protect released nucleic acid from cellular nucleases (Ogram *et al.*, 1995).

There are different commercial RNA isolation kits, but it has been found that they are extremely variable. In addition, archaeal mRNA is not poly A tailed so it is difficult to use any kit designed specifically to isolate eukaryotic mRNA. Moreover, isolating RNA from halophilic archaea required the choice of particular procedures and reagents that performed well at high salinity. Therefore, the new method of RNA isolation as mentioned previously is far more efficient than standard protocols and gave better results. The method includes lysis by solubilization of the cell membrane by detergent. Most lysis-denaturant solutions may not be efficient extractants for nucleic acids, so usually alkaline extractants with at least 0.1 M phosphate are the most efficient extractants (Ogram *et al.*, 1987). However, here slightly acidic (pH 5.3) sodium acetate was used to improve the isolation and to prevent hydrolysis of RNA

under alkaline conditions. Also, protein denaturants such as DEPC, and detergents such as SDS, were employed to inactivate RNase.

3.4.2.1 Analysis of isolated RNA

The extracted RNA was characterized with respect to its size and composition. The RNA quality of different samples of total RNA was determined by measuring A_{260}, which was between 0.05-0.1 and exhibited an A_{260}/A_{280} ratio of 1.5-1.6. The concentration of RNA was obtained by using the formula $1A_{260} \equiv 40$ μg/ml and was found to be between 0.15-0.2 μg/μl, taking into consideration that almost half the concentration was genomic DNA and the rest is total RNA as shown in Figure 3.1.

Additionally, the quality of the total RNA isolated was monitored by gel electrophoresis, but surprisingly the efficiency of extraction of total RNA was not always a reliable guide to the success of the subsequent RT-PCR of mRNA. The agarose gel shows that the isolated RNA is contaminated with genomic DNA; this was to be expected, as no DNase treatment was included in the procedure. Moreover, two major electrophoretic bands were observed in the recovered RNA and assumed to be the 23S and 16S rRNA molecules (3.2 Kbp and 1.5 Kbp, respectively); the mRNA lies in between (Figure 3.1). It has been found that 84% of total RNA is ribosomal RNA (Chant *et al.*, 1986).

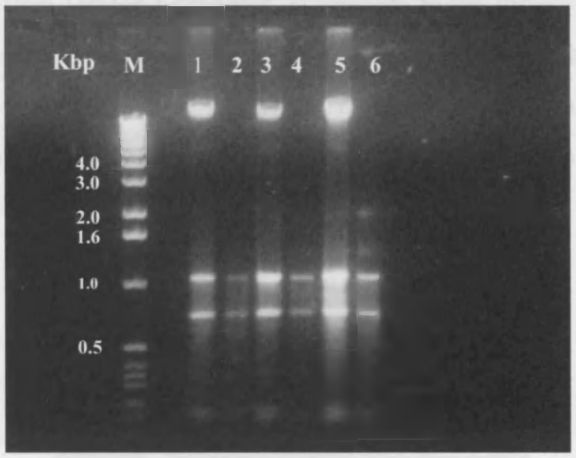

Figure 3.1: Agarose gel of total RNA of *Hfx. volcanii*.
Marker lane (M) contains 1kb ladder, with sizes in kilo base pairs as shown. The gel is a 1% agarose gel showing products of total RNA isolation, where lanes 1, 3 and 5 represent untreated isolated RNA showing the contaminated genomic DNA while lanes 2,4 and 6 represent conventional DNase treated samples of isolated RNA.

3.4.2.2 Purification of isolated RNA

RT-PCR is one of the molecular techniques that require high-quality RNA, especially free from DNA, in high yield. Then, it is important to find DNase that has markedly higher affinity for DNA, thus being more effective in removing trace quantities of DNA contamination than conventional DNase and guaranteed to lack any contaminating RNase activity that may affect the isolated RNA. During purifications the main points to be taken into consideration are try to avoid heating RNA samples to inactivate DNase, which can lead to chemical degradation of RNA by divalent cations present in the DNase buffer.

The isolated RNA samples shown in Figure 3.1 were purified from genomic DNA using two different reagents: Deoxyribonuclease I Amplification Grade reagent and Turbo^{TM} DNase. At the end of the RNA purification, the samples were examined by electrophoresis on a 1% (w/v) agarose gel (Figure 3.2). Also, after treatment, each RNA sample was subjected to PCR; none of the reactions revealed a PCR product, indicating that the RNA samples were now free of DNA.

From experimental observation it has been concluded that Turbo DNase reagents are better than DNase I reagents, especially as the former reagents use novel DNase inactivation reagents rather than the use of EDTA followed by heating. Besides that, it ensures the removal of DNase enzyme from the reaction mix and removes the divalent cations from the reaction buffer or carried over from the RNA sample (Prediger and Chacko, 2003).

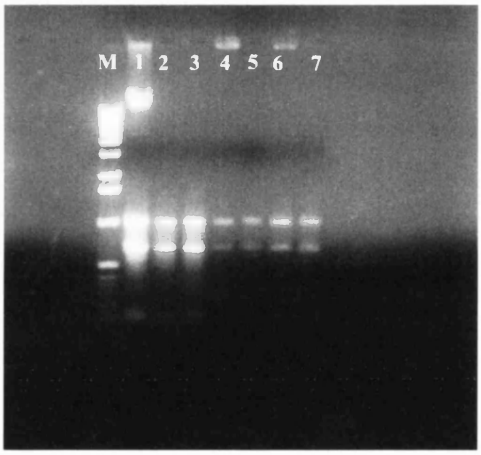

Figure 3.2: Purification of total RNA of *Hfx. volcanii.*
Marker lane (M) contains 1kb ladder. The gel is a 1% agarose gel showing products of total RNA purification. Lane 1 shows total RNA before purification, while lanes 2-7 represent purified RNA samples. Lane 2 and 3, DNase I treated samples using 5µl and10µl of RNA sample, respectively. Lanes 4-7 show Turbo DNase treated samples where lanes 4 and 5 using 5µl while lanes 6 and 7 using 10µl of RNA sample. The gel confirmed that using turbo DNase is better than DNase I and the greater amounts of RNA used the higher the concentration resulted.

3.4.3 RT-PCR

Different techniques are available to perform RT-PCR, either one-tube or two-tube methods. In the first one, all the reverse transcribed RNA (cDNA) is available for amplification, whereas in the second one, only a subsample is amplified. The methods are not valid without assurance of the absence of DNA.

3.4.3.1 One step Access RT-PCR system

Access RT-PCR is a new simplified technique RT-PCR system; it is the one that couples both reverse transcription and PCR amplification in a one-tube system. This technique includes an optimized single-buffer system that permits detection of RNA transcripts without a requirement for buffer addition in between the RT and PCR reactions, which reduces the potential for contaminating the samples.

Due to the above reasons Access RT-PCR was initially chosen to perform RT-PCR on total RNA isolated from *Hfx. volcanii.* Bands of the expected size resulted with the control RNA provided with kit, whereas negative results were obtained with *Hfx. volcanii* RNA. Although many trials and modifications were performed to optimize the reaction, no success was achieved. These failures may be due to the high G and C nucleotide content in *Hfx. volcanii* genome that necessitates a higher denaturation temperature above the optimum temperature of Tfl polymerase of the kit; or it might be something in the procedure of RNA isolation that interacts with one of the reagents of the kit leading to the failure of the process.

3.4.3.2 Two step RT-PCR

Due to the lack of success with Access RT-PCR, an alternative two-step RT-PCR procedure was used. The same procedure was successfully used with *Halobacterium* sp. strain NRC-1 (Wang *et al.*, 2004).

The two step RT-PCR resulted in bands of the expected size of transcribed genes of the complex, which was confirmed by running 1% (w/v) agarose gel. The RT-PCR confirmed that each gene of the multienzyme complex is transcribed (Figures 3.3 and 3.4) and also, by using different combination and sizes of primers, that all four genes are transcribed as an operon (Figures 3.5 and 3.6).

The figures below represent analysis by gel electrophoresis of RT-PCR of *Hfx. volcanii* RNA using gene specific PCR primers.

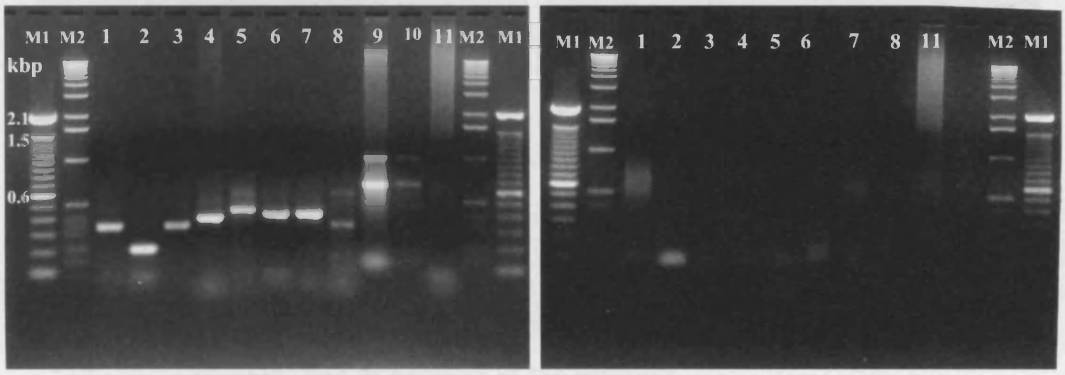

a) PCR: (+) Reverse transcriptase **b) PCR: (-) Reverse transcriptase**

Figure 3.3: Generation of short fragments of each gene of the complex (< 500 bp).
Marker lanes M1 and M2 contain 100 bp ladder and 1kb ladder, respectively, with sizes in kilo base pairs as shown. The gel is a 1.3% agarose gel showing products of RT-PCR using primers of short messages. Lanes 1, 2 and 3: E1α of 343, 203 and 345 bp. Lane 4: E1β 392 bp. Lane 5: E2 447 bp, lanes 6 and 7: E3 of 416 bp (duplicate) and lane 8: GDH 342 bp. Lanes 9 and 10: untreated RNA and turbo-treated RNA and lane 11: PCR control.
RT-PCR products in this gel using the primers mentioned in p.37 and p.38 as: FE1α + R1E1α, F2E1α + R1E1α, F3E1α + RE1α, FE1β + R1E1β, FE2 + R1E2, FE3 + R1E3 (duplicate) and FGDH + R1GDH respectively.

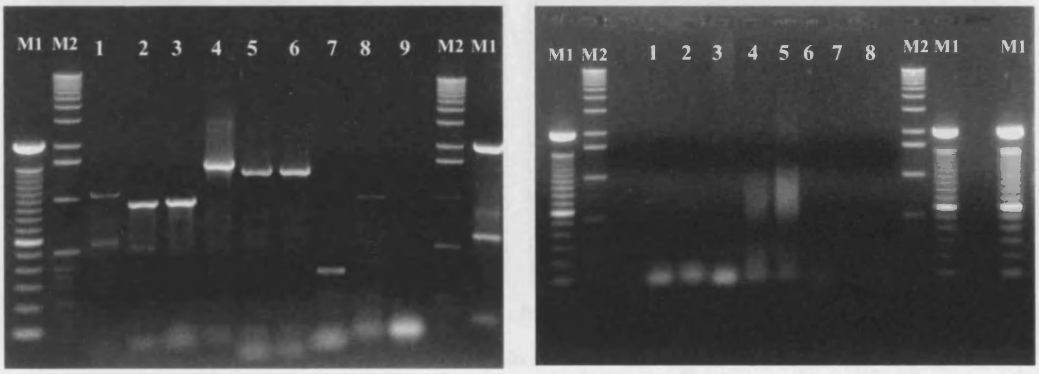

a) PCR: (+) Reverse transcriptase **b) PCR: (-) Reverse transcriptase**

Figure 3.4: Generation of long fragments of each gene of the complex (> 500 bp).
Marker lanes M1 and M2 contain 100 bp ladder and 1kb ladder. The gel is a 1.3% agarose gel showing transcripts of RT-PCR using primers of long products. Lanes 1 and 2: E1α of 1091 and 951 bp. Lane 3: E1β 966 bp, lane 4: E2 1544 bp and lanes 5 and 6: E3 1408 bp (duplicate). Lane 7 and 8: GDH of 343 and 1002 bp respectively and lane 9: PCR control.
RT-PCR products in this gel using the primers mentioned in p.37 and p.38 as: FE1α + RE1α, F2E1α + RE1α, FE1β + RE1β, FE2 + RE2, FE3 + RE3 (duplicate), FGDH + R1GDH and FGDH + RGDH respectively.

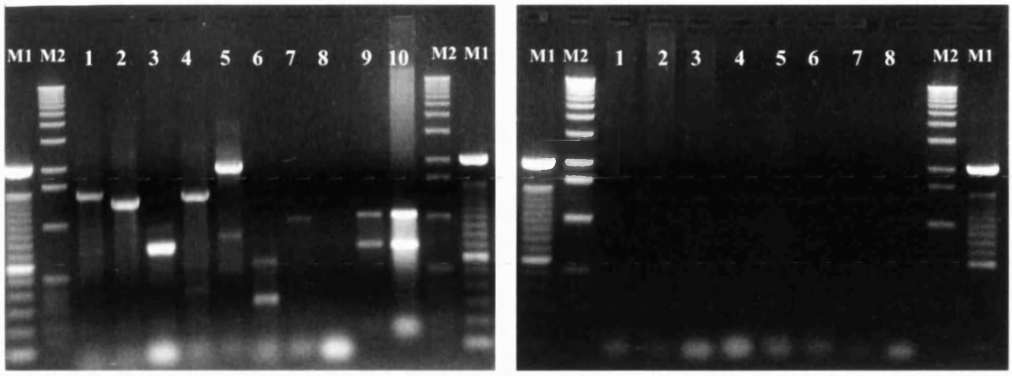

a) PCR: (+) Reverse transcriptase **b) PCR: (-) Reverse transcriptase**

Figure 3.5: Generation of fragments resulting from the use of different combination of primers of the complex.

Marker lanes M1 and M2 contain 100 bp ladder and 1kb ladder. The gel is a 1.3% agarose gel representing products of RT-PCR using combinations of primers. Lanes 1, 2 and 3: α-β transcripts of 1494,1355 and 743 bp respectively. Lane 4: β-E2 of 1437 bp and lane 5: E2-E3 of 1978 bp. Lanes 6 and 7: GDH of 343 and 1002 bp respectively. Lane 8: PCR control and lanes 9 and 10: turbo-treated RNA and untreated RNA.

RT-PCR products in this gel using the primers mentioned in p.37 and p.38 as: FE1α + R1E1β, F2E1α + R1E1β, F3E1α + R1E1β, FE1β + R1E2, FE2 + R1E3, FGDH + R1GDH and FGDH + RGDH respectively.

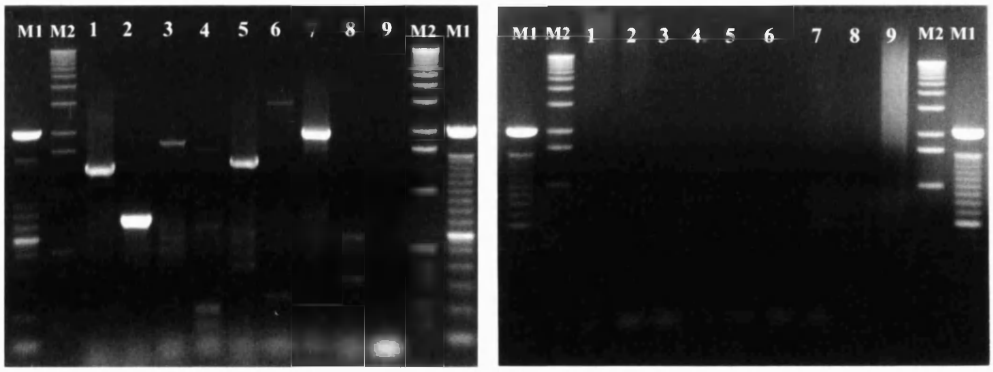

a) PCR: (+) Reverse transcriptase **b) PCR: (-) Reverse transcriptase**

Figure 3.6: Generation of more fragments resulting from the use of different combination of primers of the complex.

Marker lanes M1 and M2 contain 100 bp ladder and 1kb ladder. The gel is a 1.3% agarose gel showing products of RT-PCR using further combinations of primers. Lanes 1 and 2: α-β transcripts of 1355 and 743 bp respectively. Lane 3: α-E2 of 1794 bp and lane 4: α-E3* 3325 bp (failed). Lanes 5 and 6: β-E2 and β-E3 showing products of 1437 and 2968 bp and lane 7: E2-E3 of 1978 bp. Lane 8 short product of GDH 342 bp and lane 9 PCR control.

*α-E3 3325 bp unexpectedly failed; this may due to the large size of the transcript and instability of the RNA.

RT-PCR products in this gel using the primers mentioned in p.37 and p.38 as: F2E1α + R1E1β, F3E1α + R1E1β, F3E1α + R1E2, F3E1α + R1E3, FE1β + R1E2, FE1β + R1E3, FE2 + R1E3 and FGDH + R1GDH respectively.

Since RNA is unstable, different sizes of primers of the same gene were designed in order to avoid missing long transcripts, and to confirm the transcription of the genes as complex operon.

To confirm the validity and reproducibility of the RT-PCR reaction, each trial was performed at least three times. Also, prior to RT-PCR, all samples were proven to be free of contaminating DNA by performing control PCRs without the preceding reverse transcription step. Finally, control RT-PCR reactions, with no added SuperScript™ II Reverse Transcriptase, were carried out to ensure that no contaminating DNA was introduced during RT-PCR. Equally important as a positive control for each sample, RT-PCR was performed on the same extract with primers specific for GDH, which resulted in bands of the expected size of the transcripts. This target was chosen as a control because it is constitutive enzyme, and therefore its mRNA is known to be present.

3.5 Discussion

The presence of the OADHC operon in *Hfx. volcanii*, the existence of the activity of E3 and its substrate all add more question to the list to be answered. What is the function of this operon, are these genes transcribed and what is the level of transcription. Finally, if they are transcribed are they translated into active proteins?

In the present chapter, transcription of the OADHC operon had been studied using RT-PCR. *Hfx. volcanii* is an excellent model for molecular biological studies, as it is easily grown and maintained in the laboratory in hypersaline medium, and its genome is relatively stable compared to other halophiles. These properties permitted the use of *Hfx. volcanii* as a representative archaeal model to study the highly sensitive RT-PCR technique.

The study of interest is *in vivo* transcription that requires the isolation of total RNA or preferably mRNA. Most eukaryotic mRNAs have relatively stable polyadenylic acid tails at the 3' end. Therefore, the isolation of large quantities of high quality mRNA from eukaryotic cells has been achieved by affinity purification through annealing this sequence to immobilised poly (dT) sequences. However, it is difficult to isolate prokaryotic mRNA by the same method, mainly due to great instability or lack of poly (A) sequence in mRNA (Cao and Sarkar, 1992) and it could be degraded easily by exonucleases. Therefore, another method has been developed to enrich prokaryotic mRNA by removing rRNA from the total RNA preparation (Su and Sordillo, 1998). However, this method is a time consuming and not easily performed. Due to that, total *Hfx. volcanii* RNA has been used in the current RT-PCR studies.

In the present study, total RNA was isolated and used in RT-PCR to detect transcription of the genes of the putative OADHC operon. The results confirmed the transcription of the complex as a complete message and also the transcription of each gene of the operon. Also, the data strongly indicates the transcription of each gene of OADHC by using gene specific primers, and the use of combination of primers of the complex confirms the transcription of the complex as an operon. These results confirm and extend the previous finding of Northern studies of *Hfx. volcanii* RNA (Jolley *et al.*, 2000), which highlighted a single RNA band at 5.2 Kb, but this is not such a definite demonstration of transcription of an operon as that obtained in this chapter. Moreover,

a previous study indicates that the overall pattern of particular protein bands was comparable to that obtained with mRNAs in RT-PCR and the appearance of proteins is somewhat delayed when compared to transcripts, reflecting the higher sensitivity of RT-PCR as compared to immunoblotting (Klein *et al.*, 2000). This study supports the efficiency and accuracy of RT-PCR compared to Northern studies.

Thus, the *Hfx. volcanii* operon is present, transcribed, the activity of one of the enzymes of the complex E3 is present; and then the question is are the transcripts also translated into active E1 and E2 proteins? The answer to this question might best be gained by studying homologous expression of the complex genes in *Hfx. volcanii*, followed by activity and substrate specificity studies of the individual enzymes and the whole complex.

Growth studies of Hfx. volcanii

4.1 Introduction

We have discovered dihydrolipoamide dehydrogenase (DHlipDH), its substrate lipoic acid and gene sequences corresponding to a 2-oxoacid dehydrogenase multienzyme complex operon in halophilic archaea; in addition to that, we have now shown that all genes of the complex are transcribed as an operon *in vivo*. These findings raise many questions as to why halophilic archaea have genes for OADHC when they have alternative and active ferrodoxin oxidoreducatase enzymes that catalyse the equivalent reactions. Furthermore, no activity of any OADHC has been detected in these organisms.

In order to answer these questions, the present chapter studies the function and level of expression of DHlipDH and the OADHC multienzyme complexes in halophilic archaea by growing *Hfx. volcanii* under different metabolic conditions that may lead to an increase in the expression of DHlipDH and which in turn could reflect the expression of the complex. These studies were performed by monitoring the pattern of growth of *Haloferax* under different nutrient conditions and then measuring the enzymic activity of DHlipDH, E1, and the whole complex activity.

The level of citrate synthase, the first enzyme of the citric acid cycle, was measured as an internal control. The oxidation of most nutrients is completed in this cycle, and it was therefore thought that the level of citrate synthase might be reasonably constant in different growth conditions.

4.2 Materials

Cell culture: *Haloferax. volcanii* (DSM No. 3757) was obtained from DSMZ the Deutsche Sammlung von Mikroorganismen und Zellkulturen GmbH Braunschweig, Germany (German collection of Microorganisms and Cell Culture). Yeast extract, peptone and branched-chain amino acids were supplied by Fisher Scientific, Loughborough, UK, while agar and tryptone were from Sigma-Aldrich, Gillingham,

UK. Bacto™ Yeast Extract, Bacto™ Casamino Acids and Bacto™ Agar were obtained from BD-Biosciences, Oxford, UK, whereas Bacteriologicalpeptone was from Oxoid, Basingstoke, UK. Unless mentioned otherwise, the rest of the chemicals were supplied from Sigma-Aldrich, Gillingham, UK, with high commercial purity.

4.3 Methods

4.3.1 Strains and Culture Conditions

Hfx. volcanii was grown in 18% (w/v) salt-water modified growth medium (MGM1) consisting of 14.4% (w/v) NaCl, 1.8% (w/v) $MgCl_2.6H_2O$, 2.1% (w/v) $MgSO_4.7H_2O$, 0.42% (w/v) KCl, 0.5% (w/v) peptone and 0.1% (w/v) yeast extract, pH 7.2, at 42°C with shaking at 200 rpm (Mevarech and Werczberger, 1985).

Minimal medium was used for growth experiments and consisted of the same salts as modified growth medium with 0.5% (v/v) glycerol, 0.05% (w/v) sodium succinate (other carbon or energy sources can be used), 5 mM NH_4Cl, 1mM K_2HPO_4 buffer, 20 mM Tris-HCl (pH 7.5), and 0.1% (v/v) trace elements solution. The trace elements solution consisted of 0.36 mg/ml $MnCl_2.4H_2O$, 0.44 mg/ml $ZnSO_4.7H_2O$, 2.3 mg/ml $FeSO_4.7H_2O$ and 0.05 mg/ml $CuSO_4.5H_2O$, prepared in pure water and filter sterilized (Dyall-Smith, 2004). Growth was routinely monitored by measuring optical density at λ 600 nm.

Where required, the medium was solidified by the addition of 1.5% (w/v) agar. Agar plates were prepared to a depth of around 5-8 mm (in contrast to normal 3mm) and incubated at 42°C wrapped in a plastic bag or in an airtight container to avoid desiccation and salt crystal formation (DasSarma and Fleischmann, 1995). Cultures were left on the bench or in the refrigerator in well-sealed glass bottles or flasks, or on plates sealed in plastic. Frozen stocks were maintained at -80°C (maximum of 2 years) or in liquid nitrogen (maximum of 15 years) in the same medium containing 20% (v/v) and 15% (v/v) glycerol, respectively (Dyall-Smith, 2004).

E. coli strains were routinely grown in Luria-Bertani (LB) broth (1% (w/v) NaCl, 1% (w/v) tryptone and 5% (w/v) yeast extract) at 37°C with shaking at 200 rpm or on agar plates containing LB medium supplemented with 1.5% (w/v) agar at 37°C

for the time required. Strains were stored at -80°C in LB with 20% (v/v) glycerol or on plates sealed in plastic in the fridge.

4.3.2 Growth studies of *Hfx. volcanii*

The doubling time and growth pattern of *Hfx.volcanii* were determined. In all batch cultures an inoculum of approximately 5% of the culture volume was used, prepared under the same conditions and in the same medium as in the growth experiment. To improve the growth, cultivation was carried out in an Erlenmeyer flask (500 ml volume with 100 ml of medium) with orbital shaking at 170-200 rpm, at 42°C. After inoculating the medium, a zero time reading was measured and the growth was monitored by OD_{600nm} measurements and samples were removed at known times for assay of enzymic activities.

4.3.2.1 Growth of *Hfx.volcanii* using different carbon sources

Cultures were prepared using the minimal medium with different carbon sources using the naturally occurring isomers D-carbon source and L-amino acids. For example, 0.25% or 0.5% of glycerol, glucose or sodium citrate, 0.25% of pyruvate, L-lactate, sodium acetate, L-alanine, L-glutamate and L-valine, and 0.3% of L-leucine or L-isoleucine, were used. With some carbon sources such as glucose and pyruvate, and with all branched-chain amino acids, lipoic acid (DL- 6,8 Thiocticacid ± α lipoic acid) was added to a final concentration of 0.2 mM.

4.3.2.2 Growth of *Hfx. volcanii* anaerobically

Anaerobic cultures were grown using modified growth medium (MGM2) consisting of 18.8% (w/v) NaCl, 4.3% (w/v) $MgSO_4.7H_2O$, 0.25% (w/v) KCl, 0.07% (w/v) $CaCl_2.2H_2O$, 50 mM Tris-HCl (pH 7.2), 0.5 % (w/v) bacto-tryptone, and 0.3 % (w/v) bacto-yeast extract (Cline *et al.*, 1989). The media were distributed into 250 ml bottles in 50 ml aliquots; some were supplemented with 0.7% arginine, others with 50 mM sodium nitrate (Soppa, 1998), some with both, and the remaining left with no supplementation. The bottles were sealed with rubber septa and autoclaved. The bottles were inoculated using a sterile syringe with a starting culture of aerobically

grown *Hfx. volcanii* in MGM2 with no supplement when OD_{600nm} ~ 1. Then the cultures were flushed with nitrogen for 15-20 min and the bottles were incubated at 42°C at 50 rpm. Growth was monitored by withdrawing a sample with a syringe while flushing with nitrogen.

4.3.2.3 Gel filtration

In the case of *Hfx. volcanii* cell extracts analytical gel filtration was performed on an Amersham Biosciences Äkta FPLC system, using a Superdex 200 10/300GL column equilibrated with 2 M KCl or NaCl, 50 mM Tris HCl (pH 8.0), and 1 mM EDTA at a flow rate of 0.5 ml/min. For gel filtration of *E. coli* extracts, the KCl or NaCl concentration was reduced to 0.1 M.

4.4 Results

4.4.1 Growth characteristics of *Hfx. volcanii*

It has been found that during the growth of *Hfx. volcanii* the high salinity of the medium decreased the risk of contamination by nonhalophilic microorganisms. However, some moulds could grow but only after a long incubation time. Therefore, although very strict sterility may not be needed (Kushner, 1966; Oesterhelt and Stoeckenius, 1974) all the work has been done aseptically. *Hfx. volcanii* grows optimally at 42°C. It is an aerobic archaeon but oxygen solubility is known to decrease with increasing temperature and salinity. Therefore increasing the speed of the rotation by shaking to 200 rpm enhanced growth. Colour intensity of the pigmentation of *Hfx. volcanii* was found to increase with time in light conditions although growth does occur in the dark. The carotenoid content of the cells was shown to be decreased dramatically when the salt concentration of the growth medium increased (Rodriguez-Valera *et al.*, 1983). However, in other extreme halophiles it was found that their pigmentation increased at higher salt concentration (Kushwaha *et al.*, 1982). Since pigments may protect against the lethal effects of visible light, these results could explain why slow-growing extreme halophiles come to predominate at higher salt concentrations (Rodriguez-Valera *et al.*, 1983).

Also, agar plates were prepared more thickly and incubated wrapped in plastic in order to avoid dryness and formation of salt crystals (Figure 4.1).

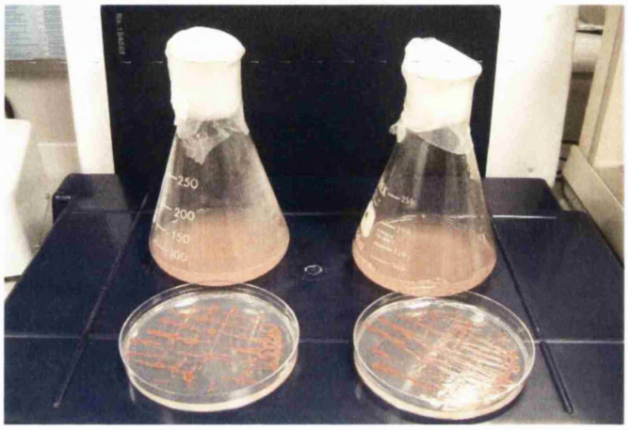

Figure 4.1: *Hfx. volcanii* growth in liquid and solid MGM1 media.

4.4.2 Growth and activity studies of *Hfx. volcanii*

4.4.2.1 Growth studies in MGM1 Medium

Testing growth of *Hfx. volcanii* in complex media containing 18% and 25% (w/v) of the total salts showed that it could grow in both with slightly better growth at 18% salt (Figure 4.2). The generation time (the time required for the population to double) was 3-5 hours and the growth rate was 0.2 generation/hour (Figure 4.3). Thus, this organism has a relatively long generation time, compared to other microorganisms such as *E. coli* that have a 12-17 min doubling time. Growth was monitored by measuring the growth (turbidity) at a wavelength of 600 nm since it is away from the 400-500 nm range of carotenoid colour absorbance

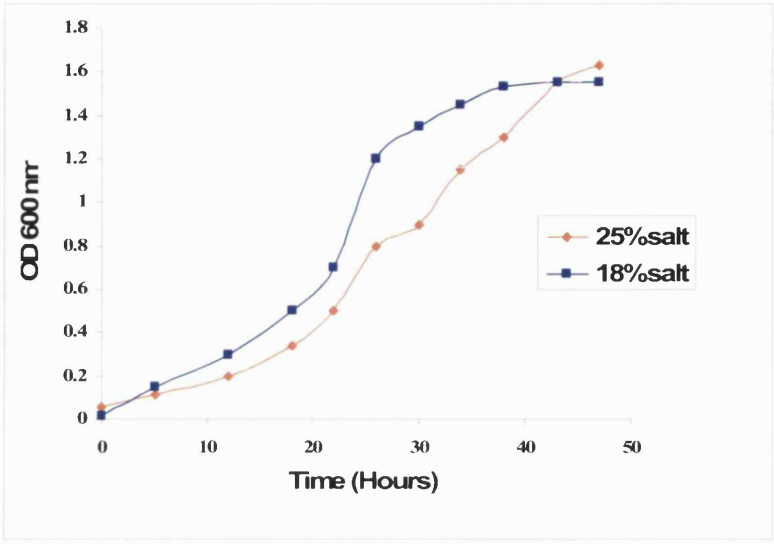

Figure 4.2: Growth profile of *Hfx. volcanii* in MGM1 media.

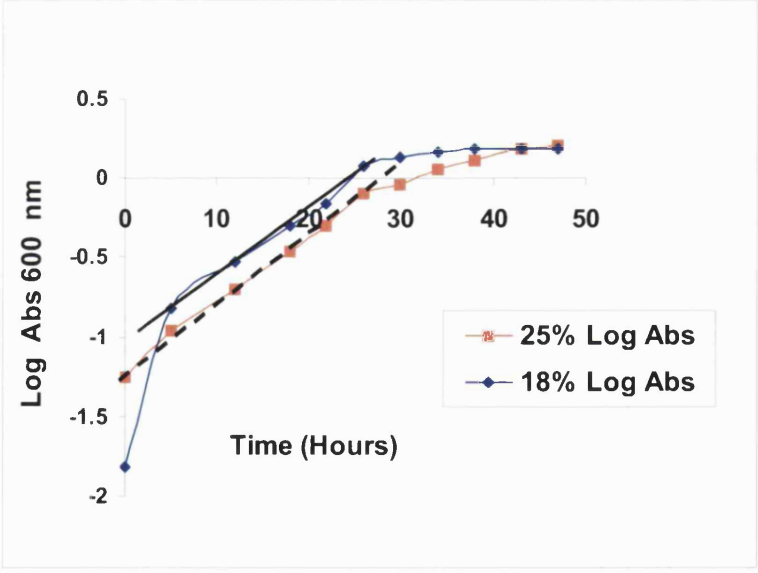

Figure 4.3: Generation time of *Hfx. volcanii* in 25% and 18% salt concentration.
Generation time in 18% [salt] = LN2/ slope = 4.8 hours.
Growth rate in 18% [salt] = 1/generation time = 0.2 generation/hour.

4.4.2.2 Enzyme activity studies of *Hfx. volcanii* grown in MGM1 medium

DHlipDH, citrate synthase, E1 and whole complex activities were monitored at various times during the growth of *Hfx. volcanii* in MGM1 medium. In the present study, DHlipDH specific activity of *Hfx. volcanii* growing in 2 M NaCl was 0.22 (U/mg) in the cell extract and citrate synthase specific activity was 0.35 (U/mg) (Table 4.1 (p.69), Figure 4.4 and Figure 4.5). However, other groups had found that DHlipDH specific activity was 0.01 (U/mg) (Vettakkorumakankav *et al.*, 1992) while citrate synthase from *Hfx. volcanii* had an optimal activity between 1 M and 3 M NaCl and its specific activity was 0.08 (U/mg) in the cell extract (James *et al.*, 1994). These differences may be due to variation in medium content or incubation conditions.

It is clear that the DHlipDH activity increased 3 fold during growth and the citrate synthase activity almost doubled (Figure 4.4 and 4.5). Moreover, neither E1 nor any complex activity could be detected when assayed with any of the 2-oxoacid substrates during the growth of *Hfx. volcanii* in MGM1 medium.

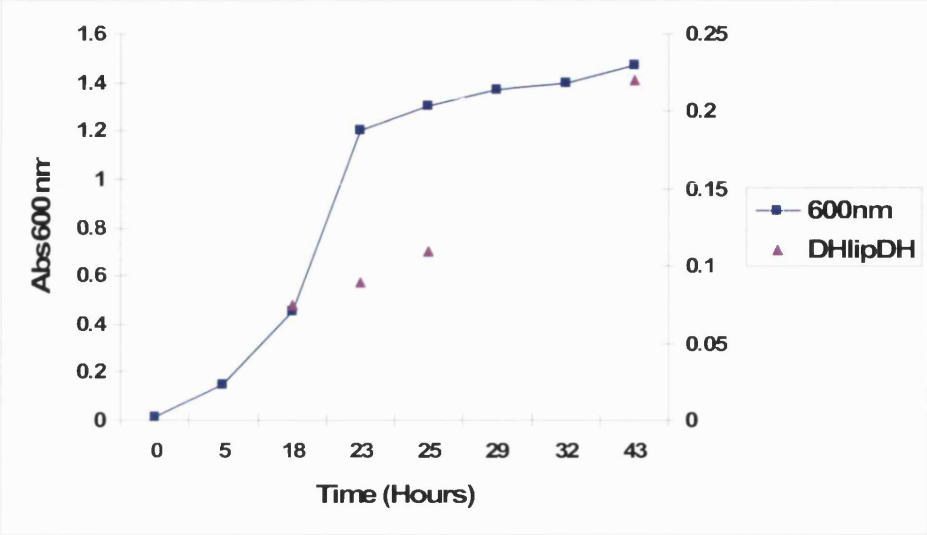

Figure 4.4: Growth of *Hfx. volcanii* in MGM1 and DHlipDH activity.
Y2-axis is DHlipDH specific activity (U/mg).

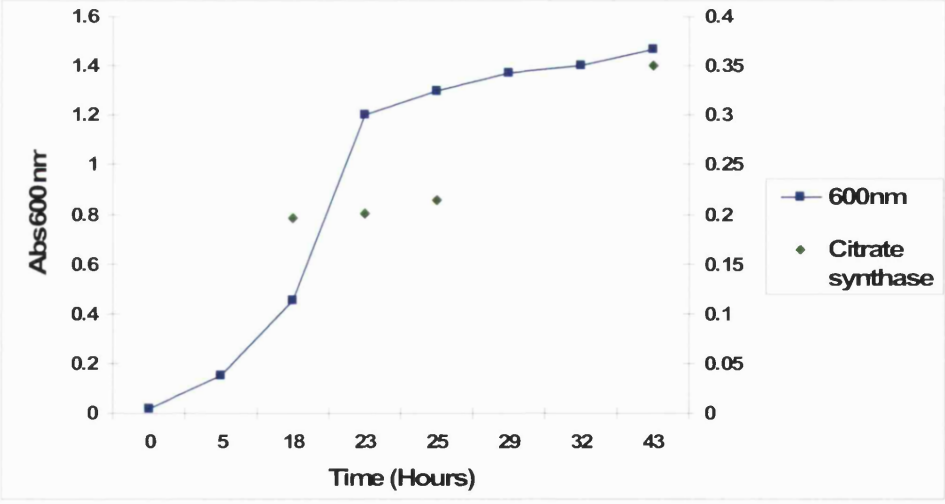

Figure 4.5: Growth of *Hfx. volcanii* in MGM and citrate synthase activity.
Y2-axis is citrate synthase specific activity (U/mg).

4.4.2.3 Growth studies of *Hfx. volcanii* using different carbon sources

In an attempt to increase the expression of the OADHC in *Hfx. volcanii,* a variety of carbon sources were chosen according to their entry positions in the pathways of central metabolism (Figure 4.6).

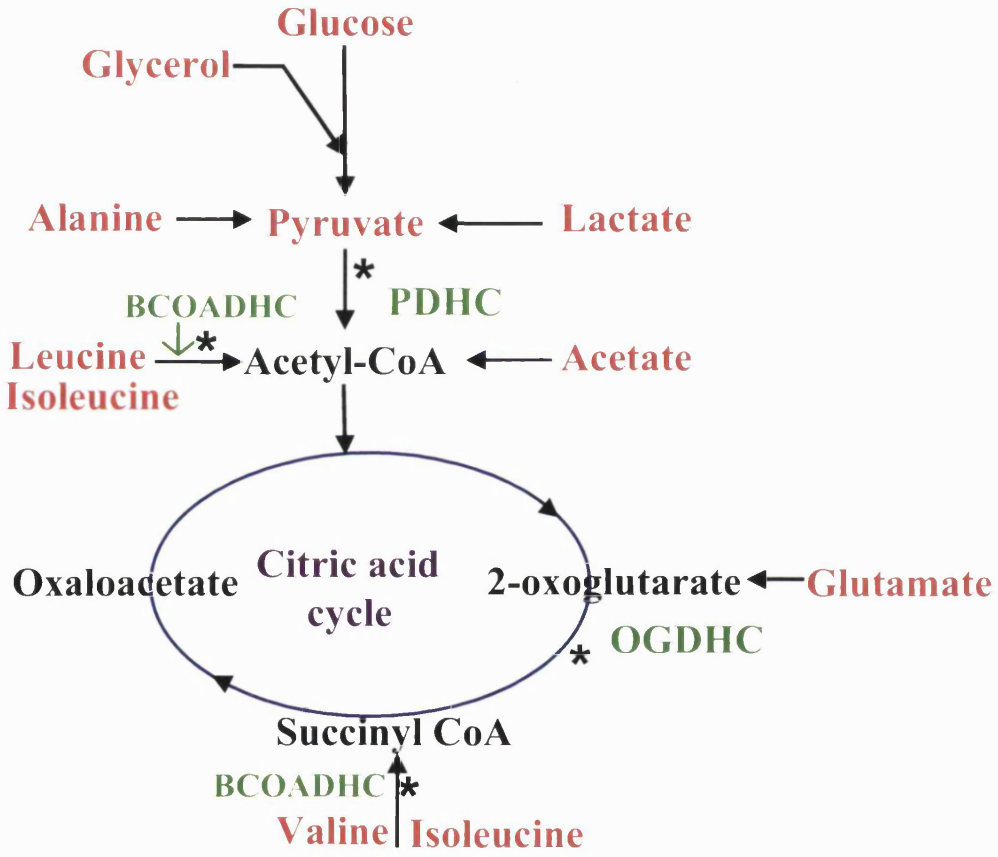

Figure 4.6: Central Metabolic pathways.

***Shows where the 2-oxoacid dehydrogenase multienzyme complexes have a metabolic role in aerobic bacteria and eukaryotes.**
PDHC: Pyruvate dehydrogenase complex, OGDHC: 2-Oxoglutarate dehydrogenase complex and BCOADHC: Branched-chain 2-oxoacid dehydrogenase complex.

Table 4.1 summarises the growth density of *Hfx. volcanii* on different carbon sources. Growth on glucose, glycerol and pyruvate seemed to be as good as in a complex

medium (Figures 4.7, 4.8, 4.9 and 4.10). On the other hand, on alanine, acetate, citrate, lactate and glutamate, *Hfx. volcanii* took a longer time to grow, with glutamate, alanine and citrate producing the longest generation time (Figures 4.11 and 4.12). Its growth seemed to be poorer (less turbidity) in a minimal medium than in MGM1, yet in both minimal and complex media, OD_{600nm} ~1.4 at the maximum.

The pH of the minimal media was found to start at pH 7.7. However, despite the presence of buffers in the medium, the pH dropped slightly during *Hfx. volcanii* growth using glucose and glycerol. This was presumably due to acid production during metabolism. $NaHCO_3$ (0.5%) was added to the minimal medium with glucose and glycerol but no difference in growth intensity was observed (Figure 4.13). This result agrees with an earlier study that found $NaHCO_3$ partly prevented the pH drop and allows very limited growth (Kauri *et al.*, 1990).

Different concentrations of glucose and glycerol (0.25% and 0.5%) were used but no significant differences in growth or in enzyme activity were recorded (Figures 4.7, 4.8, 4.9, 4.10 and 4.13). However, in the case of sodium citrate there was no growth with a concentration of 0.25% but there was significant growth and activity when the concentration increased to 0.5%.

Moreover there was no growth, or only a negligible one, on the branched-chain amino acids L-leucine (0.3%), L-isoleucine (0.3%) and L-valine (0.25%). However, after a prolonged incubation of 8-12 days, the OD_{600nm} reached ~ 0.4 with isoleucine and leucine, while with valine it took longer and reached an OD_{600nm} = 0.1 after which growth started to decline again. Moreover, subculture into new media was carried out but no growth subsequently occurred.

Another attempt was made to grow *Hfx. volcanii* on branched-chain amino acids using a slight modification from the above procedure by using a different starting culture: *Hfx. volcanii* grown under intense light on complex medium Hv-YPC as described in Chapter 5 (Section 5.3.2.7), which contains 0.17% (w/v) Casamino Acids and a higher salt concentration than MGM1. The growth was higher and faster with each of the branched-chain amino acids than in the previous trial. The growth was fastest with isoleucine, reaching an OD_{600nm} = 1.3 after 3 days, while with leucine the growth reaches OD_{600nm} ~ 1 after 5 days; with valine growth was the slowest reaching

OD_{600nm}= 0.5 after five days. To validate these results, a starting culture of Hv-YPC lacking Casamino Acids was used and the growth was found to be slower and pass through a longer lag phase than the growth in Hv-YPC medium with Casamino Acids. Generally, it decreased two fold compared to Hv-YPC with Casamino Acids. These results coincide with another study which found that both ribosome content and the growth rate were more than two fold higher in *Hfx. volcanii* cells growing exponentially on Casamino Acids compared with cells growing on glucose (Zaigler *et al.*, 2003).

Finally, attempts were made to stimulate the growth of *Hfx. volcanii* on certain carbon sources by the addition of lipoic acid. It was found that there is no difference in the growth with or without lipoic acid (Table 4.1).

4.4.2.4 Enzyme activity studies of *Hfx. volcanii* grown on different carbon sources

Table 4.1 summarizes the growth density and enzymic activity of *Hfx. volcanii* growing on different carbon sources. Since prokaryotes lack mitochondria, as also do some eukayotes such as *Trypanosoma brucei*, DHlipDH may sometimes be found to be specifically associated with the plasma membrane (Danson *et al.*, 1987). For this reason, cell extracts were prepared by sonication as mention in Chapter 2 and also using a French press, which it is less disruptive than sonication; however, no difference in enzymic activity was observed between the extracts prepared using the two methods.

When *Hfx. volcanii* was grown on a sole carbon source, the starting culture was grown in MGM1, but for the second trial of growth with only glucose, pyruvate, branched-chain amino acids or complex medium, Hv-YPC was used for the growth of *Hfx. volcanii* as starting cultures. These results are shown in table 4.1. The use of Hv-YPC as a starting culture led to an increase in the activity of both DHlipDH and citrate synthase compared to MGM1. Using isoleucine as an example to detect the effect of Casamino Acids presence in Hv-YPC, it can be concluded that the presence of Casamino Acids leads to an increase in enzymic activity. This could be the cause of the growth and increase of enzymic activity when *Hfx. volcanii* was grown in a synthetic media with one of the branched-chain amino acids. The Casamino Acids may

prepare the cells to grow on branch-chain amino acids and the effect could be also due to a higher salt concentration in Hv-YPC medium than in MGM1. Table 4.2 describes the growth density with certain carbon sources such as MGM1, pyruvate, glucose and branched-chain amino acids, using MGM1 as starting culture. The results show slower growth density and even no growth with valine compared with growth using Hv-YPC as starting culture. Also lower DHlipDH and citrate synthase activity than with the one using Hv-YPC as starting culture was observed. However, the ratio of DHlipDH to citrate synthase activity shows no large differences between the two media as a starting culture.

Moreover, using different concentrations of glycerol (0.25% and 0.5%) gave no difference in enzymic activity. Also, during the long generation time with alanine, both enzymic activities tend to increase at the beginning of growth then the activities decrease along with growth (Figures 4.11 and 4.12). There was no significant increase in the DHlipDH activity with any of the carbon sources and always citrate synthase activity doubled the activity of DHlipDH. In contrast, the growth of *Hfx. volcanii* on branched-chain amino acids led to a significant increase in DHlipDH activity compared to citrate synthase. Also, the ratio of DHlipDH to citrate synthase increased 2-3 fold.

Additionally, no difference resulted from the addition of lipoic acid to the medium in terms of the growth density or to enzymic activity. Thus, the addition of lipoic acid is of no importance to the expression of DHlipDH.

To summarise, the only growth conditions that lead to a rise of the DHlipDH-citrate synthase ratio are branched-chain amino acids. Also, it has been found that Hv-YPC medium is better to generate a starter culture than MGM1 due to the presence of casamino acids. No overall OADHC of *Hfx. volcanii* or E1 activity could be detected under any of the growth conditions.

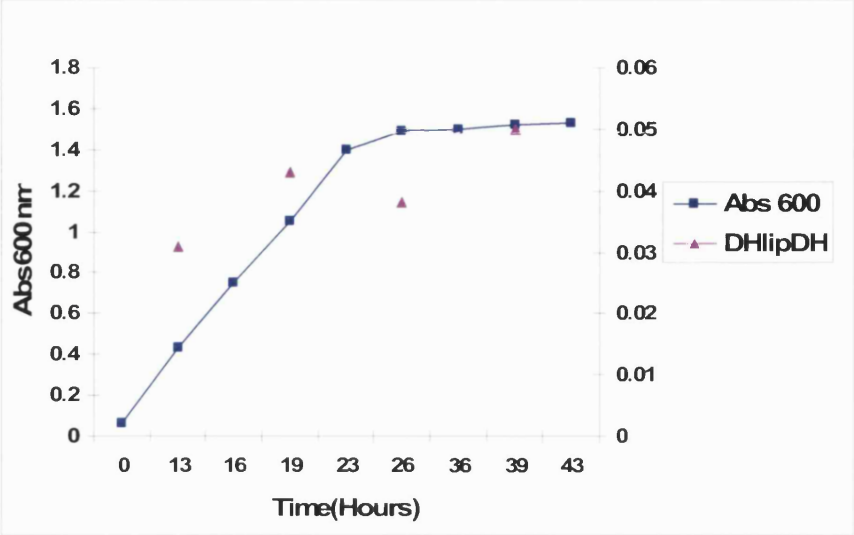

Figure 4.7: Growth and DHlipDH specific activity of *Hfx. volcanii* on 0.25% glycerol.
Y2-axis is DHlipDH specific activity (U/mg).

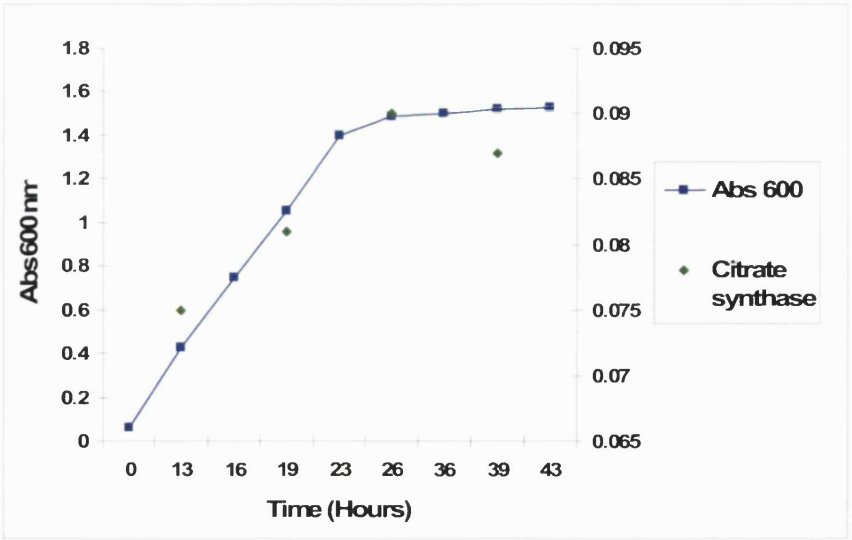

Figure 4.8: Growth and citrate synthase specific activity of *Hfx. volcanii* on 0.25% glycerol.
Y2-axis is citrate synthase specific activity (U/mg).

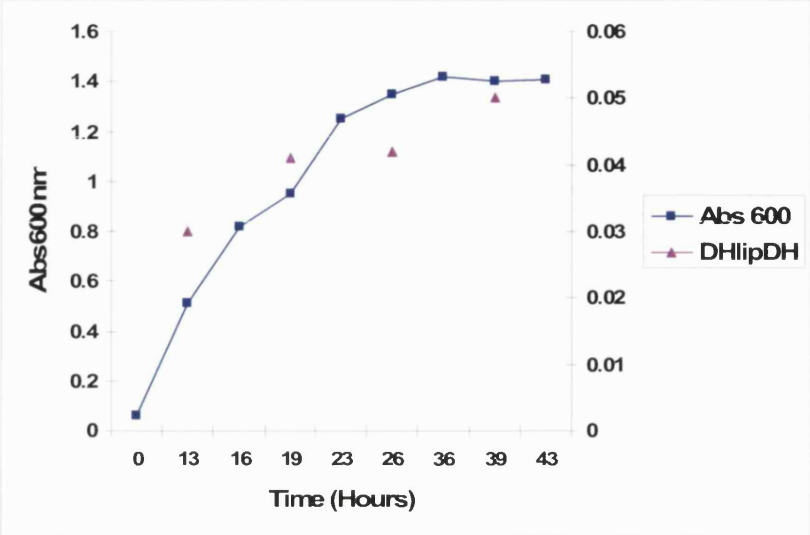

Figure 4.9: Growth and DHlipDH specific activity of *Hfx. volcanii* on 0.5% glycerol.
Y2-axis is DHlipDH specific activity (U/mg).

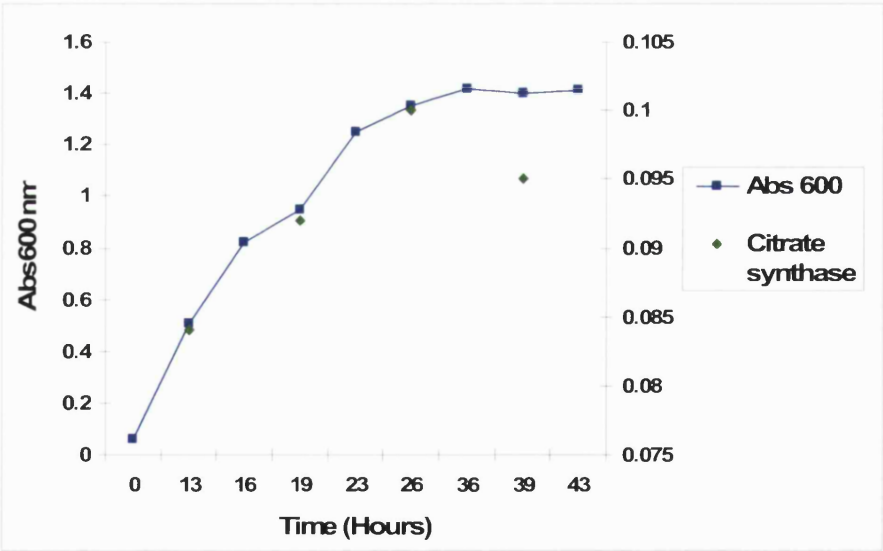

Figure 4.10: Growth and citrate synthase specific activity of *Hfx. volcanii* on 0.5% glycerol.
Y2-axis is citrate synthase specific activity (U/mg).

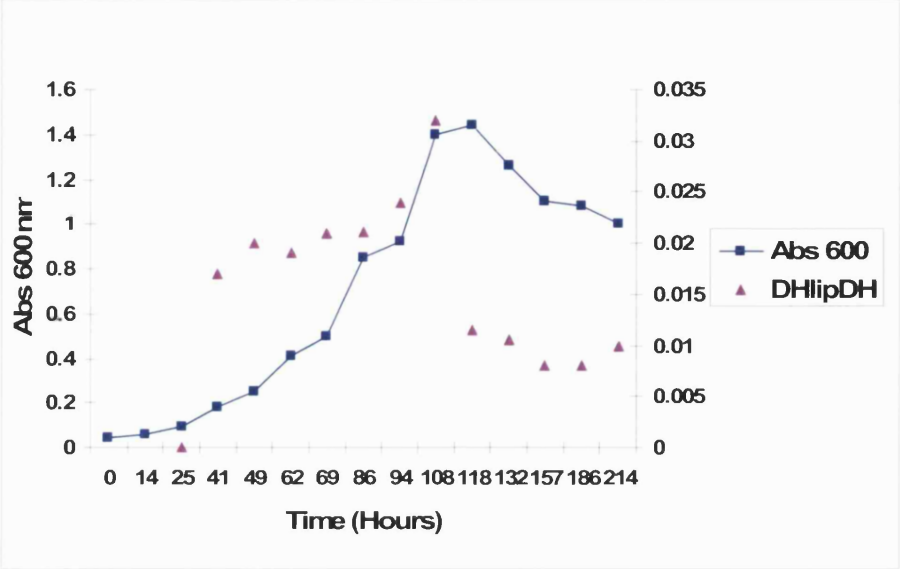

Figure 4.11: Growth and DHlipDH specific activity of *Hfx. volcanii* on 0.25% alanine.
Y2-axis is DHlipDH specific activity (U/mg).

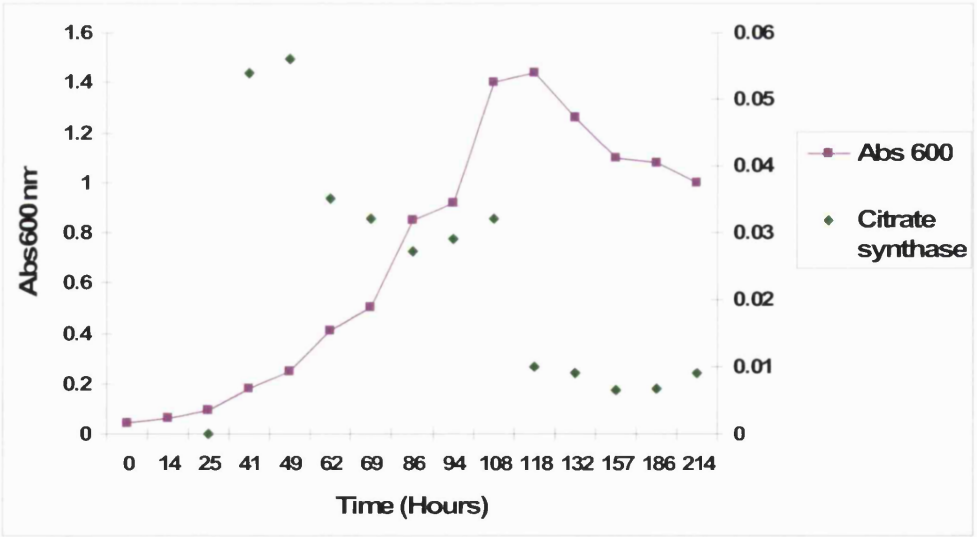

Figure 4.12: Growth and citrate synthase specific activity of *Hfx. volcanii* on 0.25% alanine.
Y2-axis is citrate synthase specific activity (U/mg).

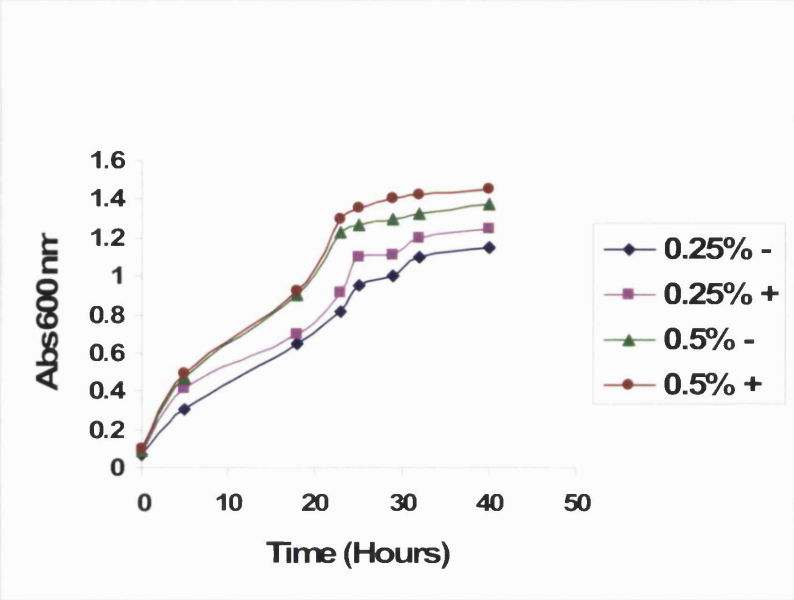

Figure 4.13: Growth of *Hfx. volcanii* using different concentrations of glucose, ±$NaHCO_3$.

Table 4.1: Growth of *Hfx. volcanii* on a variety of carbon sources.

C source	Growth density	DHlipDH *[1]	CS activity*[1]	DHlipDH: CS*[2]
MGM1	+++	**0.22**	**0.35**	**0.63**
MGM1 (+lip)	+++	**0.20**	**0.32**	**0.63**
Pyruvate	+++	**0.20**	**0.40**	**0.5**
Pyruvate (+lip)	+++	**0.35**	**0.65**	**0.54**
Glucose	+++	**0.25**	**0.50**	**0.50**
Glucose (+lip)	+++	**0.30**	**0.60**	**0.50**
Glycerol	+++	**0.05**	**0.10**	**0.50**
Acetate	++	**0.40**	**0.70**	**0.57**
Glutamate	+	**0.03**	**0.12**	**0.25**
Citrate	+	**0.02**	**0.02**	**1.13**
Alanine	++	**0.03**	**0.06**	**0.50**
Lactate	+	**0.10**	**0.35**	**0.29**
Isoleucine	+++	**0.93**	**0.62**	**1.50**
Isoleucine (+lip)	+++	**0.85**	**0.65**	**1.30**
Ile no casa	++	**0.71**	**0.57**	**1.25**
Ile no casa (+lip)	++	**0.64**	**0.64**	**1.00**
Leucine	++	**0.90**	**0.65**	**1.38**
Leucine (+lip)	++	**0.80**	**0.58**	**1.21**
Valine	+	**0.70**	**0.55**	**1.27**
Valine (+lip)	+	**0.60**	**0.49**	**1.22**

*[1]Activity expressed in U/mg protein, measured at late log phase of growth at OD_{600nm} between 0.9-1.1.
CS: Citrate synthase.
*[2] Specific activity ratio of DHlipDH to citrate synthase.
(+lip): lipoic acid was added to the medium.
Ile no casa: isoleucine-using Hv-YPC as starting culture lacking casamino acids.
+++ (OD_{600nm} > 1), ++ (OD_{600nm} 0.5-1) and + (OD_{600nm}< 0.5).

Table 4.2: *Hfx. volcanii* growth pattern and enzymic activity of certain carbon sources using MGM1 as starting culture.

C source	Growth density	DHlipDH *[1]	CS activity*[1]	DHlipDH: CS*[2]
MGM1	+++	**0.17**	**0.39**	**0.44**
Pyruvate	++	**0.08**	**0.19**	**0.39**
Glucose	++	**0.06**	**0.19**	**0.31**
Isoleucine	++	**0.56**	**0.42**	**1.33**
Leucine	+	**0.50**	**0.37**	**1.19**
Valine	—	—	—	—

*[1]Activity expressed in U/mg protein, measured at late log phase of growth at OD_{600nm} between 0.9-1.1.
CS: Citrate synthase.
*[2] Specific activity ratio of DHlipDH to citrate synthase.
+++ (OD_{600nm} > 1), ++ (OD_{600nm} 0.5-1) and + (OD_{600nm}< 0.5).

4.4.2.5 Growth of *Hfx. volcanii* anaerobically

In the first trial to grow *Hfx. volcanii* anaerobically (under N_2 gas) using MGM1 or minimal medium with addition of 50 mM $NaNO_3$, no growth occurred. The reason for this is unclear, although it is possible that the medium lacks some vitamins or trace elements that are needed only under anaerobic respiration (personal communication, Prof. Jorg Soppa, Geothe University, Frankfurt, Germany).

The second trial of anaerobic growth was with MGM2. Growth was highest with MGM2 plus $NaNO_3$ (OD_{600nm} = 0.488), less with MGM2 plus $NaNO_3$ and arginine (OD_{600nm} = 0.35) but even less with MGM2 (OD_{600nm} =0.09) only or MGM2 plus arginine (OD_{600nm} = 0.11); these readings were taken after almost 250 h (Figure 4.14 and Table 4.3). This represents the importance of $NaNO_3$ in anaerobic growth as it functions as a terminal electron acceptor. On the other hand, the DHlipDH activity under anaerobic growth was found to be always lower than citrate synthase activity except with $NaNO_3$, where DHlipDH activity was little higher.

In parallel the same experiment was performed aerobically and growth was excellent reaching (OD_{600nm} = 1.3) within 64 h using MGM2 medium only or by the addition of arginine, $NaNO_3$ or both together (Figure 4.15 and Table 4.4). The enzymic activities were monitored for both anaerobic and aerobic growth; both DHlipDH and citrate synthase specific activities tend to be higher under anaerobic condition growth than aerobic. Also, the ratio of DHlipDH to citrate synthase specific activity was always found to be < 1 under both conditions, except with $NaNO_3$ anaerobically, it was > 1, which indicates an increase of expression of DHlipDH during the growth of *Hfx. volcanii* anaerobically with $NaNO_3$.

As with the aerobic cultivation no complex activity or E1 activity could be detected. It could be concluded that the anaerobic growth does not increase the expression of DHlipDH or complex activity except with anaerobic growth with $NaNO_3$ that had led to an increase in DHlipDH expression, but no complex activity could be detected.

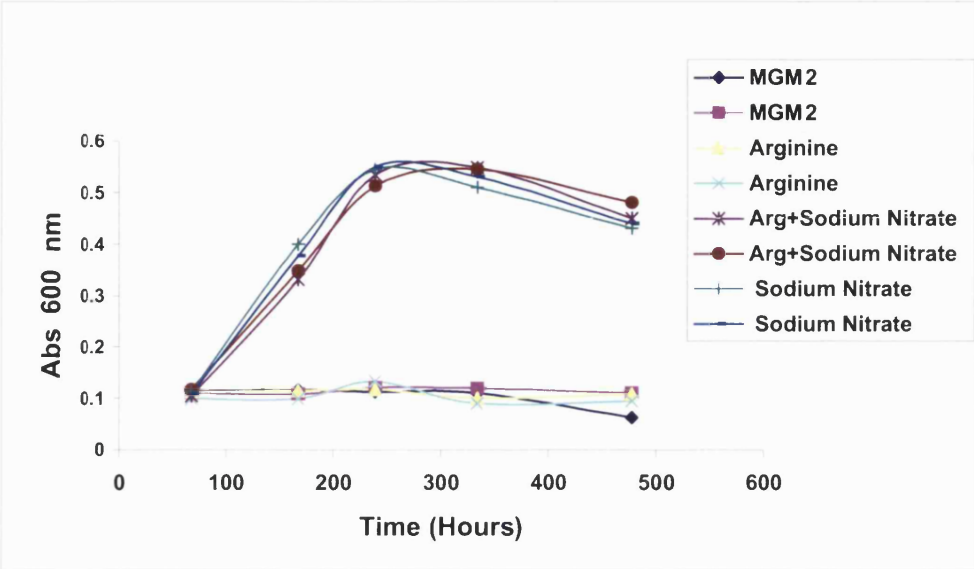

Figure 4.14: Growth of *Hfx. volcanii* anaerobically in MGM2.
Each trial was performed twice, MGM2: modified growth medium. Arginine: MGM2 with arginine only. Arg + Sodium Nitrate: MGM2 with arginine and $NaNO_3$. Sodium Nitrate: MGM2 with $NaNO_3$ only.

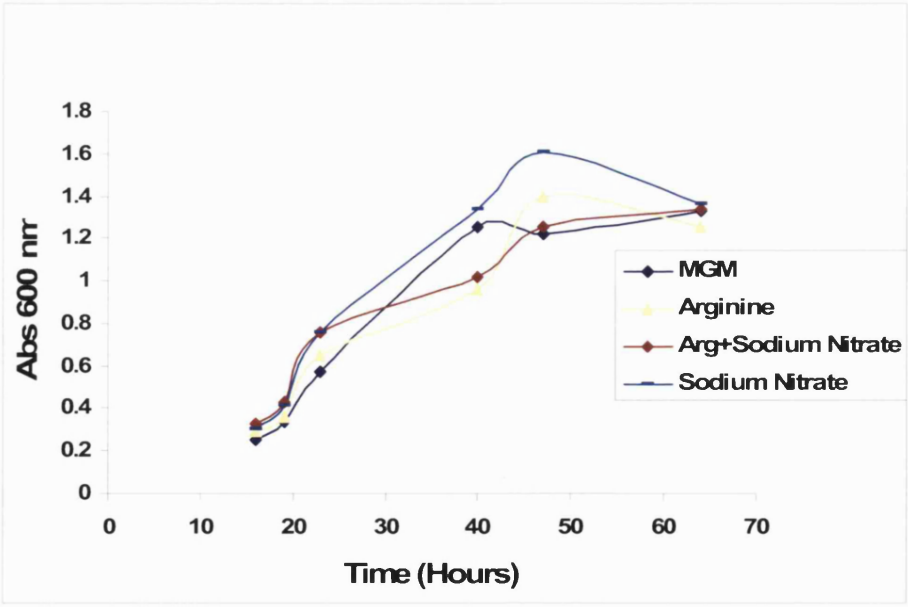

Figure 4.15: Growth of *Hfx. volcanii* aerobically in MGM2.
MGM2: modified growth medium. Arginine: MGM2 with arginine only. Arg + Sodium Nitrate: MGM2 with arginine and $NaNO_3$. Sodium Nitrate: MGM2 with $NaNO_3$ only.

Table 4.3: *Hfx. volcanii* anaerobic growth pattern and enzymic activity growing in MGM2.

C source	Growth density	DHlipDH *[1]	CS activity*[1]	DHlipDH: CS*[2]
MGM2	+	**0.15**	**0.31**	**0.48**
Arginine	+	**0.22**	**0.32**	**0.66**
Arg + NO_3^-	++	**0.29**	**0.53**	**0.54**
$NaNO_3$	++	**0.35**	**0.30**	**1.16**

MGM2: modified growth medium. Arginine: MGM2 with arginine only. Arg + NO_3^-: MGM2 with arginine and $NaNO_3$. $NaNO_3$: MGM2 with $NaNO_3$ only.
*[1]Activity expressed in U/mg protein, measured at late log phase of growth at OD_{600nm} between 0.9-1.1.
CS: Citrate synthase.
*[2] Specific activity ratio of DHlipDH to citrate synthase.
+++ (OD_{600nm} > 1), ++ (OD_{600nm} 0.5-1) and + (OD_{600nm}< 0.5).

Table 4.4: *Hfx. volcanii* aerobic growth pattern and enzymic activity growing in MGM2.

C source	Growth density	DHlipDH *[1]	CS activity*[1]	DHlipDH: CS*[2]
MGM2	+++	**0.05**	**0.04**	**0.75**
Arginine	+++	**0.02**	**0.05**	**0.40**
Arg + NO_3^-	+++	**0.03**	**0.05**	**0.60**
$NaNO_3$	+++	**0.03**	**0.05**	**0.60**

MGM2: modified growth medium. Arginine: MGM2 with arginine only. Arg + NO_3^-: MGM2 with arginine and $NaNO_3$. $NaNO_3$: MGM2 with $NaNO_3$ only.
*[1]Activity expressed in U/mg protein, measured at late log phase of growth at OD_{600nm} between 0.9-1.1.
CS: Citrate synthase.
*2 Specific activity ratio of DHlipDH to citrate synthase.
+++ (OD_{600nm} > 1), ++ (OD_{600nm} 0.5-1) and + (OD_{600nm}< 0.5).

4.4.2.6 Gel filtration

Since the activity of the *Hfx. volcanii* OADHC could not be detected with any of the carbon sources, the concentrated cell extract was passed through an analytical gel filtration column to see if DHlipDH is associated with any complex or if it is free in solution. The recovered fractions were assayed for DHlipDH, citrate synthase and OADHC activity.

The cell extracts of *Hfx. volcanii* growing on isoleucine, acetate and anaerobically with $NaNO_3$ were chosen for their high activity of DHlipDH. As presented in Figure 4.16, the gel filtration resulted in a single DHlipDH peak, which shows the dimeric enzyme ($M_r \approx 119{,}000$) (Danson *et al.*, 1984) to be unassociated with any other protein. As usual, citrate synthase activity was measured as it is used as a molecular weight marker; citrate synthase is a homodimer with a total relative molecular mass (M_r) of approximately 86,000 (James *et al.*, 1994). It has been found that with anaerobic growth both enzymic activities recovered from the gel filtration were very low compared to the activity recovered from samples grown aerobically on acetate and isoleucine.

Figure 4.17 shows gel filtration data of an *E. coli* cell extract, prepared in the same manner as for *Hfx. volcanii*. The filtration resulted in 3 peaks of DHlipDH activity. One was associated with PDHC activity and another represent the uncomplexed DHlipDH at $M_r \approx 100{,}000$. A third peak eluted in the void volume and may represent membrane-associated DHlipDH or aggregated material. In *E. coli* the citrate synthase is a hexameric enzyme of $M_r \approx 270{,}000$, and elutes between free and complex E3.

In conclusion, no complexed DHlipDH could be detected using cell extracts of *Hfx. volcanii* compared with *E. coli* extract; only free DHlipDH is recovered. Also, none of the growth conditions that have been used led to the detection of complex activity or complexed DHlipDH.

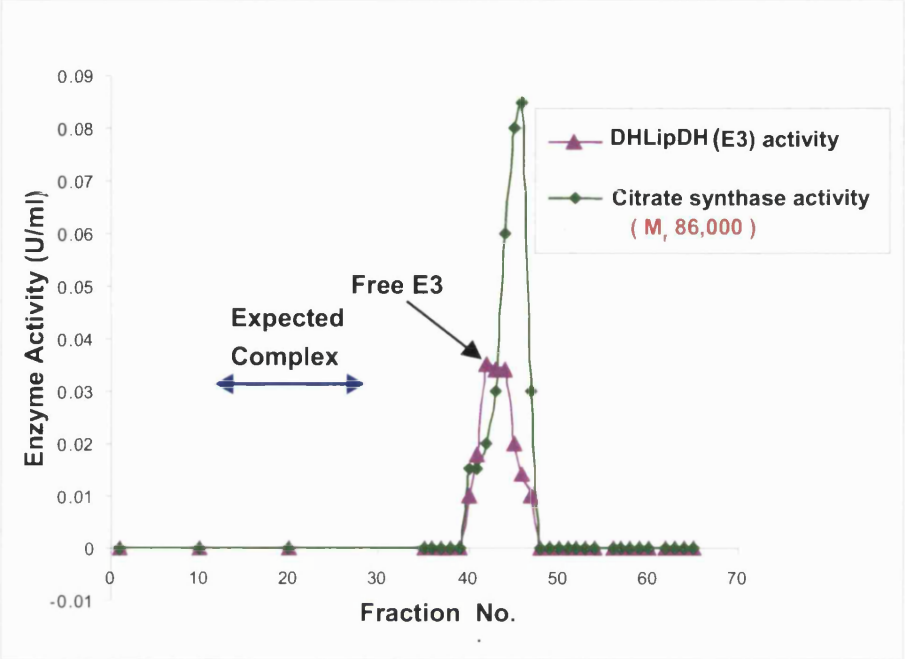

Figure 4.16: Gel filtration of *Hfx. volcanii* cell extract.

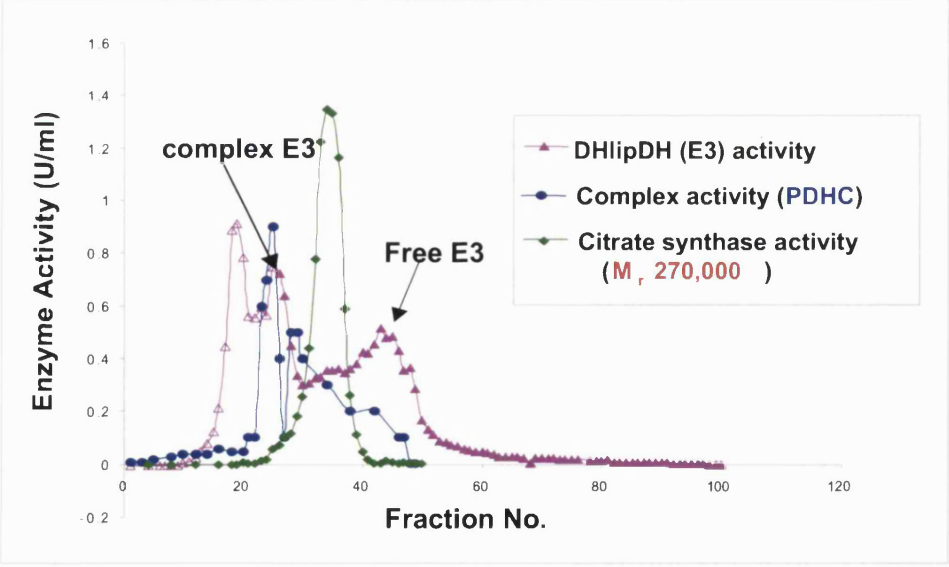

Figure 4.17: Gel filtration of *E. coli* cell extract.

4.5 Discussion

The main objective of this chapter was to see if the putative OADHC could be induced by growing *Hfx. volcanii* under different nutrient conditions, and whether these also lead to an increase in DHlipDH expression.

Firstly, the optimal salt conditions for growth of *Hfx. volcanii* were tested. The optimum salt concentration for growth varies between different halophilic archaea (ranging between 15% to 25%) but most will grow at 23% (w/v) total salt. It has been found that *Hfx. volcanii* grows optimally at 18% salt concentration.

Growth of *Hfx. volcanii* on different carbon sources did not lead to the detection of OADHC or E1 activity with any of the known substrates. The activity of DHlipDH was detected in all carbon sources, with no significant activity increase except a slight increase during growth on acetate and a significant increase with branched-chain amino acids. The metabolism of acetate is through the glyoxylate cycle. This cycle has some enzymes in common with the citric acid cycle but there are two exclusive enzymes: isocitrate lyase and malate synthase. These have been detected in *Hfx. volcanii* and their activity increased when the carbon source was acetate (Oren and Gurevich, 1995; Serrano *et al.*, 1998).

Although previously *Hfx. volcanii* had failed to grow on branched-chain amino acids (Jolley *et al.*, 1996b), in this study growth was achieved. Growth on branched-chain amino acids generally, and isoleucine especially, led to a significant increase of DHlipDH activity compared to other carbon sources, but no whole complex activity could be detected. It has been shown that DHlipDH from kidney mitochondria dissociates more readily from the branched-chain 2-oxoacid dehydrogenase complex than from pyruvate and 2-oxoglutarate dehydrogenase complexes. Even in cell extracts of kidney mitochondria that contain uncomplexed DHlipDH, the branched-chain 2-oxoacid dehydrogenase activity is stimulated 2 to 3 fold by the addition of DHlipDH (Pettit *et al.*, 1978). Although the DHlipDH activity increased significantly during growth of *Hfx. volcanii* on branched-chain amino acids, no complex activity could be detected, and therefore it might be worth trying the addition of purified *Hfx. volcanii* DHlipDH to overall complex assays.

Furthermore, one study has found that the presence of branched-chain amino acids in the growth medium resulted in only small increases (1.3-1.7 fold) in *Enterococcus faecalis* gene expression, compared to 1.7 to an almost 4-fold increase in gene expression when grown with branched-chain 2-oxoacids (Ward *et al.*, 1999; Ward *et al.*, 2000). Therefore, since in the present study the growth of *Hfx. volcanii* on branched-chain amino acids led to a significant increase in DHlipDH activity but with no active complex, it is worth trying to grow *Hfx. volcanii* on branched-chain 2-oxoacids.

Another attempt to stimulate the activity of DHlipDH was through the addition of lipoic acid to the growth medium of *Hfx. volcanii* with certain carbon sources. Lipoic acid forms an important component of the E2-lipoyl domain of the OADHCs, and in *E. coli* it can be synthesized endogenously or scavenged from the environment (Miller *et al.*, 2000). Given the incomplete nature of the *Hfx. volcanii* genome, it is not known if the lipoic acid is supplied by endogenous and/or exogenous pathways. However, in the case of *Hfx. volcanii* no difference in growth intensity or in the enzyme activity was detected in the presence of lipoic acid.

Additionally, anaerobic growth of *Hfx. volcanii* was performed but no significant increase in growth or enzymic activity of either DHlipDH or complex activity could be measured, except with the addition of sodium nitrate to MGM2 that led to an increase in DHlipDH compared to the internal marker enzyme. However, no OADHC activity could be detected.

Since the activity of the *Hfx. volcanii* OADHC could not be detected with any of the carbon sources or growth conditions, a cell extract was passed through an analytical gel filtration column to detect if the expressed DHlipDH is associated with any complex or if it is free in solution. Only free DHlipDH could be identified compared with *E. coli* extract.

It should be noted that a gene encoding an E1 subunit of OADHC was induced in *Hfx. volcanii* in a glucose medium (Zaigler *et al.*, 2003). This E1 gene differs from the E1 genes of the operon concerned with the present investigation in this thesis (Jolley *et al.*, 2000; Wanner and Soppa, 2002); also the gene is not associated with an E2 gene and no specific function of the expressed protein has been detected. Thus *Hfx.*

volcanii encodes at least three different E1 proteins. However, due to the absence of a complete genome sequence of *Hfx volcanii*, further conclusions are not possible.

The question of why no OADHC activity can be detected in halophilic archaea remains unresolved. As previously confirmed in Chapter 3, the genes of OADHC are transcribed as an operon, although the level of transcription has not been determined. It has been found that a low mRNA level might accompany reduced translational efficiency because decreased ribosomal protection of mRNA will increase its exposure to endonucleases (Gustafsson *et al.*, 2004; Wu *et al.*, 2004). Also, in various eukaryotic organisms, small RNAs can induce DNA methylation and/or heterochromatin (i.e., transcriptional silencing) at the homologous genomic locus (Matzke and Birchler, 2005). Moreover, it could be that the complex is transcribed but only E3 is expressed, or that whole complex is produced but it is unstable to the conditions used to lyse the *Hfx. volcanii* cells. Finally, it may be that the true 2-oxoacid substrate has not yet been found and thus no activity is being detected.

Consequently, it was decided that homologous expression should be performed to determine if the genes can be transcribed and translated into an active enzyme *in vitro* and then to determine substrate specificity if they are active. This is described in Chapter 5.

Homologous expression in Hfx. volcanii

5.1 Introduction

Expression of halophilic proteins in the native organism has potential advantages over expression in *E. coli*. Despite the advantages of using *E. coli*, such as rapid growth, high biomass levels and its well-known and developed genetics, there may be difficulty in expressing halophilic genes in a low ionic strength internal environment that can lead to problems with protein folding, activity and stability. Our group found that the yields of *E. coli*-expressed halophilic enzymes citrate synthase and DHlipDH were greater than those obtained by purification of the enzyme from the native organism, but the products were either soluble yet inactive or insoluble inclusion bodies that required either reactivation or refolding of the recombinant halophilic enzyme (Connaris *et al.*, 1999). Moreover, a functional *in vitro* transcription system of halophilic archaea is not yet available, and thus the majority of the studies on the transcription initiation and regulator proteins of *Hfx. volcanii* and *Hbt. salinarum* have been done *in vivo*, by using the various promoters of the gvp genes involved in gas vesicle formation of *Hbt. salinarum* and *Hfx. mediterranei* (Danner and Soppa, 1996; Gregor and Pfeifer, 2005; Hofacker *et al.*, 2004; Patenge *et al.*, 2000; Pfeifer *et al.*, 2001; Zimmermann and Pfeifer, 2003).

From this basis, the work was initiated to express halophilic OADHC back into *Hfx. volcanii*. A small number of shuttle vectors have been developed over the last few years that are able to replicate in both *E. coli* and *Hfx. volcanii*. This ability is due to the inclusion of the origins of replications for both species (Allers *et al.*, 2004; Holmes *et al.*, 1991; Holmes *et al.*, 1994; Lam and Doolittle, 1989). Similarly, the vectors are selectable in each host by display of two types of antibiotic resistance or antibiotic resistance and nutritional requirements.

Following the discovery of DHlipDH, its substrate lipoic acid, and gene sequences corresponding to a 2-oxoacid dehydrogenase multienzyme complex operon in halophilic archaea, we have now shown that all genes of the complex are transcribed as an operon *in vivo*. However, no complex activity could be detected by growing *Hfx.*

volcanii on different carbon sources, and so the catalytic activity of the complex components could not be determined. In order to solve this obstacle, over expression of the genes of OADHC back into its native organism, *Hfx. volcanii*, was performed in this chapter. Moreover, heterologous expression of E1 was also performed in *E. coli*, and this is described in Chapter 6.

5.2 Materials

Cell culture: Yeast extract and peptone were supplied by Fisher Scientific, Loughborough, UK, while agar, carbencillin disodium salt, tryptone, polyethylene glycol (PEG, Average MW 600) and thymidine were from Sigma-Aldrich, Gillingham, UK. Bacto™ Yeast Extract, Bacto™ Casamino Acids and Bacto™ Agar were obtained from BD-Biosciences, Oxford, UK, whereas Bacteriological peptone was from Oxoid. Basingstoke, UK. Unless otherwise mentioned, all other chemicals were supplied from Sigma-Aldrich, Gillingham, UK, with high commercial purity.

Molecular biological studies: Oligonucleotide primers were obtained from MWG-Biotech AG, Germany. SP6 and T7 sequence primers were obtained from Novagen, USA. Restriction enzymes, Taq DNA polymerase, pGEM®-T Easy vector system, JM109 competent cells, and T4 DNA ligase were supplied by Promega, Southampton, UK. QIAEX II kit was provided by Qiagen, GmbH, Germany. dNTP was obtained from Bioline, London, UK. NucleoSpin® Plasmid Kit was from BD-Biosciences Clontech, USA. Vectors pIL11, pTA233, nonmethylating *E. coli* strain GM121, and expression strain *Hfx. volcanii* H98 were provided by Dr. Thorsten Allers, University of Nottingham, UK. Isopropyl-β-D-thiogalactopyranoside (IPTG), and 5-bromo-4-chloro-3-indolyl-β-D-galactopyranoside (X-gal) were supplied by Sigma-Aldrich, Gillingham, UK. Site-directed mutagenesis kit was obtained from Stratagene, Amsterdam the Netherlands. Low DNA mass ladder, 1kb, and 100 bp ladders were from Invitrogen, Paisley, UK.

5.3 Methods

5.3.1 Cloning of OADHC genes into pGEM®-T Easy vector

5.3.1.1 Oligonucleotide primer sequence design

Oligonucleotide primers were designed using the Primerselect programme from a genetic analysis computer package (Primer Premier, version 4.04, Premier Biosoft International, Palo Alto, CA, USA) using the identified OADHC sequence of *Hfx. volcanii* as mention in Chapter 2 (Section 2.5.1). Primers were designed with homology immediately upstream and downstream of the open reading frames of the OADHC. Primers were adjusted to incorporate *Xba*I and *Hind*III restriction sites in the forward and reverse primers, respectively. The restriction sites were selected according to the restriction map of the vector pIL11, after mapping the restriction sites of the OADHC using Biology SDSC Workbench (http://workbench.sdsc.edu). The addition of a number of bases upstream of the restriction site of each enzyme is to facilitate binding of these restriction enzymes (New England Biolabs, catalogue) Hitchin Herts, UK

FE1α *Xba*I : 5' - TGCT▼CTAGAGTGAGCGTGCTTCAACGCG - 3'

RE1α *Hind*III: 5' - CCCA▼AGCTTTCATTCTCTGAGGAATCCTTCGTCG - 3'

FE1β *Xba*I: 5' - TGCT▼CTAGAATGAGCAGTCAGAACCTCACCATCG - 3'

RE1β *Hind*III: 5' - CCCA▼AGCTTTCAGAAGTTCACCGCCTCACG - 3'

FE2 *Xba*I: 5' - TGCT▼CTAGAATGGCGCTCAAGGAATTCAAACTCC - 3'

RE2 *Hind*III: 5' - CCCA▼AGCTTTTATTCTAACACCAGCAGTTTGGGG - 3'

FE3 *Xba*I: 5' - TGCT▼CTAGAATGGTCGTCGGAGACATCGC - 3'

RE3 *Hind*III: 5' - CCCA▼AGCTTTCACCGATTCAGGGTGTGAATCG - 3'

In the above oligonucleotide sequences, TGC and CCC: are extra bases that were added to permit the binding of restriction enzymes *Xba*I and *Hind*III to the PCR products. C▼ATATG and G▼GATCC are restriction sites of *Nde*I and *Bam*HI respectively.

Due to the large size of the E1α-β insert, two extra forward primers were designed in order to sequence within the insert:

AB seq1 **5' - TCGACAAGGCGAAGAACC - 3' (from 710 to 727 bp)**

AB seq2 **5' - GTTCAACCACGCATACGC - 3' (from 1002 to 1019 bp)**

Both primer sequences were checked in order not to be found elsewhere in the E1 (α-β) gene or within pGEM®-T vector sequence.

5.3.1.2 Polymerase chain reaction (PCR) amplification of OADHC genes

PCR was performed as mentioned in Chapter 2 (Section 2.2.4.3) followed by running 5μl of PCR product on 1.3% agarose gel as also described in Chapter 2 (Section 2.2.4.4).

5.3.1.3 DNA extraction from agarose gel

Gel extraction was used to purify PCR products of the correct size and restriction-digested vectors and their inserts. In cases where the DNA was to be excised and purified, 0.8% (w/v) gels with large wells and low voltage (60-70 V) were used for the loading of the remaining PCR product or digested samples. The bands were excised using a sterile razor blade under UV light of long wavelength (~ λ_{350nm}) to minimize DNA damage. Gel extraction was performed using QIAEX II kit following the recommended protocol. At the end, 5 μl of the extraction product was analyzed on a 1% (w/v) agarose gel alongside 4 μl of low DNA mass ladder for quantitative estimations, as described in Chapter 2 (Section 2.2.4.4). The remainder of the reaction was stored at -20°C to be used in ligation.

5.3.1.4 A-tailing PCR products

The reaction was performed in a 0.5 ml thin-walled tube, by the addition of 5.2 μl of the extraction product, 1 μl 10x reaction buffer free of $MgCl_2$, 2mM of $MgCl_2$, 2mM of dATP and 5 units of Taq DNA polymerase to a final volume of 10 μl. The tube was incubated at 70°C for 30 min.

5.3.1.5 Ligation of A-tailed PCR products into pGEM®-T Easy vector

The pGEM®-T Easy vector system (Figure 5.1) was used as an intermediate cloning vector to clone the eluted A-tailed PCR products, following the recommended protocol. Appropriate amounts of eluted insert DNA were ligated to 1 µl pGEM®-T Easy vector (50 ng) in 10-20 µl with incubation overnight at 4 °C. The concentration of extracted DNA was estimated by comparison to DNA mass standards on the gel. The pGEM®-T Easy vector is approximately 3 kb and supplied at 50 ng/µl. To calculate the appropriate amount of PCR product (insert) to include in the ligation reaction, the following equation was used:

$$\frac{\text{ng of vector} \times \text{kb size of insert}}{\text{kb size of vector}} \times \text{insert: vector molar ratio*} = \text{ng of insert}$$

*Ratio of 2:1 (insert: vector) always was used.

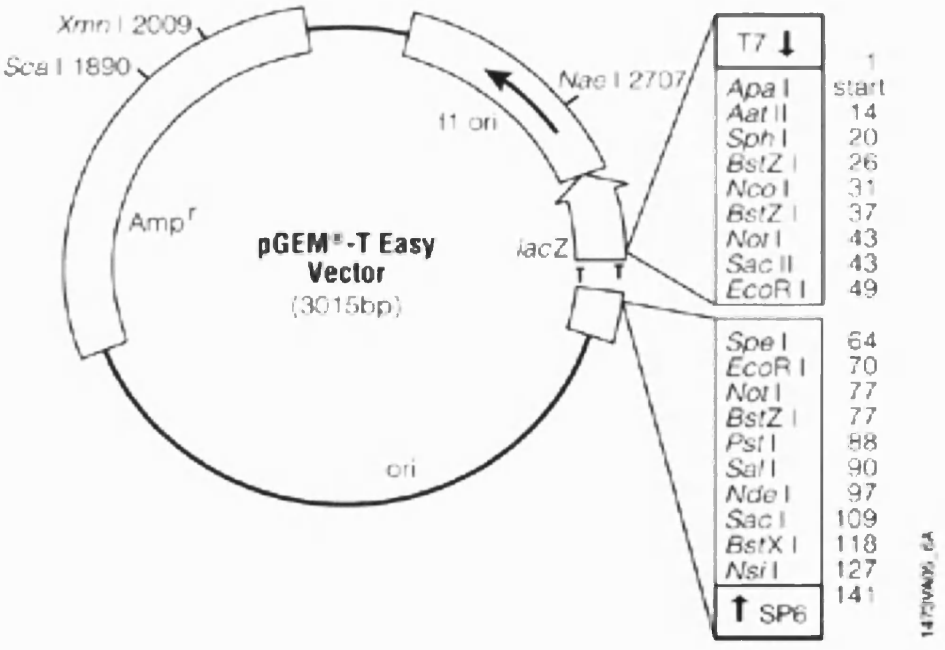

Figure 5.1: Circular map of pGEM®-T Easy vector .
Amp^r denotes the ampicillin/carbencillin resistance gene. The T-overhangs are indicated in the *Lac Z* region, which is disrupted upon the insertion of a DNA fragment and forms the basis of blue/white screening. F1 ori is the origin of replication in *E.coli*. Inserts can be sequenced using SP6 and T7 promoter primers. http://www.promega.com/vectors.

5.3.1.6 Transformation of JM109 *E. coli* competent cells

10 µl of ligation reaction was used to transform 50 µl high efficiency JM109 *E. coli* (ampicillin/carbencillin sensitive strain) competent cells (1 x 10^8 cfu/µg DNA) using the supplied protocol (Promega technical manual of pGEM®-T and pGEM®-T Easy vector Systems). SOC medium was always used during transformations. 100 ml SOC medium contains 2 g tryptone, 0.5 g yeast extract, 0.2 ml of 5 M NaCl, 0.019 g KCl, 1 ml of each 1 M $MgCl_2.6H_2O$ and 1 M $MgSO_4.7H_2O$, and 0.36g of D-glucose. The final pH was pH 7, and the medium was then autoclaved and stored in the fridge. There was certain modification to the protocol such as, heat shocking the cells for 90 s at exactly 42°C. Each plate was supplemented with 100 µl SOC medium, 100 µl 2% x-gal (dissolved in N, N- dimethyl formamide) and 100 µl of 100mM IPTG (dissolved in distill water and filter sterilized) spread on the surface of LB agar plates supplemented with 50 µg/ml carbencillin as mention in Chapter 2 (Section 2.2.1) and left to dry before use to facilitate blue/white colony screening. 100 µl of the transformants were plated on one plate. For the second plate cells were centrifuged and ~ 800 µl of the supernatant was removed; the pellet was then resuspended with the remaining supernatant and then plated to increase the concentration of transformants. Transformants were selected by overnight incubation at 37°C.

5.3.1.7 Miniprep purification of plasmid DNA

10 ml LB medium containing 10 µl of 50 µg/ml carbencillin was inoculated with the transformants or from a master plate streak, and incubated at 37°C overnight shaking at 200 rpm. The cells were pelleted at 11,000 x g for 9 min at room temperature. The plasmid DNA was extracted and purified using a NucleoSpin® Plasmid Kit, as recommended in the manual provided with the kit. At the end, 5 µl of the reaction product was analyzed on a 0.8% (w/v) agarose gel alongside circular pGEM-T vector without insert to detect any size shift indicating successful ligation. The remainder of the reaction was stored at -20°C.

5.3.1.8 Sequence of DNA minipreps

Sequencing of plasmid DNA from selected transformants was performed using SP6 and T7 terminator primers; at least three minipreps of each insert were sent for sequencing. Samples were sequenced at Molecular Biological Services in the Department of Biology and Biochemistry, University of Bath, on a 3700 DNA analyser (Applied Biosystems, USA).

Results were analysed by aligning the determined sequences with corresponding gene sequences of the identified OADHC sequence of *Hfx. volcanii* as mention in Chapter 2 (Section 2.2.4.1), using the BioEdit Sequence Alignment Editor software package (© 1997-2004 Tom Hall, Isis Pharmaceuticals, downloaded from http://www.mbio.ncsu.edu/BioEdit/bioedit.html).

5.3.2 Cloning of OADHC into pIL11 and pTA233

5.3.2.1 pIL11 and pTA233 vectors

Both pIL11 and pTA233 plasmids were supplied in an *E. coli* host strain on LB with ampicillin agar slants. Miniprep purification of each plasmid was performed as described in Section 5.3.1.7.

pIL11 is a replication vector that multiplies in *E. coli* only. It is a 2845 bp vector that posses the *Hfx. salinarum* ferredoxin promoter (*fdx* promoter) for gene over-expression in *Hfx. volcanii* (Figure 5.2). pIL11 lacks a *Lac Z* region, so that there is no possibility of blue/white screening.

pTA233 is a shuttle expression vector that can multiply in both *Hfx. volcanii* and *E. coli.* It is a 7429bp vector and works well with clones up to 4 kb (Figure 5.3). However, pTA233 plasmid vector based on pHV2 has a relative copy number of around 6, which is nowhere near as high as ColE1-based plasmids such as pUC19.

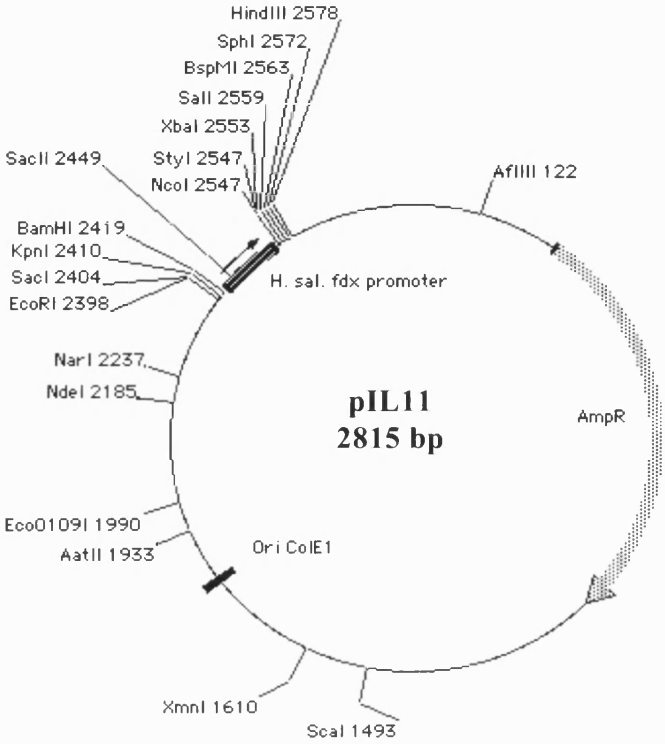

Plasmid name: pIL11
Plasmid size: 2815 bp
Constructed by: Moshe Mevarech lab
Construction date:
Comments/References: Based on pUC19: bp 1-2424 = pUC19 bp 2686-263, bp 2552-2814 = pUC19 bp 262-1. NcoI site (C^CATGG) contains ATG for cloning gene after H. sal. fdx promoter, for overexpression in Hf. volcanii.

Figure 5.2: Circular map pIL11 vector.
The vector map of pIL11 shows the ampicillin/carbencillin resistance gene (AmpR). Ori ColE1 represents the origin of replication in *E. coli*, and *fdx* promoter represents the ferredoxin promoter from *Hbt. salinarum* for over-expression in *Hfx. volcanii.* Also, the *Nco*I site (C^CATGG) contains an ATG codon for cloning the target gene after the *fdx* promoter. The pIL11 vector lacks a *Lac Z* region and therefore does not permit blue/white screening.

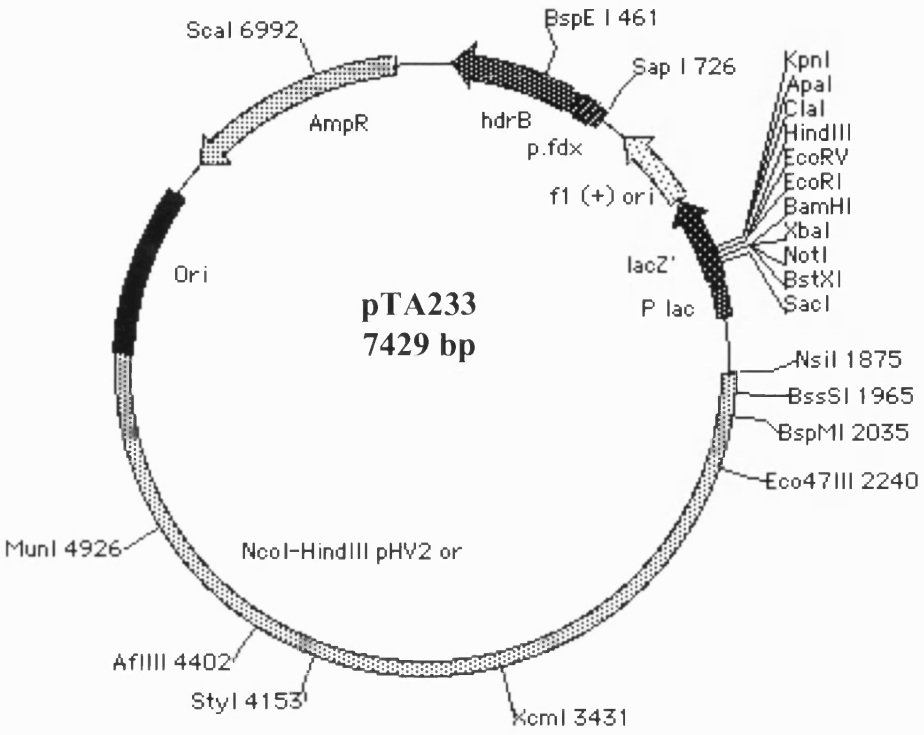

Figure 5.3: Circular map of pTA233 expression vector.
pTA233 is a shuttle vector based on pTA192 vector. The map illustrates the *Lac Z* region, which is disrupted upon insertion of a DNA fragment and forms the basis of blue/white screening. The f1 (+) ori is the single-stranded DNA replication origin of the filamentous phage f1. The hdrB thymidine gene is a selectable marker that complements ΔhdrB *Hfx. volcanii* thymidine auxotrophy and is preceded by *fdx* promoter. The map also shows the ampicillin/carbencillin resistance gene (AmpR) selectable marker followed by ori: the origin of replication of *E. coli*. The *Nco*I-*Hind*III pHV2 or is the region that contains the origin of replication for *Hfx. volcanii* (Allers *et al.*, 2004).

5.3.2.2 Double digestion

For recombinant expression, the OADHC genes were recloned from pGEM-T into the *Xba*I and *Hind*III sites of pIL11 replication vector, and then into *Hind*III and *Bam*HI sites of pTA233 expression shuttle vector, respectively.

Firstly, samples of vector and insert were prepared by double digestion. This was performed in sterile 0.5 ml thin wall tubes: 10 µl of the vector or insert, 5 µl 10x buffer B, 5 µl 100x BSA and 1.2 µl of each enzyme to a final volume of 50 µl sterile Milli Q water. The mixture was gently vortexed and incubated at 37°C for 24 h. Also, in parallel a single digest was performed following the same procedure but using one restriction enzyme only. At the end of the incubation period, 5 µl of reaction product was visualized on a 0.8% (w/v) agarose gel as described in Chapter 2 (Section 2.2.4.4).

5.3.2.3 Cloning into pIL11

After the fragments had been separately ligated into pGEM®-T, the vectors were transformed into JM109 competent cells. From these, plasmid minipreps were subjected to enzyme digestion using *Xba*I and *Hind*III. pIL11 vector was similarly digested and both preparations were gel purified (Section 5.3.1.3). The inserts were then cloned into pIL11 as mentioned in Section 5.3.1.5. The concentration of eluted digested product used was estimated by comparison with DNA mass standards. After transformation into JM109 competent cells, (Section 5.3.1.6) minipreps of plasmid pIL11 with OADHC inserts were purified (Section 5.3.1.7) and then double digested, using *Hind*III and *Bam*HI.

5.3.2.4 Cloning into pTA233

The genes along with the ferredoxin promoter were excised from pIL11 with *Hind*III and *Bam*HI, and were ligated into pTA233 vector into *Hind*III and *Bam*HI cloning sites following the same procedure as mentioned in Section 5.3.2.3.

5.3.2 5 Preparation of GM121 (dam$^-$) competent cells

Several colonies of *E. coli* GM121 were inoculated into 10 ml of LB media and were incubated overnight at 37°C with shaking at 180 rpm. 1 ml of the overnight culture

was inoculated into 100 ml LB in a 500 ml flask and incubated at 37°C with shaking at 180 rpm for 2 h. The culture was then chilled on ice for 30 min and transferred to two pre-chilled 50 ml falcon tubes. The cells were centrifuged at 3,000 x g for 5 min at 4°C, and each pellet was resuspended in 12.5 ml of sterile, ice-cold 100 mM $CaCl_2$ and 12.5 ml of 40 mM $MgSO_4$, and incubated on ice for 30 min. Cells were centrifuged as before and resuspended in 2.5 ml of 100 mM $CaCl_2$ and 2.5 ml of 40 mM $MgSO_4$; prechilled sterile glycerol was then added to 10% of the total volume. 250 µl aliquots were pipetted into chilled 1.5 ml tubes, frozen in dry ice/methanol and stored at –80°C.

5.3.2 6 Transformation of GM121 competent cells

The miniprep DNA of each clone of OADHC in pTA233 was transformed into JM109 competent cells; from here, a new miniprep was retransformed into GM121 as described in Section 5.3.1.6 to generate unmethylated DNA. This was followed by selection of GM121 transformants and plasmid prep of unmethylated PTA233 for transformation into the expression strain *Hfx. volcanii* H98.

5.3.2.7 Growth of *Hfx. volcanii* expression strain H98

The *Hfx. volcanii* host strain H98 is of (*ΔpyrE2 ΔhdrB*) genotype (Allers *et al.*, 2004). A deletion of both *pyrE2* and *hdrB* genes confers both uracil and thymidine auxotrophy in rich medium (Hv-YPC) respectively. The *Hfx. volcanii* H98 was grown in rich medium (Hv-YPC) that was composed of two separate solutions. The first is 30% concentrated salt water (SW), consisting of 24% (w/v) NaCl, 3% (w/v) $MgCl_2.6H_2O$, 3.5% (w/v) $MgSO_4.7H_2O$, 0.7% (w/v) KCl and 20 ml of 1 M Tris-HCl, pH 7.5, all dissolved in warm water to a final volume of one litre. The second part of the medium is 10x YPC, which consists of 8.5 g yeast extract (Difco), 1.7 g peptone (Oxoid) and 1.7 g Casamino Acids (Difco), dissolved in distilled water to a final volume of 170 ml, and adjusted to pH 7.5 with 1 M KOH. For liquid Hv-YPC medium (18% SW final), 200 ml of 30% SW medium was mixed with 33 ml of 10x YPC into a clean 500 ml Duran bottle and made to a final volume of 333 ml with distilled water. For solid Hv-YPC, 100 ml distilled water, 200 ml of 30% SW and 5 g agar (Difco) were mixed in a 500 ml Duran bottle, and the contents were dissolved by microwave heating with

continuous mixing between the heating phases. Finally, to each 300 ml batch 30 ml of 10x YPC was added and then autoclaved. After autoclaving, the media were allowed to cool to about 57°C and then 2 ml of 0.5 M $CaCl_2$ and filter sterilised thymidine were added, giving a concentration of 40 µg thymidine/ml.

5.3.2 8 Transformation of *Hfx. volcanii* strain H98 competent cells

Unmethylated pTA233 with the cloned inserts was transformed into *Hfx. volcanii* H98 expression strain to effect the expression of the OADHC genes.

Transformation of H98 strain was carried out using polyethylene glycol (PEG) 600 (Cline *et al.*, 1989; Dyall-Smith, 2004). A freshly inoculated culture (10 ml Hv-YPC with thymidine) was grown overnight until late log phase ($A_{650} \approx 0.8$) and then harvested at 4,500 x.g for 8 min at room temperature. The pellet was washed in 2 ml sterile buffered spheroplasting solution (14.61g NaCl, 0.5 g KCl, 12.5 ml 1 M Tris-HCl pH 8.5, 37.5 g sucrose and distilled water to 250 ml) and the cells were pelleted as above. Then very gently the pellet was resuspend in 600 µl buffered spheroplasting. For each transformation, 200 µl of cells was transferred to a clean 2 ml round-bottom tube. Spheroplasts formed on the addition of 20 µl 0.5 M EDTA (pH 8.0), and the contents were mixed by inverting followed by incubation at room temperature for 10 min. Meanwhile, the DNA samples were set up in a 30 µl total volume [10 µl dam^- DNA or 10 µl sterile H_2O as control, 15 µl sterile unbuffered spheroplasting solution (5.84 g NaCl, 0.2 g KCl, 15 g sucrose and distill water to 100 ml adjust pH to 7.5 with 1 M NaOH) and 5 µl of 0.5 M EDTA pH 8.0]. After 10 min DNA was added to the spheroplasts and was left for 5 min. After 5 min, 250 µl of 60% PEG 600 (480µl of PEG 600 dissolved in 320 µl unbuffered spheroplasting solution) was added to each transformation, gently mixed and left at room temperature for 30 min. Then 1.5 ml sterile spheroplasts dilution solution (76 ml 30% SW, 15 g sucrose, 0.75 ml of 0.5 M $CaCl_2$ and distilled water to 100 ml) was added, mixed and left at room temperature for 2 min. The cells were harvested at 4,500 x g for 8 min at room temperature and the supernatant removed. 1 ml of sterile regeneration solution (150 ml 30% SW, 25 ml 10x YPC, 37.5 g sucrose, 1.5 ml of 0.5 M $CaCl_2$ and distilled water to 250 ml) plus 60

μg/ml sterile thymidine was added, and the whole pellet was transferred to 4 ml sterile tube. To avoid resuspending the pellet at this stage, the tube was left undisturbed at 45°C for 1.5-2 h. At the end of the incubation period the pellet was resuspended by tapping the side of the tube and returned back to 45 °C with shaking at 150 rpm; after 3 h, the cells were transferred to a 50 ml Falcon to increase the surface area. Then the cells were transferred to a 2 ml tube and pelleted at 4,500 x g for 8 min at room temperature and the supernatant removed. The pellet was resuspended gently in 1 ml sterile transformant dilution solution (150 ml 30% SW, 37.5 g sucrose, 1.5 ml of 0.5 M $CaCl_2$ and distilled water to 250 ml). Finally, 100 μl was plated on Hv-YPC (without thymidine) plates using dilutions 10^{-1}, 10^{-2} and 10^{-3} in transformant dilution solution, and incubated at 45°C, sealed in plastic.

After 6 days, when the colonies had grown, three colonies from each transformation were picked into three 50 ml flasks with 20 ml Hv-YPC and incubated at 45°C shaking at 180 rpm. When the OD_{600nm} had reached ≥ 1.2, cells were harvested and stored at –20°C for further studies.

5.3.2.9 Analysis of transformants

Firstly, the cell extract of each clone was used to study enzymic activity (E1) as mentioned in Chapter 2 (Section 2.2.2.7). Secondly, 5 ml cell broth was used to prepare a miniprep of plasmid DNA as mentioned in Section 5.3.1.7, which was then subjected to double digestion using *Hind*III and *Bam*HI restriction enzymes following the protocol described in Section 5.3.2.2. Thirdly, SDS-PAGE was carried out for each cell extract and cell debris as mentioned in Chapter 2 (Section 2.2.4.5).

5.3.3 Site-directed mutagenesis

Five mutants of OADHC genes were created for future structural and enzymic studies. Mutants Mut E1α, Mut E1β, Mut E1α-β, Mut E2 and Mut E3 were generated using the QuikChange site-directed mutagenesis kit as recommended by the supplier, with OADHC clones in pIL11 as template. Primers are shown below, with the mutated base highlighted in red and the original genomic sequence displayed above.

The listed primers and their reverse complement are shown below:

Original E1α: 5' - GCA GCC ATG G T$^{\nabla}$CTAGA GTG AGC GTG C - 3'

Mut FE1α: 5' - GCA GCC ATG G T$^{\nabla}$C GGA GTG AGC GTG C - 3'

T was removed and G substituted for A, thereby replacing the AGA (arginine) with GGA (glycine)

Mut RE1α: 5' - G CAC GCT CAC TCC GA C CAT GGC TGC - 3'

TA

Mut FE1β: 5' - GCA GCC ATG G T$^{\nabla}$C GGA ATG AGC AGT CAG AAC C - 3'

Mut RE1β: 5' - G GTT CTG ACT GCT CAT TCC GAC CAT GGC TGC - 3'

TA

Mut FE2: 5' - GCA GCC ATG G T$^{\nabla}$C GGA ATG GCG CTC AAG G - 3'

Mut RE2: 5' - CCT TGA GCG CCAT TCC GAC CAT GGC TGC - 3'

TA

Mut FE3: 5' - GCA GCC ATG G T$^{\nabla}$C GGA ATG GTC GTC GG - 3'

Mut RE3: 5' - CC GAC GAC CAT TCC GAC CAT GGC TGC - 3'

After the synthesis of the mutant strand, resultant DNA was transformed into XL1-blue supercompetent cells as mentioned in Section 5.3.1.6, followed by miniprep purification of plasmid DNA as described in Section 5.3.1.7. The minipreps of the mutant clones were sequenced as described in section 5.3.1.8 using special primers designed ~ 60 bp upstream or downstream of the mutation site. The primer sequences were checked in order not to be found elsewhere in the pIL11 sequence or even in the gene sequence itself. Due to the large size of the E1α-β mutant, two extra tubes were sent to be sequenced including primers within the E1α-β sequence as mentioned in Section 5.3.1.1.

Forward and reverse sequence primers are described below:

FP11seq2: 5' - CGTGGCAGTACGCTGG - 3'

RP11seq: 5' - GTGTGGAATTGTGAGCGG- 3'

The genes with the correct sequence were aligned, then they were cloned into pTA233 vector as mentioned in Section 5.3.2.4, transformed into JM109 and then into GM121 dam$^-$ *E. coli*, followed by transformation into expression strain *Hfx. volcanii* H98 as described in Section 5.3.2.8.

5.4 Results

5.4.1 Cloning of OADHC genes into pGEM®-T Easy vector

5.4.1.1 PCR amplification of OADHC genes

Using primers designed with homology upstream and downstream of the open reading frames, the complex genes (E1α, E1β, E2, E3 and E1α-β) were successfully PCR-amplified from a genomic extract of *Hfx. volcanii*. The amplification was confirmed by bands of the expected size visualized on a 1.3% (w/v) agarose gel (Figure 5.4).

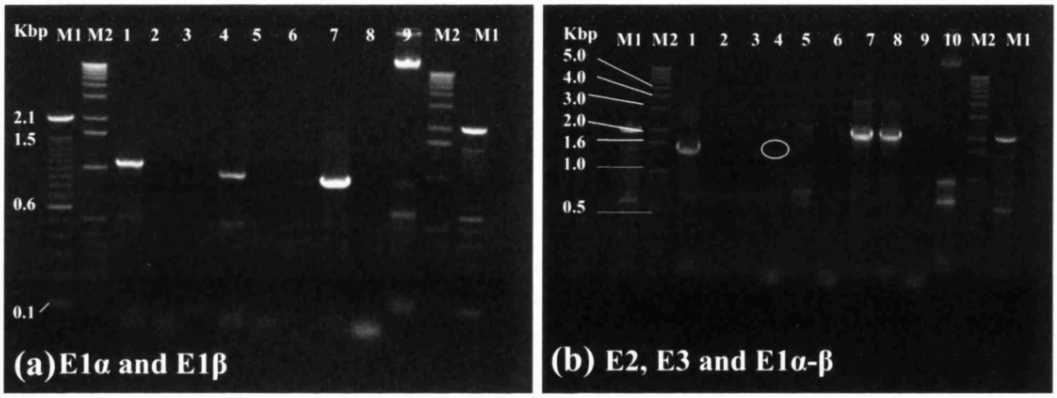

Figure 5.4: PCR amplification of *Hfx. volcanii* OADHC genes.
The gel is a 1.3% agarose gel showing products of PCR amplification. Marker lanes M1 and M2 contain 100 bp ladder and 1kb ladder, respectively, with sizes in kilo base pairs as shown. Gel (a): Lane 1: E1α of 1107 bp, lane 4: E1β 984 bp and lane 7: E1β 984 bp (primers without restriction sites). Controls without forward or reverse primer of E1α and E1β respectively are shown in lane 2, 3,5 and 6. Lane 8: PCR control and lane 9 genomic DNA extract. Gel (b): Lane 1: E2 of 1566 bp, lane 4 E3 (faint) of 1428 bp, and lane 7and 8 E1α-β 2091 bp (duplicate). Lanes 2,3,5 and 6 controls without forward or reverse primer of E2 and E3 respectively. Lane 9: PCR control and lane 10 genomic DNA extract.

5.4.1.2 DNA extraction from agarose gel

The DNA of each gene was first extracted from the agarose gel. The resultant DNA was confirmed by running 1% agarose gels, and the concentration of extracted DNA was estimated by comparison to DNA mass standards on the gel.

5.4.1.3 A-tailing PCR products

Thermostable Vent® DNA polymerase, will generate blunt-ended fragments during PCR amplification. Nevertheless, PCR fragments generated can be modified using the A-tailing procedure and then ligated into the pGEM®-T Easy vector. Using this method, only one insert will be ligated into the vector as opposed to multiple insertions that can occur with blunt-ended cloning. In addition, with T-vector cloning there is no need to dephosphorylate the vector, and there is a low background of religated vector.

5.4.1.4 Ligation of A-tailed PCR products into pGEM®-T Easy vector

The amplified A-tailed fragments were ligated into the pGEM®-T Easy vector.

5.4.1.5 Transformation of JM109 competent cells

High efficiency *E. coli* JM109 were heat-shock transformed with constructs of pGEM®-T easy vector with one of the OADHC genes (E1α, E1β, E2, E3 or E1α-β) in order to provide enough DNA to transform *Hfx. volcanii.*

5.4.1.6 Miniprep purification of plasmid DNA

At the end of miniprep purification, 5µl of each gene miniprep was visualized using 0.8% agarose gel against circular pGEM®-T Easy vector with no insert; a size shift indicates a successful cloning of each OADHC gene into pGEM®-T Easy vector (Figure 5.5).

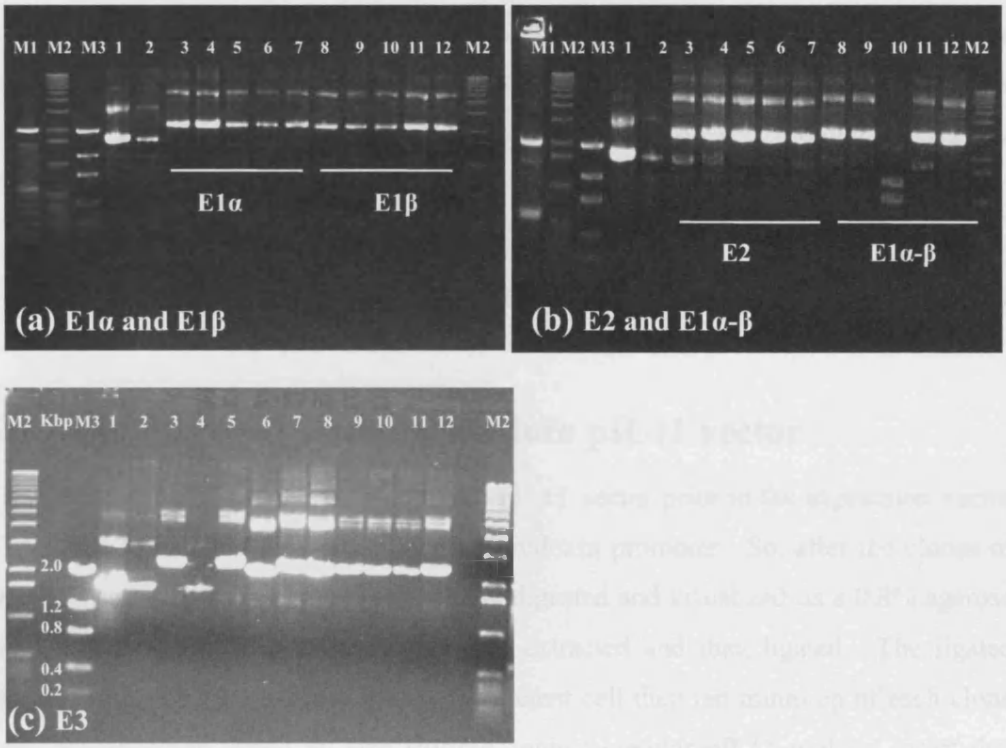

Figure 5.5: Miniprep of *Hfx. volcanii* OADHC genes after cloning into pGEM-T. Marker lanes M1, M2 and M3 contain 100 bp ladder, 1kb ladder and low DNA mass ladder respectively, with sizes in kilo base pairs as shown. The minipreps after cloning into pGEM-T are shown on a 0.8% agarose gel in (a), (b) and (c). Lanes1 and 2: circular pGEM-T without insert as a control. Gel (a) shows E1α minipreps in lanes 3-7 and E1β minipreps in lanes 8-12. The minipreps in lane 4 and 11 were completely sequenced and used in subsequent cloning experiments. Gel (b) demonstrates E2 minipreps in lanes 3-7 and E1α-β minipreps in lanes 8-12 (lane 10 is failure). The minipreps in lane 5, 4 and 12 were completely sequenced and used in subsequent cloning experiments. Gel (c) shows E3 minipreps in lanes 3-12 (lane 4 is failure). The minipreps in lane 3 and 12 were completely sequenced and used in subsequent cloning.

5.4.1.7 Sequence of DNA miniprep

Three of the clones were completely sequenced for each gene of the OADHC. The results of the sequencing experiments were checked and aligned. The clones were sequenced to identify one without mismatch errors, which then provided a reliable source of the gene for subsequent cloning. The successful cloning strategy is summarized in Figures 5.4 and 5.5.

5.4.1.8 Double digestion

The inserts were double digested from pGEM®-T Easy vector and recloned into the *Xba*I and *Bam*HI sites of pIL11 replication vector (Figure 5.6).

5.4.2 Cloning of OADHC genes into pIL11 vector

The main reason of cloning the genes into pIL11 vector prior to the expression vector pTA233 is to recover the insert plus the ferredoxin promoter. So, after the clones of OADHC and pIL11 vector had been double digested and visualized on a 0.8% agarose gel, the inserts and pIL11 vector were gel extracted and then ligated. The ligated samples were transformed into JM109 competent cell then ten miniprep of each clone were prepared and tested by size shifting against circular pIL11 without insert that indicate successful ligation and transformation (Figure 5.7). The inserts were double digested from pIL11 vector and recloned into the *Bam*HI and *Hind*III sites of pTA233 expression vector (Figure 5.8). As shown in figure 5.8 the bands resulted after double digestion of the inserts will be higher than PCR product of each insert due to the presence of the ferredoxin promoter with the insert (promoter of 128 bp).

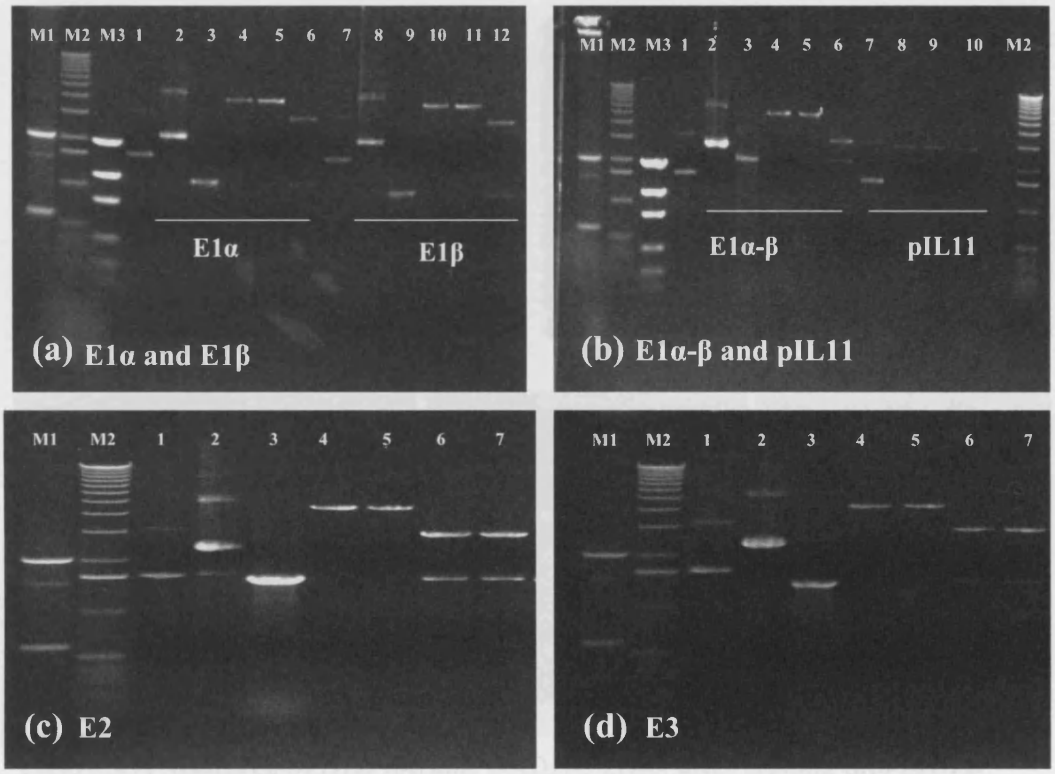

Figure 5.6: Double and single digestion of *Hfx. volcanii* OADHC genes out of pGEM-T vector.

Marker lanes M1, M2 and M3 contain 100 bp ladder, 1kb ladder and low DNA mass ladder, respectively. Double and single digest were visualized using 0.8% (w/v) agarose gel. Lane 1: circular pGEM-T without insert as a control (also lane 7 on gel (a) only), lane 2: miniprep of each gene with pGEM-T (also lane 8 on gel (a) only). Lane 3 is PCR product of each gene (also lane 9 in gel (a) only) as an insert size control. Lanes 4 and 5: single digest of each gene with *Hind*III or *Xba*I respectively (also lanes 10 and 11 in gel (a) only). Gel (a) Lanes 6 and 12, gel (b) lane 6, gel (c) lanes 6 and 7 and gel (d) lanes 6 and 7 (duplicate) show double digestion of the genes with *Hind*III and *Xba*I and the higher M_r band is the pGEM-T vector and the lower one is the insert of interest of the correct size. Gel (b) lane 7: circular pIL11 vector, lanes 8 and 9 single digest with *Hind*III or *Xba*I respectively and lane 10 double digest with both enzymes. There is no observable difference between single and double digest with pIL11 vector because the excised insert is only 25 bp in length.

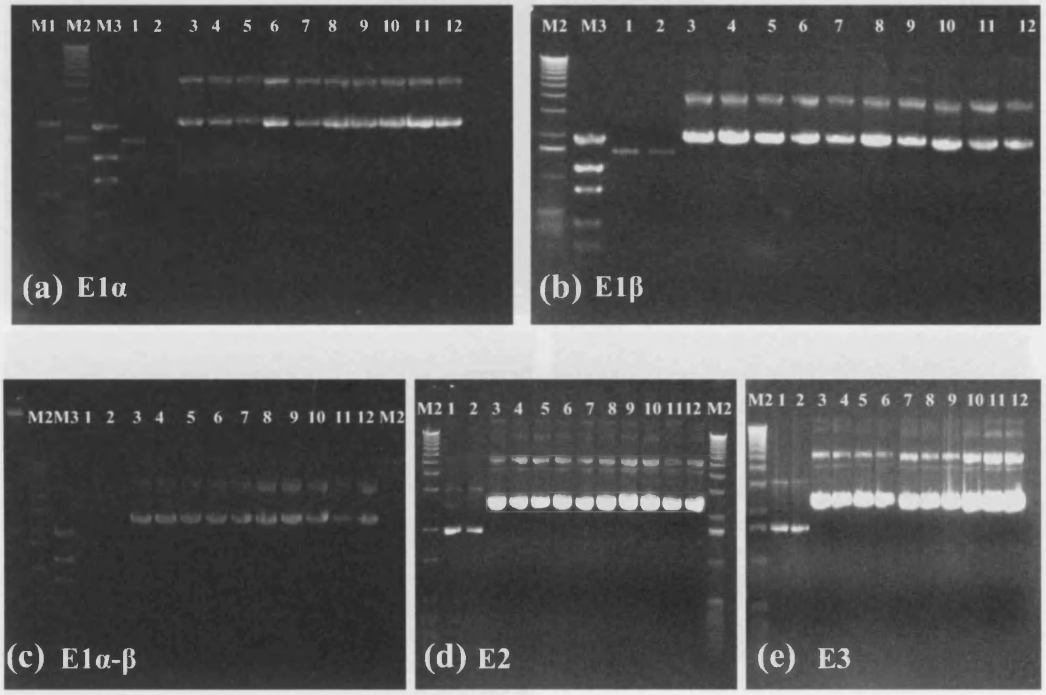

Figure 5.7: Miniprep of *Hfx. volcanii* OADHC genes after cloning into pIL11.
Marker lanes M1, M2 and M3 contain 100 bp ladder, 1kb ladder and low DNA mass ladder respectively. The minipreps are shown on a 0.8% agarose gel in (a), (b), (c), (d) and (e). A size shift indicates successful ligation of each gene of OADHC into pIL11. In gels (a), (b), (c), (d) and (e) lanes 3-12 show minipreps of E1α, E1β, E1α-β, E2 and E3 respectively after cloning into PIL11.

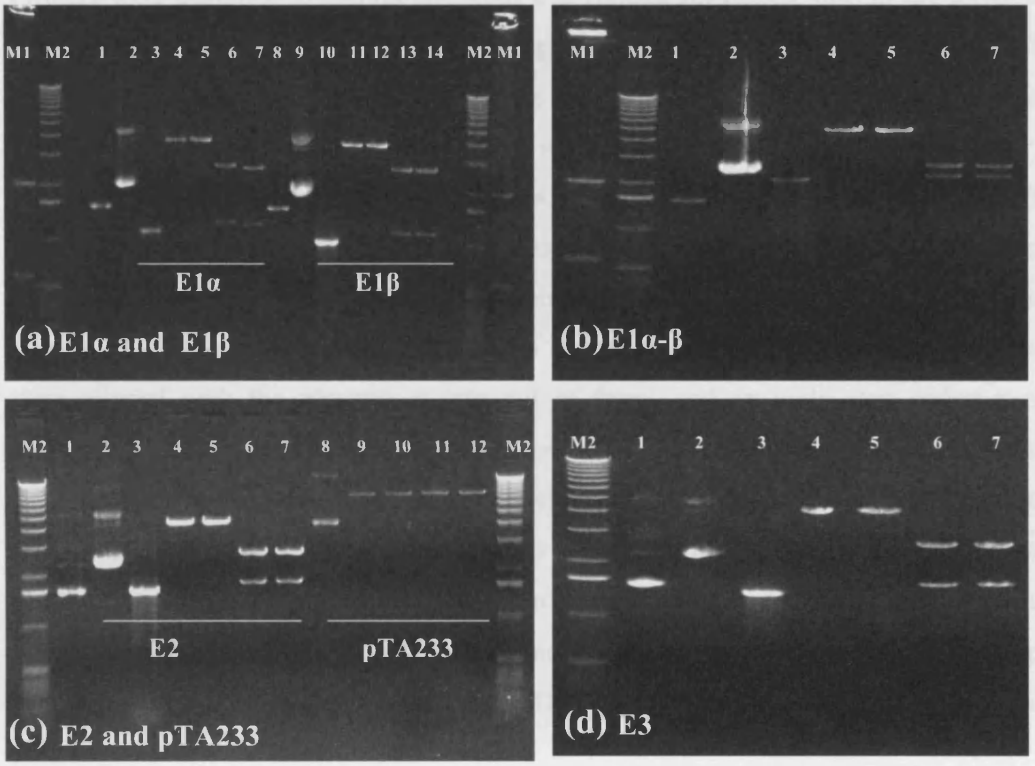

Figure 5.8: Double and single digestion of pIL11 vector containing *Hfx. volcanii* OADHC genes.

Marker lanes M1, M2 and M3 contain 100 bp ladder, 1kb ladder and low DNA mass ladder respectively. Double and single digests were visualized using 0.8% (w/v) agarose gels. Lane 1: circular pIL11 without insert as a control (also lane 8 on gel (a) only), lane 2: miniprep of each gene with pIL11 (also lane 9 on gel (a) only). Lane 3 is a PCR product of each gene (also lane 10 on gel (a) only) used as an insert size control. Lanes 4 and 5: single digest of each gene with *Hind*III or *Bam*HI respectively (also lanes 11 and 12 on gel (a) only). Gel (a) Lanes 6, 7, 13 and 14, gel (b) lanes 6 and 7 gel (c) lanes 6 and 7, and gel (d) lanes 6 and 7 (duplicate), show double digestion of the genes with *Hind*III and *Bam*HI. Two bands resulted, the higher M_r band is the pIL11 vector and the lower one is the insert of interest of the correct size, which is higher than the PCR product band due to the presence of *Fdx* promoter (128 bp). Gel (c) lane 8: circular pTA233 vector, lanes 9 and 10 single digest with *Hind*III or *Bam*HI respectively, and lane 11and 12 double digest with both enzymes.

5.4.3 Site-directed mutagenesis

Primers were designed to incorporate *Xba*I and *Hind*III restriction sites in the forward and reverse primers, respectively. According to the restriction map of pIL11, the *Nco*I site (C^CATGG) was recommended to be used in the forward primer because it contains the start codon, ATG, for cloning a gene after the *fdx* promoter. However, when the restriction map of OADHC genes was searched, an *Nco*I site maps in the E1β sequence; it was therefore decided not to use the *Nco*I site but still to use the same restriction sites for all designed primers, hoping that the start codon of the gene will be used in the expression of the protein. As a result, when the sequence of the primers were aligned with the plasmid, it was out of frame and an early stop codon was recognized if the expression started at the *NcoI* site (ATG). An early stop signal at the third codon **TAG** would prevent the production of required protein. So, in order to remove this signal, site-directed mutagenesis was performed on the OADHC genes in pIL11. As shown below, the original FE1α primer and the new mutated primer are aligned to show from where T is deleted and G is substituted for A. The early stop codon in the original primer is underlined. The same situation arises for the rest of the primers.

Original FE1α: 5' – GCA GCC ATG G T$^{\nabla}$C TAGA GTG AGC GTG C - 3'

Mut FE1α: 5' – GCA GCC ATG G T$^{\nabla}$C GGA GTG AGC GTG C - 3'

ATG: starting codon at *Nco*I site. **T$^{\nabla}$C TAGA:** restriction site of *Xba*I and **TAG:** an early stop signal.

Removing T would result in an arginine (AGA) with a positively charged R group, but replacing A with G results in glycine (GGA) with a non-polar uncharged R group. The resulting mutant with no early stop codon (TAG) can use either the ATG of *Nco*I as the start codon or the start codon of the gene itself.

Site-directed mutagenesis was used successfully to generate five OADHC mutants: Mut E1α, Mut E1β, Mut E1α-β, Mut E2 and Mut E3 in pIL11 vector. The site-directed mutagenesis was carried out in pIL11 because it is smaller in size than pTA233, the kit being applicable to vectors up to 8 kb. After the generation of the mutants, the vectors were transformed into XL1-blue supercompetent cells as

recommended by the site-directed mutagenesis kit. Around eight minipreps of each clone were prepared and tested by size shifting against circular pIL11 without insert (Figure 5.9).

Three clones were completely sequenced for each mutant of the OADHC to identify one with the correct mutation site, which then provided a reliable source of the gene for subsequent cloning. The inserts were double digested from pIL11 vector and recloned into the *Bam*HI and *Hind*III sites of pTA233 expression vector (Figure 5.10). As shown in Figure 5.10, the bands resulting after double digestion of the inserts will be higher than the PCR band of each insert due to the presence of the ferredoxin promoter (128 bp) with the insert.

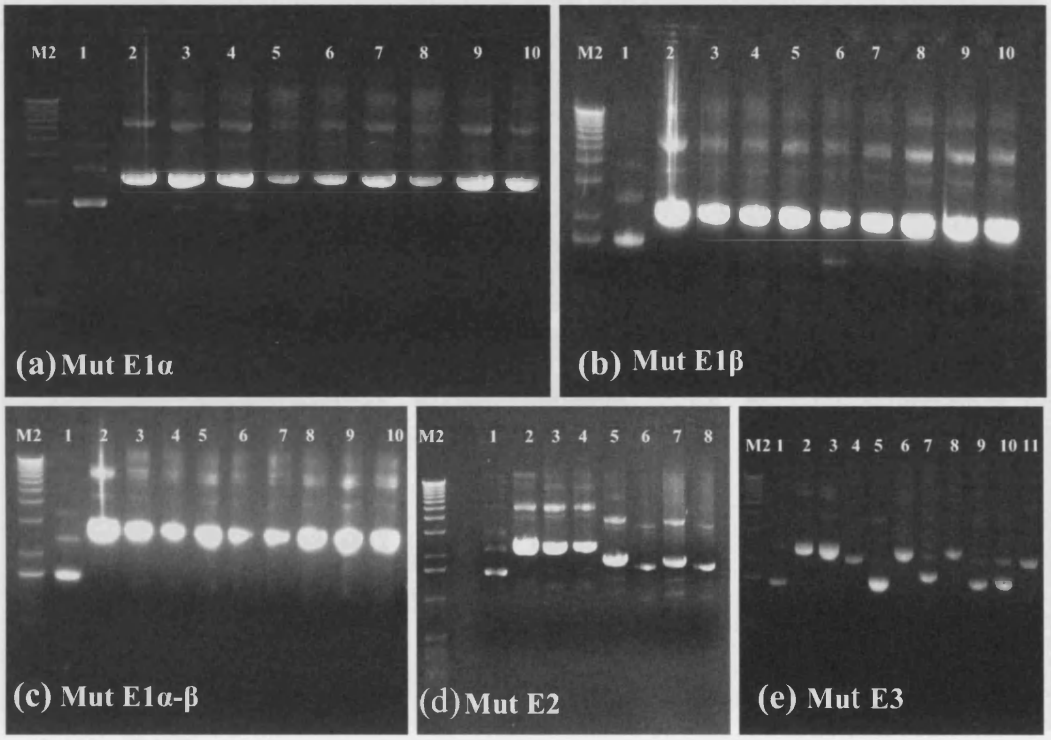

Figure 5.9: Minipreps of *Hfx. volcanii* mutated OADHC genes in pIL11.
Marker lane M2 contain 1kb ladder. The minipreps of pIL11 after mutation and transformation into XL1-blue supercompetent cells are shown on a 0.8% agarose gel in (a), (b), (c), (d) and (e). Lane 1: circular pIL11 without insert and lane 2: non-mutated pIL11 with insert as a control except in gel (e) where lanes 2 and 3 are the same duplicate. Gels (a), (b) and (c) show minipreps of mutated E1α, E1β and E1α-β minipreps, minipreps lanes: 3 of E1α, and E1β and lane 8 of E1α-β were completely sequenced and used in subsequent cloning. Gel (d) represents minipreps of E2 only preps in lanes: 3 and 4 were correct and the miniprep lane 3 was fully sequenced and used in subsequent cloning. Gel (e) shows minipreps of E3 lanes 6 and 8 were correct and the miniprep lane 6 was completely sequenced and used in subsequent cloning.

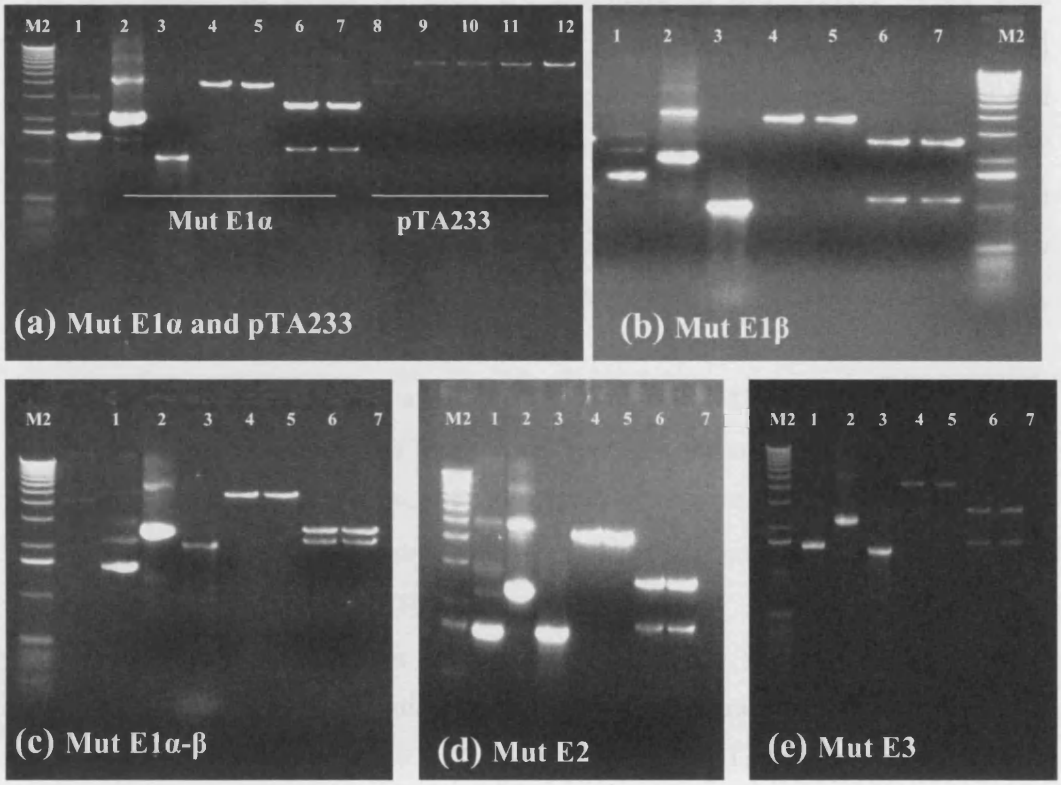

Figure 5.10: Double and single digestion of pIL11 carrying *Hfx. volcanii* mutated OADHC genes.

Marker lane M2: 1kb ladder. Double and single digests were visualized using 0.8% (w/v) agarose gel. Lane 1: circular pIL11 without insert as a control, lane 2: miniprep of each gene with pIL11. Lane 3 is a PCR product of each gene used as an insert size control. Lanes 4 and 5: single digest of each gene with *Hind*III or *Bam*HI respectively. Lanes 6 and 7 (duplicate) show double digestion of the genes with *Hind*III and *Bam*H; two bands resulted, the higher is the pIL11 vector and the lower one is the insert (higher M_r than the PCR product band due to presence of *fdx* promoter of 128 bp). Gel (a) lane 8: circular pTA233 vector, lanes 9 and 10 single digest with *Hind*III or *Bam*HI respectively and lane 11and 12 double digest with both enzymes.

5.4.4 Cloning of OADHC genes into pTA233 vector

The double-digested clones (mutated and non-mutated) and pTA233 vector were examined by electrophoresis on a 0.8% (w/v) agarose gel. After gel extraction and ligation, the vectors with inserts were transformed into JM109 competent cells and miniprep preparations were examined by electrophoresis on 0.8% agarose gels (Figures 5.11 and 5.13). Due to the large size of pTA233 vector the size shift that would indicate that the insert has been successfully incorporated was not clear, so the clones were subjected to double digestion using *Bam*HI and *Hind*III restriction enzymes, (Figures 5.12 and 5.14).

The clones that resulted after transformation into JM109 will be of methylated DNA that will be recognized as foreign DNA by *Hfx. volcanii* H98 expression strain and will be degraded. Therefore, it was important to prepare unmethylated plasmid by transformation into a non-methylating strain, dam$^-$ *E. coli* GM121, for efficient transformation of *Hfx. volcanii* (Holmes *et al.*, 1991)

So, after transformation of the plasmid pTA233 with inserts into JM109 followed by miniprep preparation, this miniprep was transformed into the dam$^-$ (GM121) *E. coli* strain (Figures 5.15 and 5.16). Also, pTA233 with no insert was transformed into GM121 in order to be able to be transformed into H98 as a control (Figure 5.16). The unmethylated plasmid was checked by agarose gel electrophoresis after single and double restriction digestion (Figures 5.15 and 5.17).

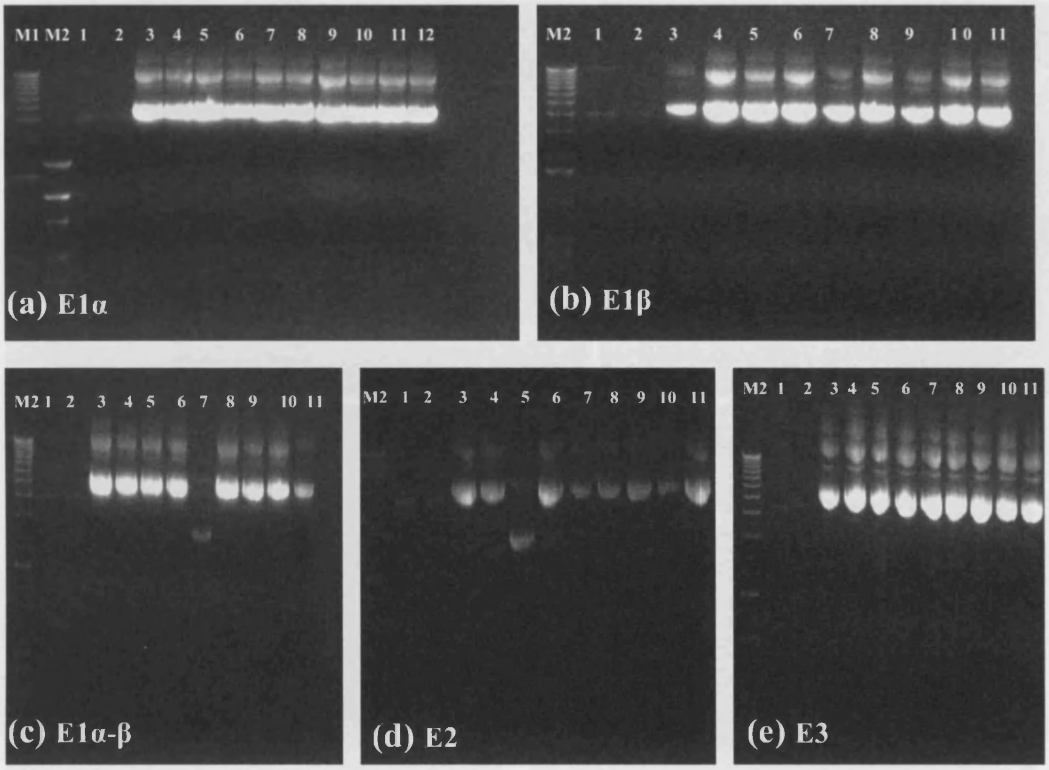

Figure 5.11: Miniprep of *Hfx. volcanii* OADHC genes after cloning into pTA233.
Marker lanes M1 and M2 contain 100 bp ladder and 1kb ladder, respectively. Lanes 1 and 2: circular pTA233 without insert as a control. The miniprep after cloning into pTA233 and transforming into JM109 cells, were visualized on a 0.8% agarose gel in (a), (b), (c), (d) and (e). All minipreps were successful except in lane 7 and lane 5 of gels E1α-β and E2 respectively. Due to the large size of the vector the size shift is not clear that could be detected by performing double digestion as in Figure 5.12.

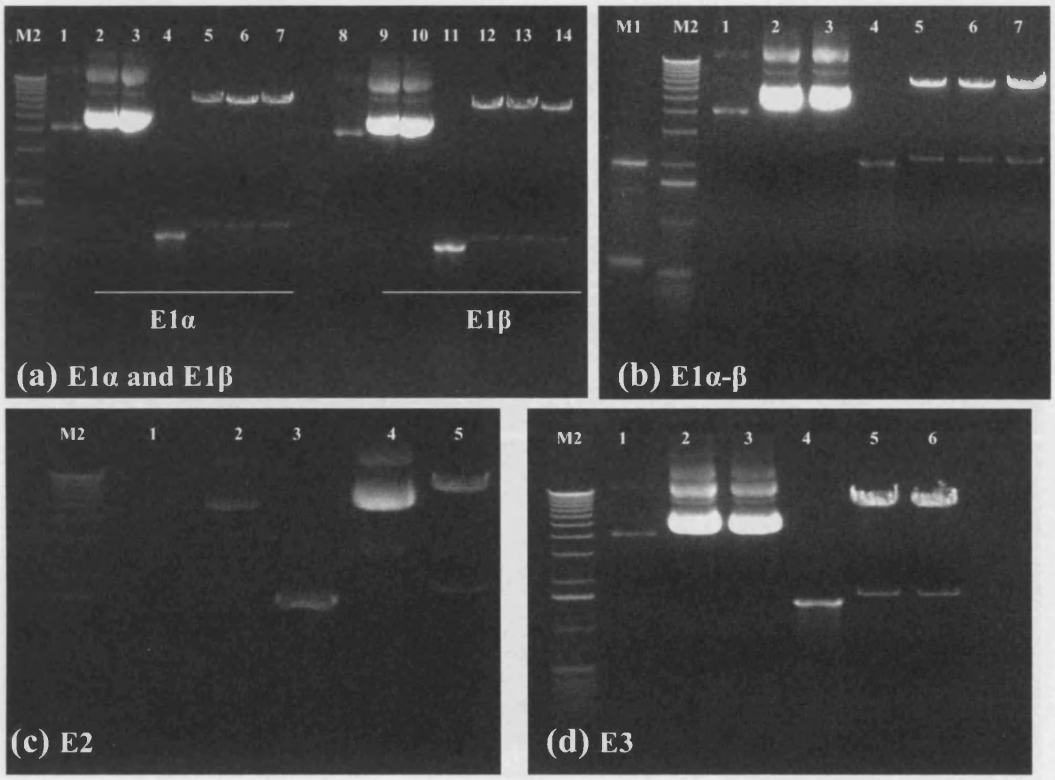

Figure 5.12: Double digestion of OADHC inserts from pTA233 vector.
Marker lanes M1 and M2 contain 100 bp ladder and 1kb ladder, respectively. Double digest of OADHC inserts after cloning into pTA233 and transformation into JM109, were visualized using 0.8% (w/v) agarose gel. Lane 1: circular pTA233 without insert as a control (also lane 8 in gel (a) only and lane 1 and 2 gel (c)). Lanes 2 and 3: miniprep of each gene with PTA233 (also lanes 9 and 10 gel (a) and lane 4 only gel (c)). Lane 4: is a PCR product of each gene used as an insert size control, and also lane 11 gel (a) and lane 3 gel (c). Double digest of each insert using *Hind*III and *Bam*HI is shown in lanes 5-7 and 12-14 gel (a), lanes 5-7 gel (b) and lane 5 gel (c) and lanes 5 and 6 gel (d). Two bands represent double digestion, the higher is the pTA233 vector and the lower one is the insert (higher M_r than the PCR product band due to presence of *fdx* promoter, 128 bp).

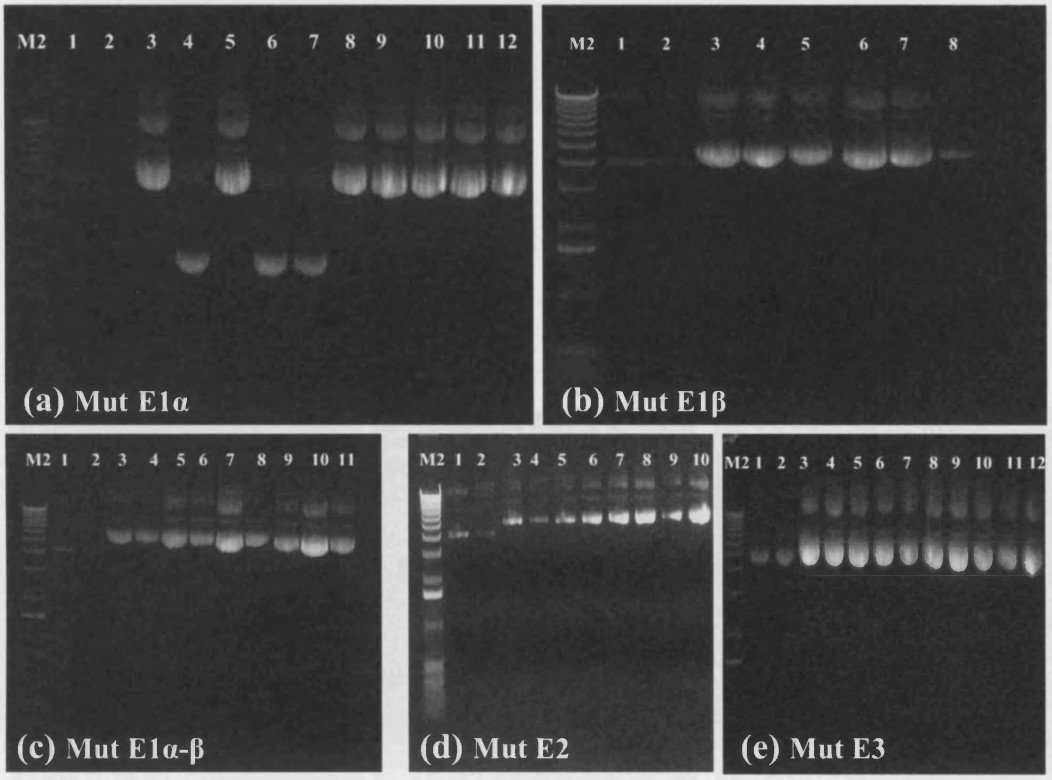

Figure 5.13: Miniprep of *Hfx. volcanii* mutated OADHC after cloning into pTA233.

Marker lane M2: 1kb ladder. Lanes 1 and 2: circular pTA233 without insert as a control. The minipreps, after cloning into pTA233 and transforming into JM109 cells, were visualized on a 0.8% agarose gel in (a), (b), (c), (d) and (e). All preparations were successful except those in lanes 4, 6 and 7 of gel (a). Due to the large size of the vector the size shift is not clear that could be detected by performing double digestion as in Figure 5.14.

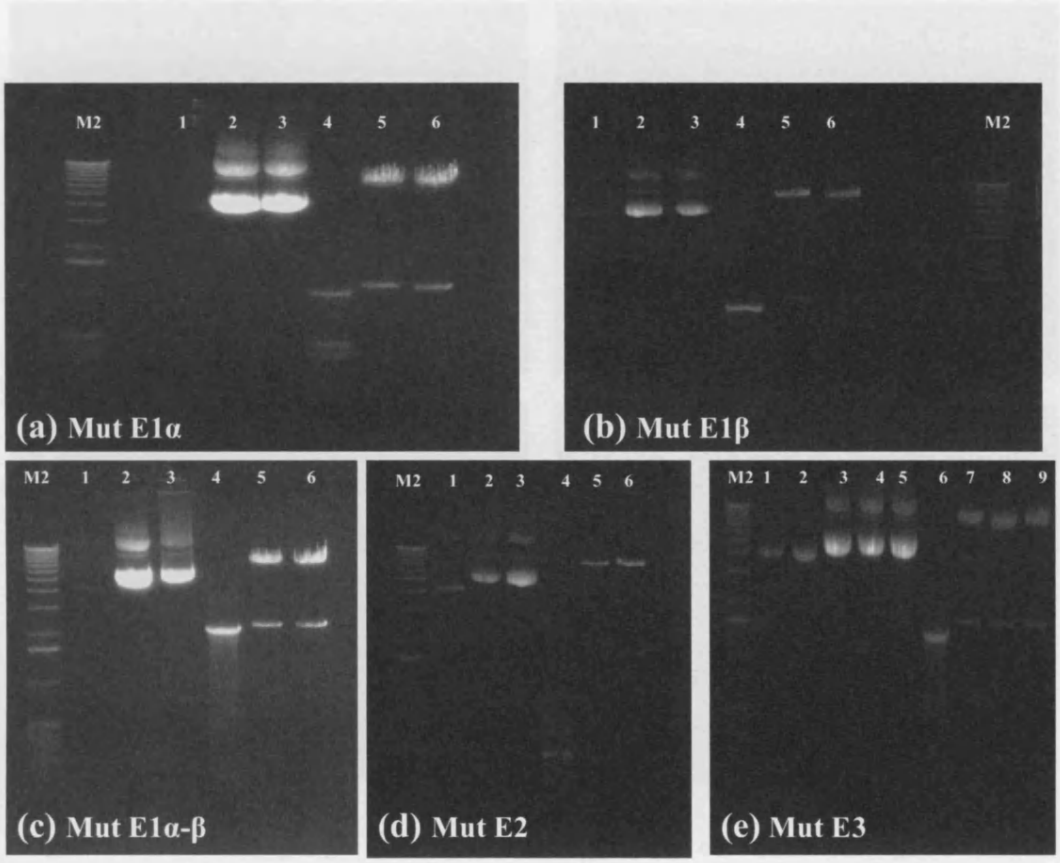

Figure 5.14: Double digestion of mutated OADHC inserts from pTA233 vector.
Marker lane M2: 1kb ladder. Double digest of mutated OADHC inserts after cloning into pTA233 and transformation into JM109, were visualized using 0.8% (w/v) agarose gel. Lane 1: circular pTA233 without insert as a control, except gel (e): both lanes 1 and 2. Lanes 2 and 3: miniprep of each mutated gene with pTA233 except gel (e): lanes 3, 4 and 5. Lane 4 is a PCR product of each gene used as an insert size control, except gel (e): lane 6. Gel (d) lane 4 was a failure. Double digest of each insert using *Hind*III and *Bam*HI is shown in lanes 5 and 6 of gels a, b, c, d and e; gel (e) double digest represented in lanes 7-9. Two bands represent double digestion, the higher is the pTA233 vector and the lower one is the insert (higher M_r than the PCR product band due to presence of *fdx* promoter, 128 bp).

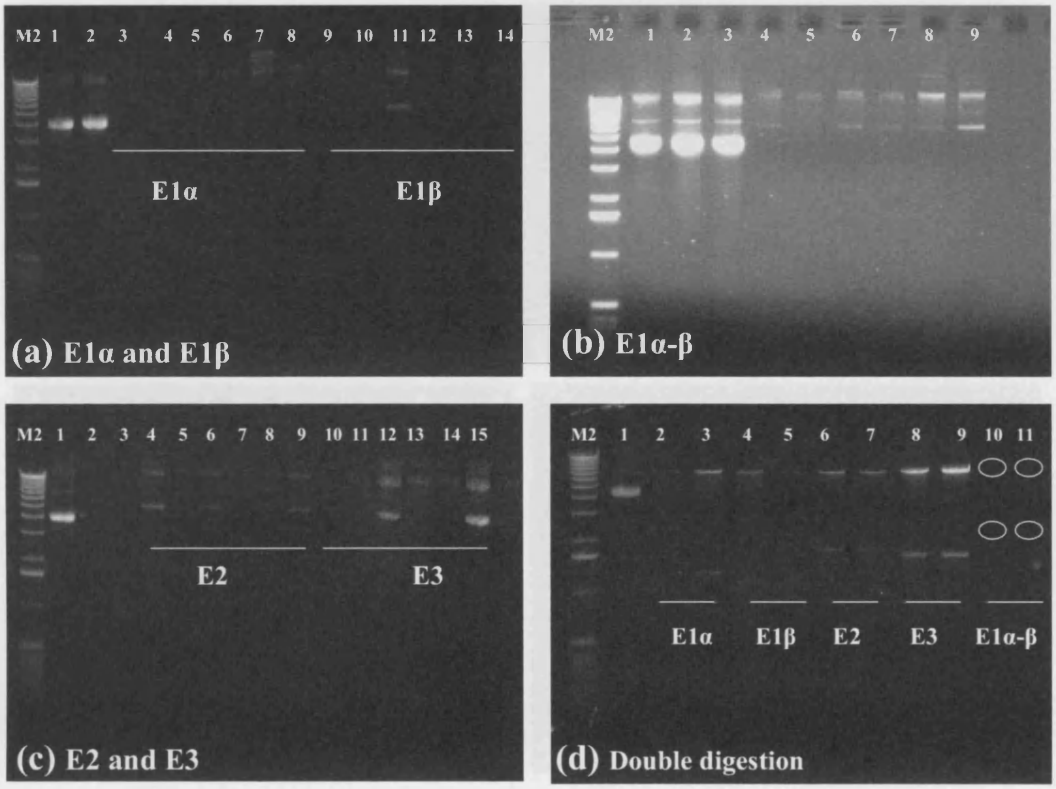

Figure 5.15: Miniprep and double digestion of OADHC genes after transformation into GM121.

Marker lane M2: 1kb ladder. Lanes 1 and 2: circular pTA233 without insert as a control; also lane 3 in gel (b) and (c). Each miniprep, after cloning into pTA233 and transformation into GM121 cells (resulting in unmethylated DNA), was visualized on a 0.8% agarose gel in (a), (b) and (c). A size shift indicates successful transformation of each gene of OADHC into pTA233; all minipreps were successful but have low DNA concentrations. Gel (d) shows a double digestion of the previous minipreps using *Hind*III and *Bam*HI. Lanes 1: circular pTA233 without insert as a control. Lanes 2-11: double digestions result with two bands the higher is the pTA233 vector and the lower one is the insert (higher M_r than the PCR product band due to presence of *fdx* promoter, 128 bp).

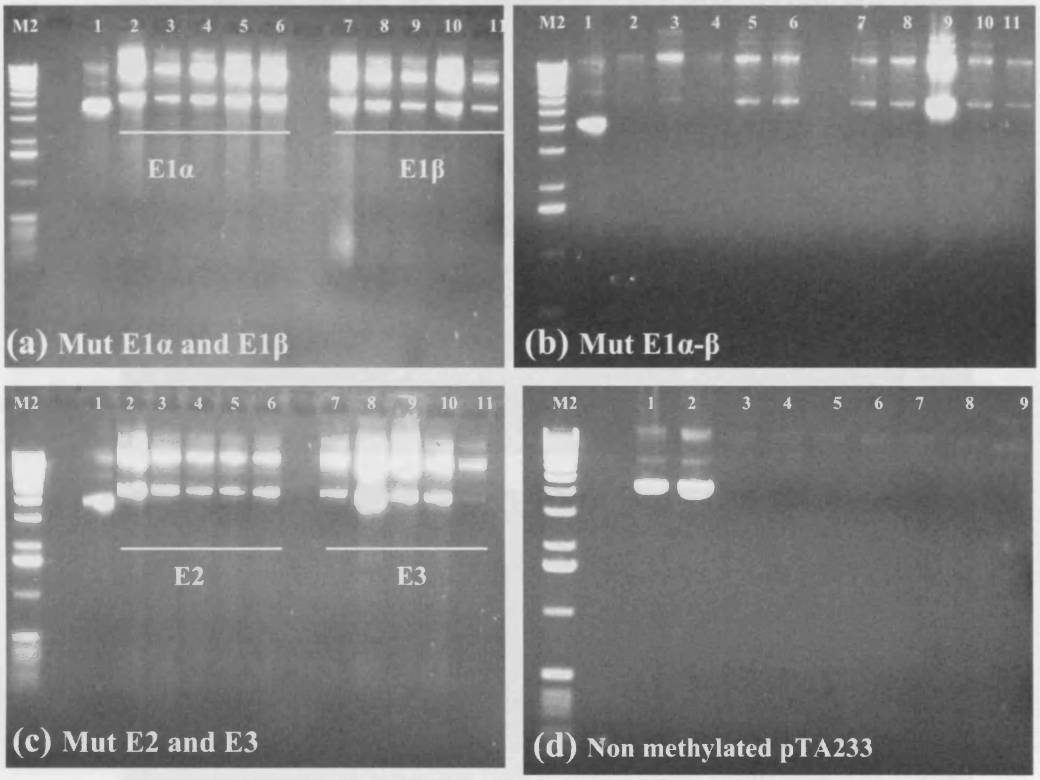

Figure 5.16: Minipreps of mutated OADHC of *Hfx. volcanii* after transformation into GM121.

Marker lane M2: 1kb ladder. Lanes 1: circular pTA233 without insert as a control, also lane 2 in gel (d). Each miniprep after cloning into pTA233 and transformation into GM121 cells (resulting in unmethylated DNA), was visualized on a 0.8% agarose gel in (a), (b) and (c). A size shift indicates successful transformation of each mutated gene of OADHC into pTA233. Gel (d) shows the transformation of circular pTA233 into GM121 ending with unmethylated vector in order to be used as a control in subsequent transformation into H98 strain.

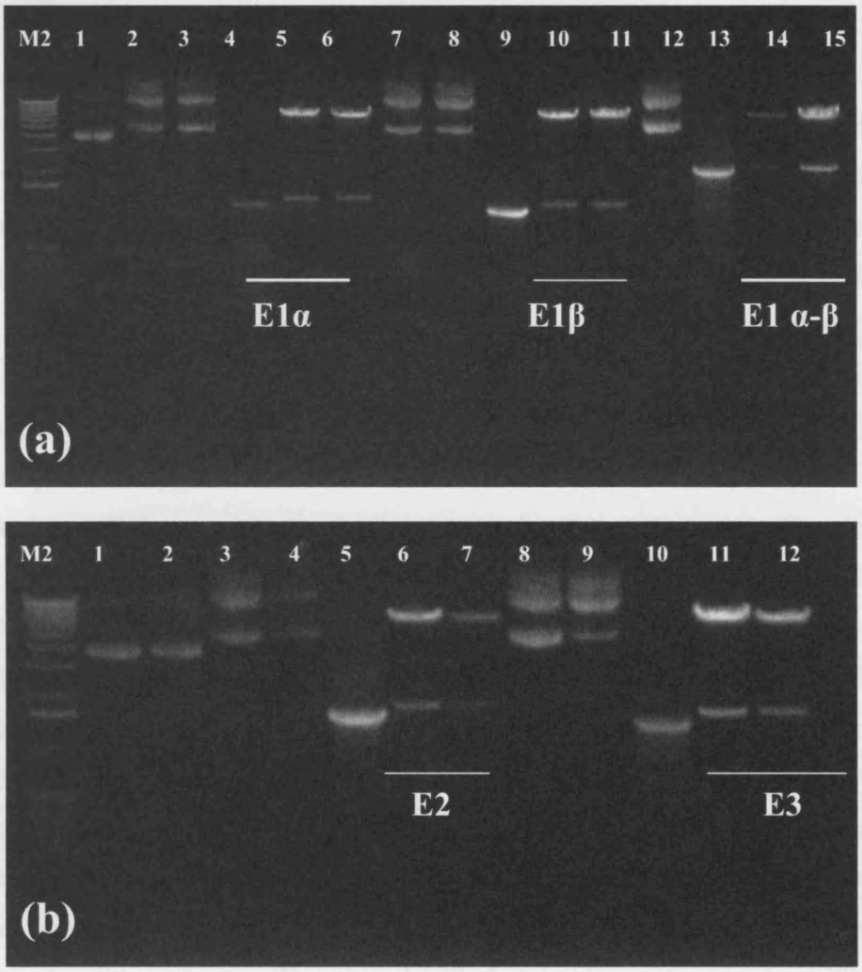

Figure 5.17: Double digestion of mutated OADHC genes of *Hfx. volcanii* after transformation in GM121.

Marker lane M2: 1kb ladder. Lanes 1: circular pTA233 without insert as a control, also lane 2 in gel (b). Gel (a) lanes: 2, 3, 7, 8 and 12 and gel (b) lanes 3, 4, 8 and 9 show miniprep of each mutated gene with pTA233. Gel (a) lanes: 4, 9 and 13 and gel (b) lanes: 5 and 10 are PCR product of each gene used as an insert size control. Double digest of each insert using *Hind*III and *Bam*HI is shown in lanes 5, 6, 10, 11, 14 and 15 gel (a) and lanes 6,7,11 and 12 gel (b). Two bands represent double digestion, the higher is the pTA233 vector and the lower one is the insert (higher M_r than the PCR product band due to presence of *fdx* promoter, 128 bp).

5.4.5 Transformation of *Hfx. volcanii* strain H98 competent cells

Hfx. volcanii strain H98 (Δ*pyrE2*, Δ*hdrB*) is a recently-developed, gene knock-out mutant based of the *pyrE2* gene, which encodes orotate phosphoribosyl transferase involved in uracil biosynthesis (Bitan-Banin *et al.*, 2003). The *hdrB* marker is a useful addition to the current genetic repertoire, as deletion of this gene confers thymidine auxotrophy in the rich medium (Hv-YPC) (Ortenberg *et al.*, 2000). The shuttle vector pTA233 was derived from pTA192 by inserting the replication origin of the *Hfx. volcanii* episome pHV2. The shuttle vector was able to transform the corresponding *Hfx. volcanii* deletion strain H98 to prototrophy for the appropriate marker (thymidine).

The procedure that was used to transform *Hfx. volcanii* is simple and reliable. But for highest efficiency and reproducibility, it is important to exercise care in two practical details, avoiding cell lysis and ensuring that the final PEG concentration is correct. So, any rough handling of the spheroplasts that may cause lysis was avoided. Also, it has been found that even if a small proportion of the cell lyse, sufficient chromosomal DNA is released to result in PEG-NaCl precipitation of DNA making it unavailable to the cells (Cline *et al.*, 1989).

Transformation was performed using the pTA233-E1α-β construct, transforming both mutated and non-mutated E1α-β. Several controls were carried out in parallel, such as transformation with water and also with unmethylated circular pTA233 vector with no insert. The control with the circular vector was to ensure any detectable enzyme activity is due to expression of transformed constructs rather than from the natural activity of the host strain.

The plates were incubated in sealed plastic bags at 45°C for 5-6 days. Colonies on Hv-YPC without thymidine took long time to grow due to regeneration of cells. Well-defined orange coloured colonies were recognized after almost 6 days with all constructs except with cells that had been transformed with water. Then the colonies were inoculated into Hv-YPC broth for 24-48 h until the OD_{600nm} reached $\geq$ 1.2. Finally, the broth culture was used for further studies as mentioned below.

5.4.6 Analysis of transformants

5.4.6.1 Recombinant E1 activity

A cell extract was prepared as mentioned in Chapter 2 (Section 2.2.2.1). The recombinant E1 (α-β construct) enzyme was incubated with TPP for 10 min at 45°C prior to assay, a lag in the production of product being observed if the reaction was initiated without prior incubation (Chapter 2, Section 2.2.2.7). E1 enzymic activity was detected and could be measured with mutated E1 rather than non-mutated E1 (Figure 5.19). Also, with a cell extract of cell transformed with pTA233 with no insert, the enzyme activity was 5-fold lower than that found with the expressed protein (Figure 5.20), confirming that the activity recovered was low, but was due to the expressed protein. Kinetic parameters were analyzed using the 3-methyl-2-oxopentanoate (deaminated isoleucine) (Figure 5.21) and pyruvate (Figure 5.22). On the other hand, due to the low observed activity, it was difficult to do kinetic studies using 4-methyl- 2-oxopentanoate (deaminated leucine) or 3-methyl-2-oxobutanoate (deaminated valine). However, no activity was found with 2-oxoglutarate. Generally, it was thought that the calculated activity was low due to the low copy number of the plasmid compared to other plasmids. The calculated parameters with these substrates are given in Table 5.1.

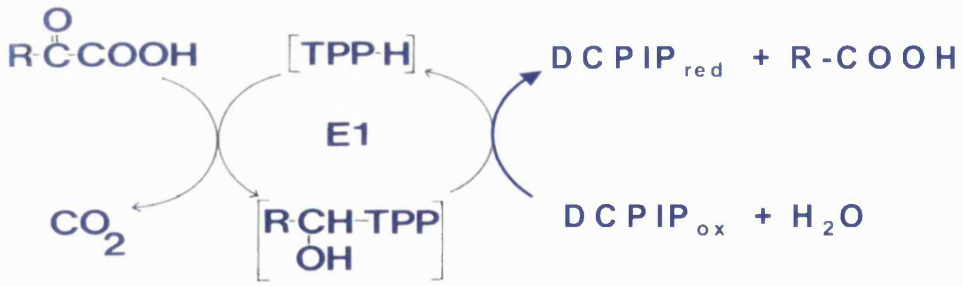

Figure 5.18: Scheme illustrating the basis of the E1 assay with DCPIP as an artificial electron acceptor.

Figures below represent spectrophotometric traces of the measurement of E1α-β enzymic activity with 3-methyl-2-oxopentanoate (deaminated isoleucine) as substrate. The activity was followed by measuring the linear decrease in absorbance at 595 nm over 15 min.

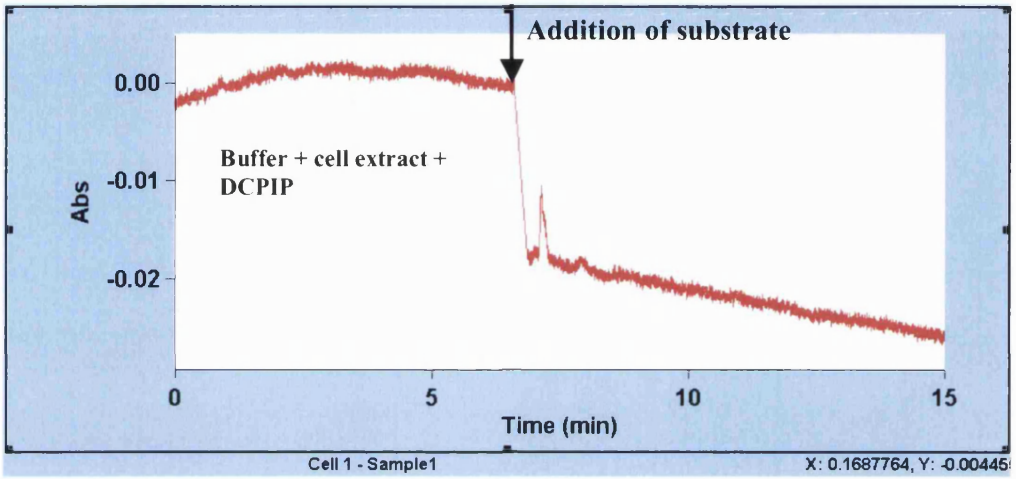

Figure 5.19: 100 µl of *Hfx. volcanii* transformed with mutated E1α-β

The first ~5 min is buffer + cell extract + DCPIP: $\Delta A_{595} = 0.0005\ A_{595}$/min.
After addition of substrate : $\Delta A_{595} = -0.0012\ A_{595}$/min.
The rate of reaction = -0.0012- 0.0005 = -0.0017 A_{595}/min. **Net rate = 0.0017 A_{595}/min.**

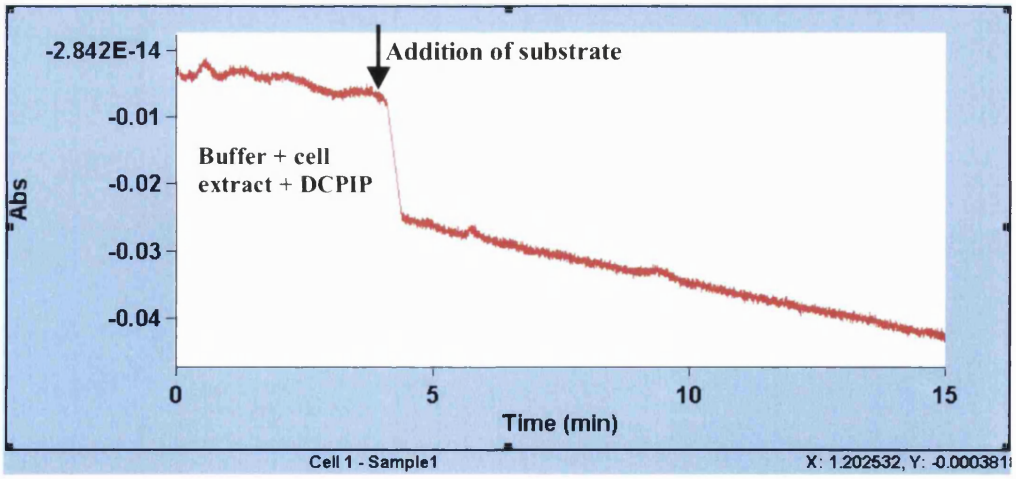

Figure 5.20: 100 µl of *Hfx. volcanii* transformed with pTA233 vector.

The first ~5 min is buffer + cell extract + DCPIP: $\Delta A_{595} = -0.0013\ A_{595}$/min.
After addition of substrate :$\Delta A_{595} = -0.0016\ A_{595}$/min.
The rate of reaction = -0.0016- (-0.0003) = -0.0003 A_{595}/min. **Net rate = 0.0003 A_{595}/min.**

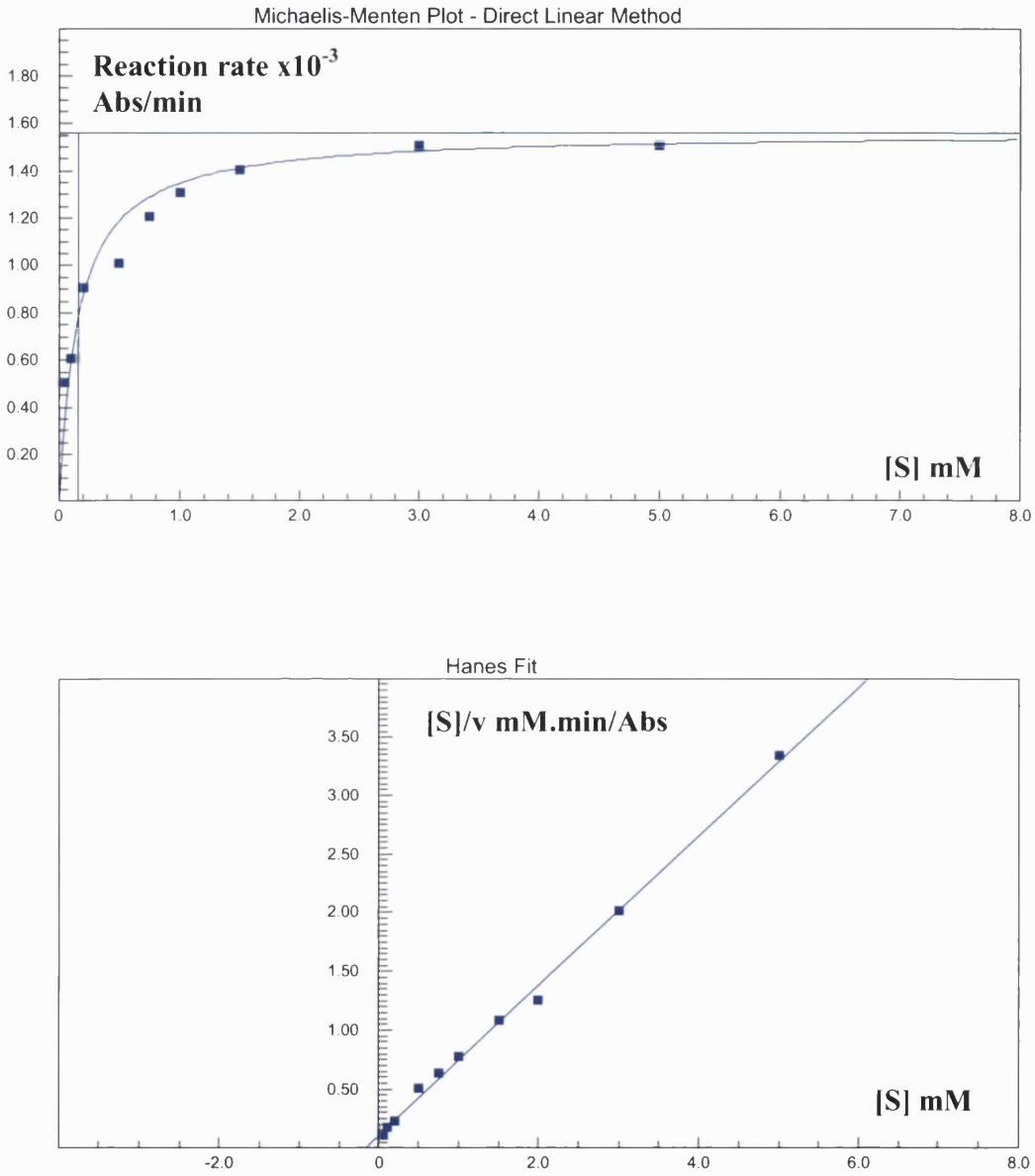

Figure 5.21: Kinetic analysis of mutated E1α-β using 3-methyl-2-oxopentanoate (deaminated isoleucine) as substrate.

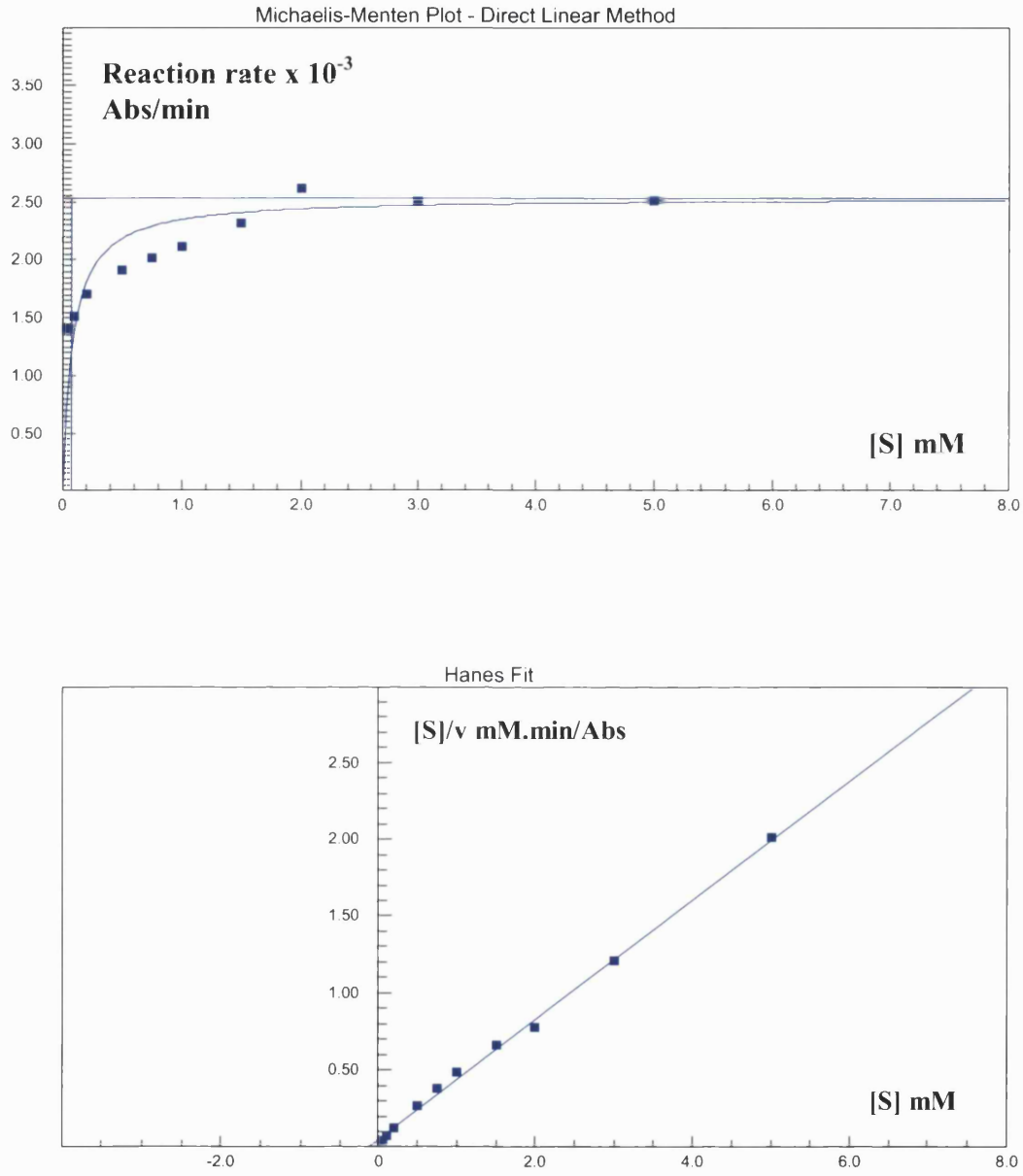

Figure 5.22: Kinetic analysis of mutated E1α-β using pyruvate as substrate.

Table 5.1: Kinetic parameters determined for recombinant E1α-β from *Hfx. volcanii* at 45°C with branched-chain 2-oxoacids, pyruvate and 2-oxoglutarate as potential substrates.

2-oxoacids substrate	V_{max} (U/mg protein)	K_m (mM)
3-Methyl-2-oxopentanoate	5.4 (± 0.1) x 10^{-4}	0.16 (± 0.1)
Pyruvate	8.5 (± 0.1) x 10^{-4}	0.08 (± 0.1)
2-Oxoglutarate	0	0

1 Unit of enzyme activity (U) is defined as 1 µmol DCPIP reduced per minute.
*Enzyme activity with both 4-Methyl- 2-oxopentanoate and 3-Methyl- 2-oxobutanoate was too low to calculate V_{max} and K_m.

5.4.6.2 Miniprep preparation and double digestion

Due to the very low activity of the recombinant E1α-β as mentioned in Table 5.1, a miniprep preparation and double digestion of the transformant were performed to confirm the presence of the insert in the plasmid and to ensure that it had not been lost during transformation. Figure 5.23 represents 0.8% agarose gel of the miniprep, double digestion of the recombinant E1α-β gene of both mutated and non-mutated and the transformation control pTA233 running against pTA233 with no insert, and PCR product of E1. With the miniprep preparation, the size shift against plasmid lacking insert indicates that the plasmid still possesses the insert. Also, running the control pTA233 vector lacking insert and transformed into H98 indicates no contamination and confirms the absence of an insert. In addition, the double digestion indicates that the plasmid still possess the insert of the correct size, although the resultant band was too faint to be visible on the photographed gel but it could be seen more clearly under UV light (Figure 5.24).

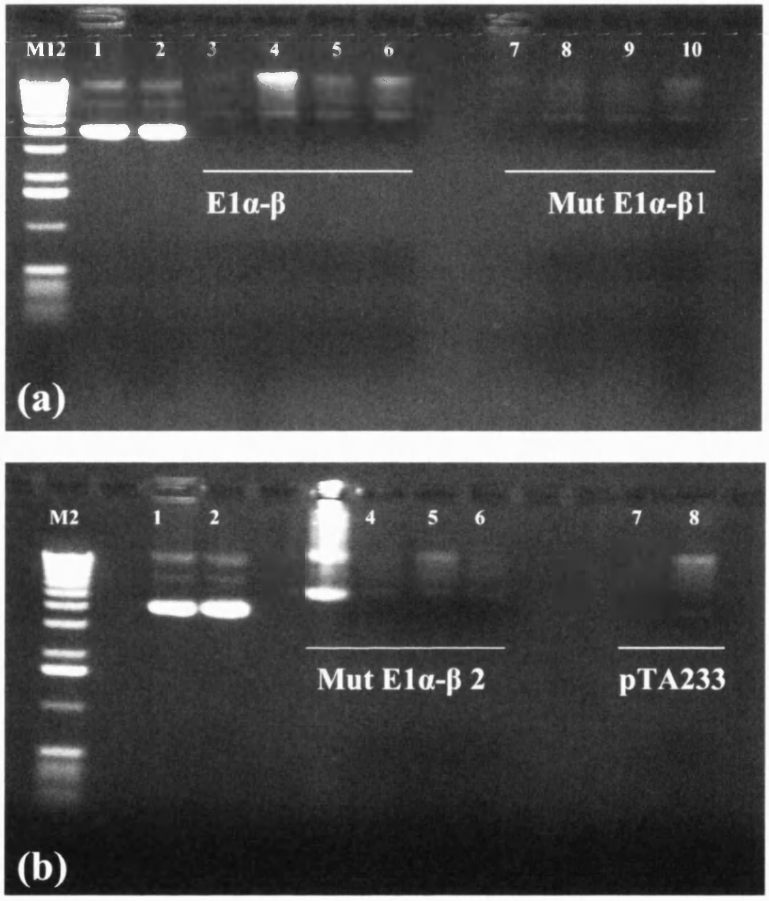

Figure 5.23: Miniprep of plasmid pTA233 containing mutated and non-mutated E1α-β after transformation into *Hfx. volcanii* H98.

Marker lane M2: 1kb ladder. Lanes 1 and 2: circular pTA233 without insert as a control. A size shift indicating successful transformation of mutated and non-mutated E1 in pTA233, into *Hfx. volcanii* H98. Gel (a) lanes 3 and 7: miniprep of construct before transformation into *Hfx. volcanii* H98; lanes 4-6: miniprep of non-mutated E1α-β construct in pTA233 after transformation into *Hfx. volcanii* H98 strain and lanes 8-10: miniprep of mutated E1α-β (1)* construct. Gel (b) lane 3 miniprep of construct before transformation; lanes 4-6: miniprep of mutated E1α-β (2)* construct, lane 7: miniprep of pTA233 before transfomation into *Hfx. volcanii* H98, and lane 8 miniprep of pTA233 after transformation into *Hfx. volcanii* H98.
*E1α-β (1) and E1α-β (2): two different clones of mutated E1α-β.

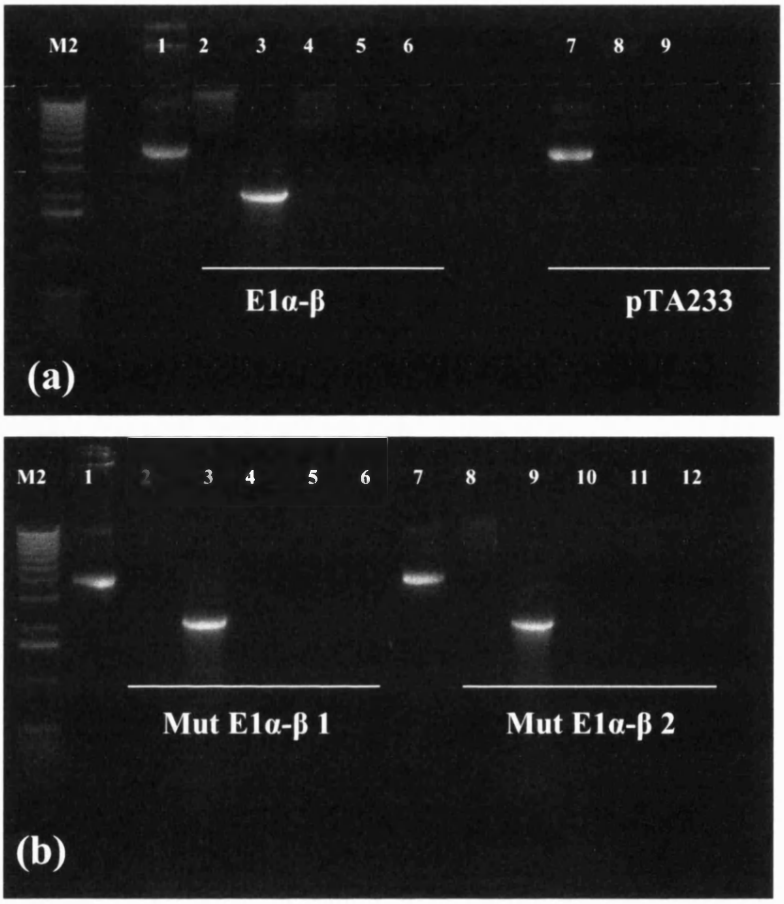

Figure 5.24:Double digestion of pTA233 containing E1α-β inserts.
Marker lane M2: 1kb ladder. Lanes 1 and 7: circular pTA233 without insert as a control. Gel (a) lanes: 2 and 8, gel (b) lanes: 2 and 8, show non-methylated miniprep of each gene with pTA233. Gel (a) lane: 3 and gel (b) lanes: 3 and 9 are PCR products of each gene used as an insert size control. Double digestion of each insert using *Hind*III and *Bam*HI is shown in gel (a) lanes 4-6 and 9 and gel (b) lanes: 4-6 and 10-12. Two bands represent double digestion; the higher is the PTA233 vector and the lower one is the insert (higher M_r than the PCR product band due to presence of *fdx* promoter, 128 bp). The bands were visible under UV light, but were of insufficient intensity to be clear on the gel photograph.
*E1α-β (1) and E1α-β (2): two different clones of mutated E1α-β.

5.4.6.2 SDS-PAGE

Both cell extracts and cell debris that were prepared by sonication (Chapter 2 Section 2.2.2.1) of *Hfx* H98 transformed with pTA233 carrying mutated and non-mutated E1α-β, and also the pTA233 control vector (no insert), were analyzed by SDS-PAGE. No difference was found in the protein profile between cells transformed with the pTA233 vector with no insert and with those transformed with pTA233 carrying the E1 gene (Figure 5.25). The predicted M_r values of the α and β polypeptide are 40971 and 36020, respectively, from the gene sequence.

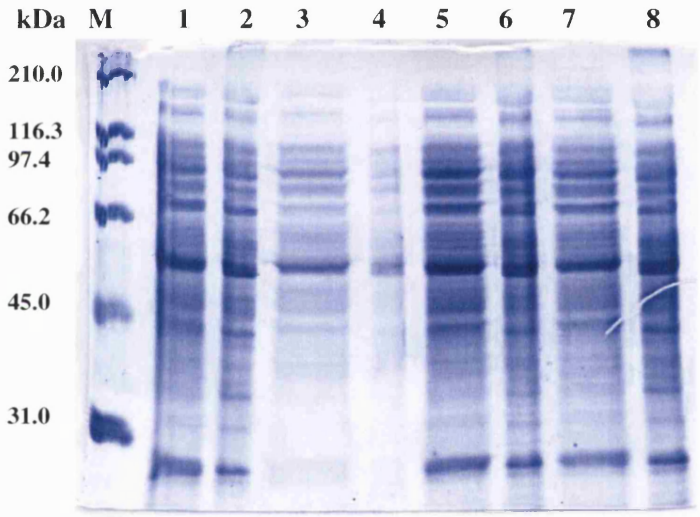

Figure 5.25: Expression of *Hfx. volcanii* recombinant E1.
This SDS-PAGE gel shows cell extracts and cell debris of *Hfx.* H98 transformed with pTA233 carrying mutated and non-mutated E1α-β and the pTA233 control vector. M: standard protein markers, **odd lanes**: soluble extract; **even lanes**: cell debris. Lanes 1 and 2: non-mutated E1α-β; lanes 3 and 4: mutated E1α-β (1)*, lanes 5 and 6: mutated E1α-β (2)* and lanes 7 and 8 pTA233.
* Two different clones of mutated E1α-β.

5.5 Discussion

The archaeon *Hfx. volcanii* was previously shown to include and transcribe the genes of a putative OADHC, but their presence remains a mystery because no enzymic activity could be found in cell extracts using any of the known OADHC substrates. Also, the activity of the *Hfx. volcanii* OADHC could not be detected after growth on any of the carbon sources or growth conditions, and inactivation of one of the genes did not lead to any nutrient phenotype (Jolley *et al.*, 1996b). Therefore, the aim of this chapter was to study the over-expression of the OADHC genes in the native organism, which may lead to measurable enzymatic activity to enable the determination of the substrate specificity of this putative complex.

Progress in archaeal molecular biology requires tools for genetic analysis. Previously it has been found that Archaea are insensitive to most of the antibiotics used in bacterial vector-host systems. But later it was reported that mevinolin, an inhibitor of eukaryotic Hmg-CoA, also strongly inhibits this enzyme in haloarchaeal extracts and prevents cell growth in liquid media (Cabrera *et al.*, 1986). Then a number of shuttle vectors had been constructed using mevinolin, other antibiotics and even nutritional requirements enabling the transformation in both *E. coli* and *Hfx. volcanii*. This will facilitate the expression of protein in their native, high-salinity environment.

In this study, clones pass through a number of cloning vectors before reaching the expression vector that was used to transform the expression strain *Hfx.* H98. pGEM-T was used to facilitate sequencing of the clones. Then the clones with the correct sequences were cloned into pIL11 cloning vector in order to recover the *fdx* promoter, before being inserted into the shuttle vector pTA233. The promoter *fdx* appeared to be one of the strongest promoters investigated, yielding large activities even during the exponential growth phase. The *fdx* gene is a typical house-keeping constitutive gene, and the expression pattern determined reflects the predominant production of *fdx* mRNA during the exponential growth phase (Gregor and Pfeifer, 2005; Pfeifer *et al.*, 1993). After cloning into the pTA233 expression vector the constructs were transformed into dam$^-$ *E. coli* strain GM121 before transforming into expression strain *Hfx* H98.

Generally there are two methylases (dam and dcm) found in most strains of *E. coli*. Dam methylase recognizes the DNA sequence GATC and methylates the adenine residue at the N-6 position, while dcm methylase recognizes the DNA sequence CCAGG and CCTGG and methylates the internal cytosine at the C-5 position. *Hfx. volcanii* has at least one restriction system that degrades methylated DNA. Specifically, this system recognizes methylated adenine residues. Therefore, transforming methylated DNA into *Hfx. volcanii* results in a 10^3 drop in transformation efficiency and the loss of most of constructs by incorporation of the resistance marker into the chromosome (Holmes *et al.*, 1991). It should be noted, however, that dam mutants tend to be unstable (Marinus, 1987), and it is not recommended to use them for routine cloning. Constructions should therefore use dam^+ strains (JM109) followed by passage through dam^- (GM121) just prior to *Hfx. volcanii* transformation.

So, the unmethylated constructs containing the E1α-β genes (both mutated and non-mutated) were transformed into the *Hfx.* H98 expression strain. The presence of the inserts plus *fdx* promoter in pTA233 was confirmed by miniprep preparation and double digestion. However, there was no evidence of any expressed protein in the soluble or insoluble fractions when run on SDS-PAGE and there was no difference between lanes with mutated and non-mutated recombinant protein, or with the lane with pTA233 without insert. So, either the recombinant protein was expressed at a very low concentration, or was possibly degraded after translation, which is unexpected since the genes are expressed in their native environment. In addition it is possible that the DNA is not completely unmethylated and the host cells recognize them as foreign genes.

There was no activity detected in the cell extracts that contain the recombinant non-mutated E1α-β with any of the OADHC substrates, possibly indicating an inactive protein due to an early stop codon. Also, no activity was found in all extracts transformed with pTA233 with no insert. However, the recombinant mutated E1 enzyme was found to possess very low catalytic activity with the branched chain 2-oxoacid, 3-methyl-2-oxopentanoate (deaminated isoleucine) and even lower activity with 4-methyl- 2-oxopentanoate (deaminated leucine) and methyl-2-oxobutanoate (deaminated valine). It is also possessed an activity with pyruvate as a substrate but no

activity could be found with 2-oxoglutarate. This low activity may be due to the nature of the expression vector pTA233, which is based on pHV2 which is a natural plasmid found in *Hfx. volcanii*, with approximately six copies per cell (Charlebois *et al.*, 1987). This low copy number may lead to a lower activity if compared to expression using other *E. coli* vectors with higher copy numbers.

These results coincide with the previous findings that the expression of E3 increased significantly when *Hfx. volcanii* was grown on branched-chain amino acids especially with isoleucine. However, no complex or E1 activity could be detected in the growth studies. Additionally, our research group has recently achieved the expression of E1 from *Thermoplasma acidophilum* in *E. coli*. They demonstrated that the protein products form an $\alpha_2\beta_2$ heterotetramer possessing the decarboxylase catalytic activity characteristic with the three branched-chain 2-oxoacids and pyruvate, but no activity with 2-oxoglutarate. This represents the first report of the catalytic function of these putative archaeal multienzyme complexes (Heath *et al.*, 2004).

It has been found that most genes rely on ATG as a start codon, while GTG and TTG are sparsely used. Also, genes with an ATG start codon tend to have a higher percentage of Shine-Dalgarno (SD) sequence than genes with either GTG or TTG. The increase was significant in 12 genomes and most pronounced in five euryarchaeal genome with the percentage having SD sequences exceeding 40% (Ma *et al.*, 2002). Considering that ATG is a more potent initiator than GTG and TTG (Ringquist *et al.*, 1992), the weak start codons GTG and TTG, in conjunction with lack of an SD sequence, might substantially reduce the expression level of a given gene. Also it has been found that some euryarchaeota (*Tp. acidophilum*, *Halobacterium* sp. Strain NRC-1) and especially crenarchaeota (*Sulfolobus solfataricus* and *Pyrobaculum aerophilum*) seem to have gradually lost conservation of both the anti-SD and the SD sequences. Accumulating evidence suggests that many single genes, or initial genes of operons, in these genomes are translated through leaderless mRNA by mechanisms that do not involve the SD-anti-SD interaction (Slupska *et al.*, 2001; Tolstrup *et al.*, 2000; Sensen *et al.*, 1996). These findings may explain the low expression of E1, since it is part of OADHC operon and the E1α is the first gene of the operon with a starting codon GTG.

Finally, the level of expression achieved for halophilic E1 is not sufficient for convenient purification and structural studies. So, for future studies, it is recommended that primers be designed to include a His-tag in order to purify the protein for further studies. Also, it is recommended that commercially available dam$^-$ and dcm$^-$strains of *E. coli* be used to increase the transformation efficiency at that stage of the cloning procedure. Moreover, it is worth trying the expression of E1α and E1β either as separate products or possibly in a coexpression system.

Heterologous expression in E. coli

6.1 Introduction

In order to have a high level of expression of the halophilic OADHC genes, it was thought sensible to express the recombinant protein in *E. coli*. Using *E. coli* has a number of potential advantages over expression in the native organism. Firstly, the rate of growth of *E. coli* is significantly faster than that of *Hfx. volcanii*, even when the later is grown optimally. Secondly, the genetic systems and techniques are at an advanced stage for *E. coli* compared to halophilic archaea, which have only recently been developed. Thirdly, expression of halophilic archaeal proteins in a low salt concentration environment has been shown to result in either soluble inactive protein or insoluble inclusion bodies that require either reactivation or refolding, yet the yields were greater than those obtained from expression in the native organism (Connaris *et al.*, 1999; Jolley *et al.*, 1996b). Also, the addition of a high-salt solution to an *E. coli* extract would be expected to precipitate many of the *E. coli* protein, leaving the halophilic protein in a near-native environment. Moreover, some halophilic proteins, such as DHlipDH, have been shown to reactivate its activity almost immediately after the addition of 2 M NaCl, even after storage for 24 h at 4°C in the absence of salt (Danson *et al.*, 1986).

Therefore, the plan was to express *Hfx. volcanii* E1α and E1β in *E. coli*, in parallel with homologous expression of OADHC in *Hfx. volcanii*. Two project students, Maria Keays (Keays, 2005) and Daniel Nicholson (Nicholson, 2005), carried out the heterologous expression using the pET system under my supervision. Maria performed the first part that included PCR amplification of E1α and E1β genes separately, cloning into pGEM-T, sequencing and the subsequent cloning of E1α into pET-19b (ampicillin resistance). Then Daniel continued with the cloning of E1β into pET-28a (kanamycin resistant), followed by transformation of the constructs separately into BL21 (DE3) pLysS expression strain. Finally, he purified and attempted the refolding of the recombinant proteins.

6.2 Materials

Cell culture: Kanamycin was from Sigma-Aldrich, Gillingham, UK. Unless otherwise mentioned, the rest of chemicals were supplied from Sigma-Aldrich, Gillingham, UK, with high commercial purity.

Molecular biological studies: pET-19b, pET-28a vectors and Bugbuster™ protein extraction reagent were supplied by Novagen, USA. *E. coli* BL21(DE3)pLysS was obtained from Promega, Southampton, UK. The rest of the cell culture and molecular materials are as mentioned in Chapter 5 (Section 5.2).

6.3 Methods

6.3.1 PCR amplification and cloning of E1α and E1β genes

The primers were designed as mentioned in Chapter 5 (Section 5.3.1.1). Primers were adjusted to incorporate *Nde*I and *Bam*HI restriction sites in the forward and reverse primers of each gene, respectively.

FE1α *Nde*I : 5' - CGCC▼ATATGAGCGTGCTTCAACGCG - 3'

RE1α *Bam*HI: 5' - CGCG▼GATCCTCATTCTCTGAGGAATCCTTCGTCG - 3'

FE1β *Nde*I: 5' - CGCC▼ATATGAGCAGTCAGAACCTCACCATCG - 3'

RE1β *Bam*HI: 5' - CGCG▼GATCCTCAGAAGTTCACCGCCTCACG - 3'

In the above oligonucleotide sequences, CGC are the extra bases that were added to permit the binding of restriction enzyme to the PCR product; C▼ATATG and G▼GATCC are the restriction sites of NdeI and BamHI, respectively.
The ATG of the restriction site of NdeI replaces the GTG start codon of *Hfx. volcanii* E1α, since the protein will be expressed in *E. coli*.

The genes encoding E1α and E1β were individually PCR-amplified from *Hfx. volcanii* genomic DNA with Vent polymerase (Chapter 2 Section 2.2.4.3), using primers that introduced restriction sites to the 5' and 3' ends of the gene product (*Nde*I and *Bam*HI). These primers also permitted the introduction of an N-terminal His tag into the protein products when expressed in the pET vector system. 5µl of PCR product were electrophoresed on 1.3% agarose gel as described in Chapter 2 (Section 2.2.4.4). Amplified DNA fragments of the correct size were purified by DNA gel extraction using a QIAEX II kit (Qiagen) following the recommended protocol (Chapter 5, Section 5.3.1.3).

Then the E1α and E1β gene products were A-tailed using *Taq* polymerase and separately ligated into the pGEM®-T easy vector intermediate cloning vector system. Each construct was then transformed separately into competent JM109 cells. Transformants were analysed by miniprep and subsequent restriction enzyme digestion using *Nde*I and *Bam*HI, followed by sequencing of selected transformants using SP6 promoter and T7 terminator primers. The experimental details are mentioned in Chapter 5 (Sections 5.3.1.4 – 5.3.1.8 and 5.3.2.2), except that double digestion with both *Nde*I and *Bam*HI buffer D was used.

For recombinant expression, E1α and E1β genes were recloned into the *Nde*I and *Bam*HI sites of pET-19b (Amp^r) and pET-28a (Kan^r) protein expression vectors, respectively (Figure 6.1 and 6.2). Samples of vector and insert were prepared by double digestion with *Nde*I and *Bam*HI as recommended. These were then ligated using T4 ligase and transformed into JM109 cells. Selected transformants were analysed by miniprep and double digestion to confirm that correct cloning of the insert had occurred.

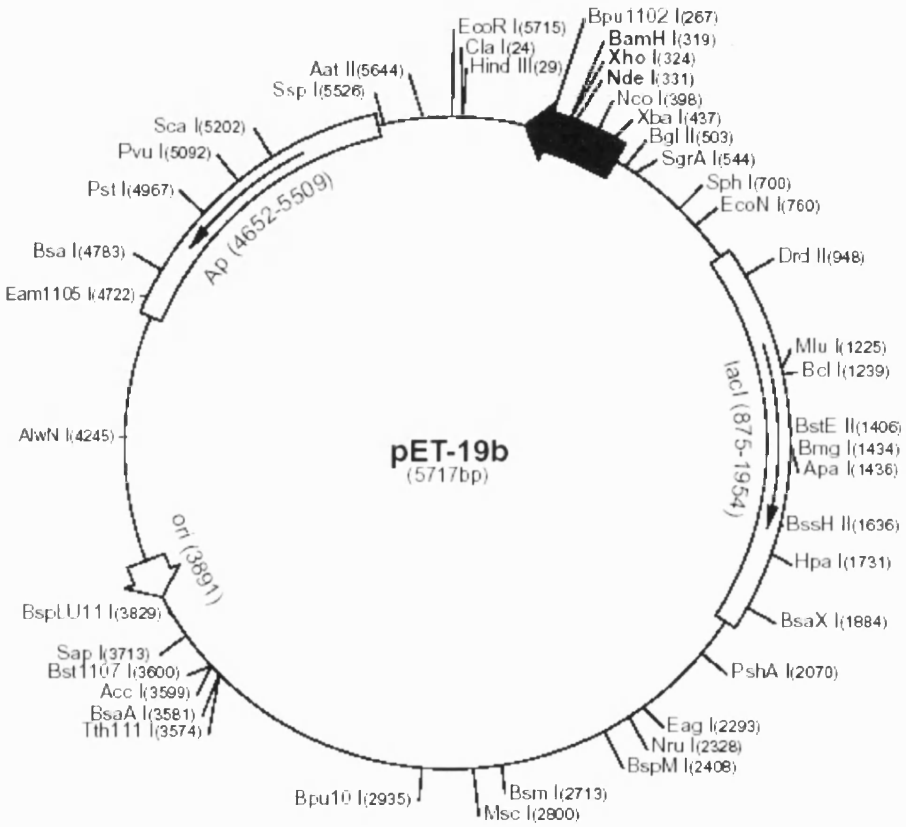

Figure 6.1: Circular map of pET-19b expression vector.
Amp^r denotes the ampicillin/carbencillin resistance gene. Ori is the origin of replication. The vector has multiple cloning sites, a T7 promoter 472-488 (upstream the inserted clone between 319-331), a T7 transcription start 471, a His•Tag coding sequence 366-395, and a *Lac*I coding sequence. This vector was used for E1α cloning.

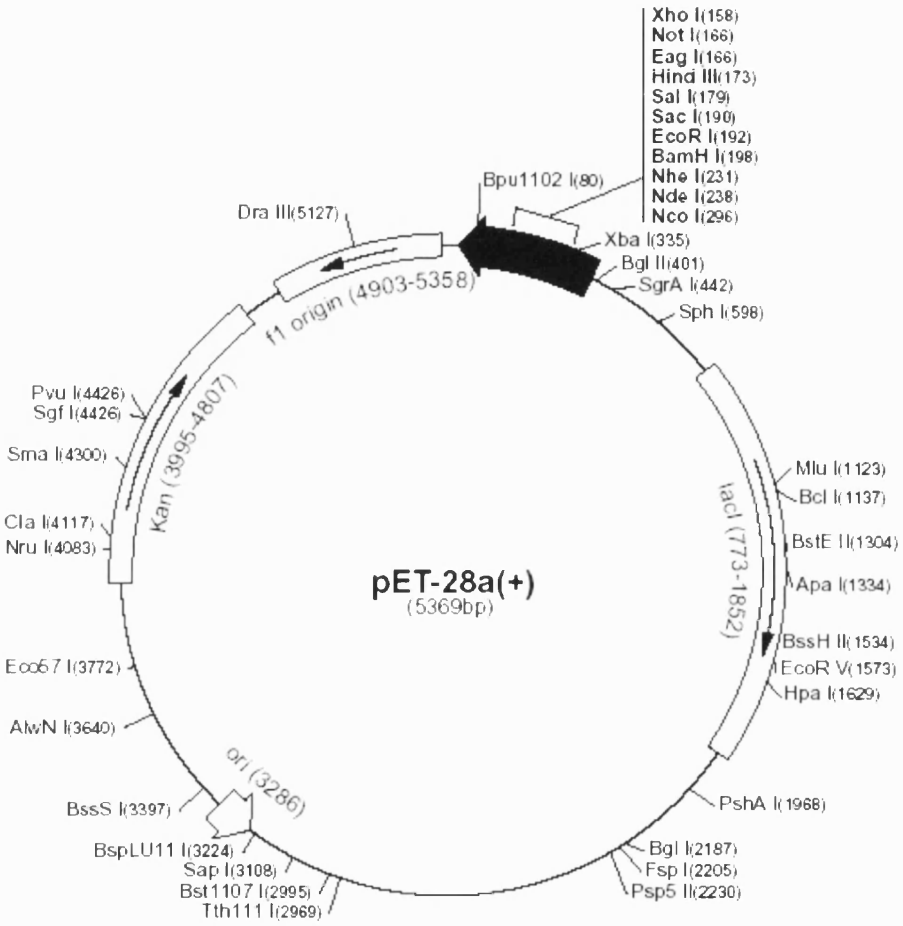

Figure 6.2: Circular map pET-28a expression vector.
Kan^r denotes the kanamycin resistance gene. Ori is the origin of replication. The vector multiple cloning sites, a T7 promoter 370-386 (upstream the inserted clone between 198-238), a T7 transcription start 369, a His•Tag coding sequence 270-287, and a *Lac*I coding sequence. This vector was used for E1β cloning.

6.3.2 Expression of recombinant E1α and E1β

E. coli BL21(DE3)pLysS allows high-efficiency protein expression of any gene under the control of a T7 promoter as is present in the pET system. Cells were separately heat-shock transformed with the pET-19b-E1α and pET-28a-E1β constructs, as recommended by the supplier. Then the transformants were plated on LB media as mention in Chapter 2 (Section 2.2.1) with chloramphenicol (34μg/ml) and either carbencillin (50μg/ml) or kanamycin (30μg/ml). Then the transformed colonies were grown in LB broth with the same composition as the LB plates. These cultures were grown at 37°C, shaking at 180 rpm, to an OD_{600nm} ~ 0.6 and then were split, with one half being induced with 1mM isopropyl-β-D-thiogalactopyranoside (IPTG) and the second left without induction. Addition of IPTG to a growing BL21(DE3)pLysS culture stimulates the production of T7 RNA polymerase, which in turn induces the expression of target gene. Expressions were performed on a small-scale of 500 ml media followed by large-scale expression in 2 L media. Samples were taken throughout 2-4 h incubation and analysed by 10% SDS-PAGE gel (Chapter 2, Section 2.2.4.5). Soluble extracts were prepared using BugBuster/Benzonase, as recommended.

Insoluble extracts were extracted followed by an inclusion-body purification using BugBuster/Benzonase, as recommended by the supplier. These purified extracts were assayed for E1 activity (Chapter 2, Section 2.2.2.7) after solubilization of insoluble protein followed by renaturation and refolding of soluble proteins.

6.3.3 Solubilization of insoluble proteins

The insoluble fraction was dissolved in solubilization buffer (20 mM Tris-Cl pH 8, containing 2 mM EDTA, 2 M KCl, 8 M urea, 50 mM dithiothreitol (DTT))(Connaris *et al.*, 1999) by sequential 1 ml additions up to a total of 5 ml of buffer (5 additions). After each addition, the solution was vortexed vigorously and was then incubated for 10 min to allow the solubilization of proteins in a high-salt environment of the buffer. Following the fifth addition, the solutions were centrifuged at 8,000 x g for 15 min. Then the supernatant (containing soluble proteins) was transferred to 1.5 ml microcentrifuge tubes in 1 ml aliquots.

6.3.4 Renaturation and refolding of recombinant E1

Refolding was initiated by slowly diluting the solubilized pellet 20-fold into renaturation buffer (20 mM Tris-Cl pH 8 containing 2 mM EDTA, 2 M KCl, 10μM TPP, 0.2 mM oxidised glutathione (GSSG), 2 mM reduced glutathione (GSH)). The buffer was added to the soluble protein very slowly drop-by-drop during 1.5 h. Following the 20-fold dilution, the renaturated protein was transferred to a 50 ml tube and gently rotated overnight (18-24 h) at 4° C.

6.4 Results

6.4.1 PCR amplification and cloning of the E1α and E1β gene

Using primers designed with homology upstream and downstream of the open reading frame, the complex genes (E1α and E1β) were successfully PCR-amplified from a genomic extract of *Hfx. volcanii*. The amplification was confirmed by bands of the expected size visualized on a 1.3% (w/v) agarose gel (Figure 6.3).

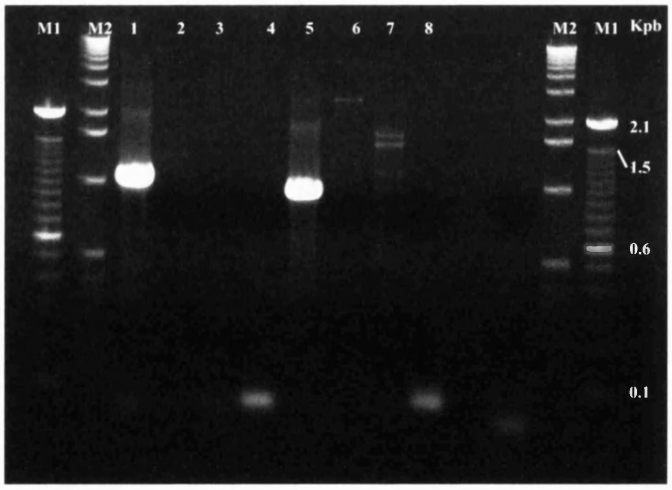

Figure 6.3: PCR amplification of *Hfx. volcanii* E1α and E1β genes.
Marker lanes M1 and M2 contain 100 bp ladder and 1kb ladder, respectively, with sizes in kilo base pairs as shown. The gel is a 1.3% agarose gel showing products of PCR amplification. Lane 1: E1α of 1107 bp, lane 5: E1β 984 bp. Controls without forward or reverse primer are shown in lane 2, 3,6 and 7 of E1α and E1β respectively. Lane 4 and 8: PCR control (lack of template).

The genes were first cloned into pGEM®-T easy vector, which efficiently recovers the A-tailed products from the Vent-amplified PCR reaction. It is an intermediate step that facilitates the sequencing of the cloned inserts using SP6 and T7 primers before proceeding to further steps in the expression procedure. High efficiency *E. coli* JM109 was separately heat-shock transformed with constructs of pGEM®-T easy vector with E1α or E1β genes. At the end a miniprep purification was performed; 5μl of each gene miniprep was visualized using 0.8% agarose gel electrophoresis against circular pGEM®-T Easy vector with no insert; a size shift indicates the successful cloning of E1α and E1β genes into pGEM®-T Easy vector (Figure 6.4). One of each successful clones of E1α and E1β was completely sequenced. The results of sequencing were checked and aligned. The clones were sequenced to identify one without mismatch errors, which then provided a reliable source of the gene for subsequent cloning. The successful cloning strategy is summarized in (Figures 6.3 and 6.4).

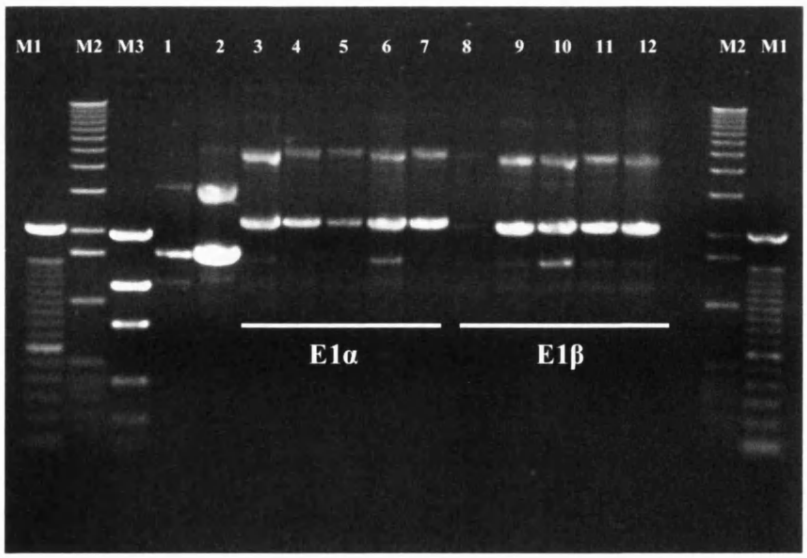

Figure 6.4: Minipreps of *Hfx. volcanii* E1α and E1β genes after cloning into pGEM-T.

Marker lanes M1, M2 and M3 contain 100 bp ladder, 1kb ladder and low DNA mass ladder, respectively. The minipreps after cloning into pGEM-T are shown on a 0.8% agarose gel. Lanes 1 and 2: circular pGEM-T without insert as a control. A size shift indicates successful ligation of E1α and E1β genes into pGEM-T. Lanes 3-7: E1α minipreps and lanes 8-12: E1β minipreps. The minipreps in lane 6 and 9 were completely sequenced and used for subsequent cloning.

The E1α and E1β genes were excised from pGEM®-T Easy vector (Figure 6.5) and cloned into the *Nde*I and *Bam*HI sites of pET-19b and pET-28a expression vectors, respectively, generating the recombinant expression vectors pET-19b-E1α and pET-28a-E1β. The ligated samples were transformed into JM109 competent cells and then minipreps of each clone were prepared and tested by size shifting against circular pET-19b and pET-28a without insert (Figure 6.6). Transformation of the constructs into JM109 was carried out in order to have enough DNA to transform the expression host BL21(DE3)pLysS.

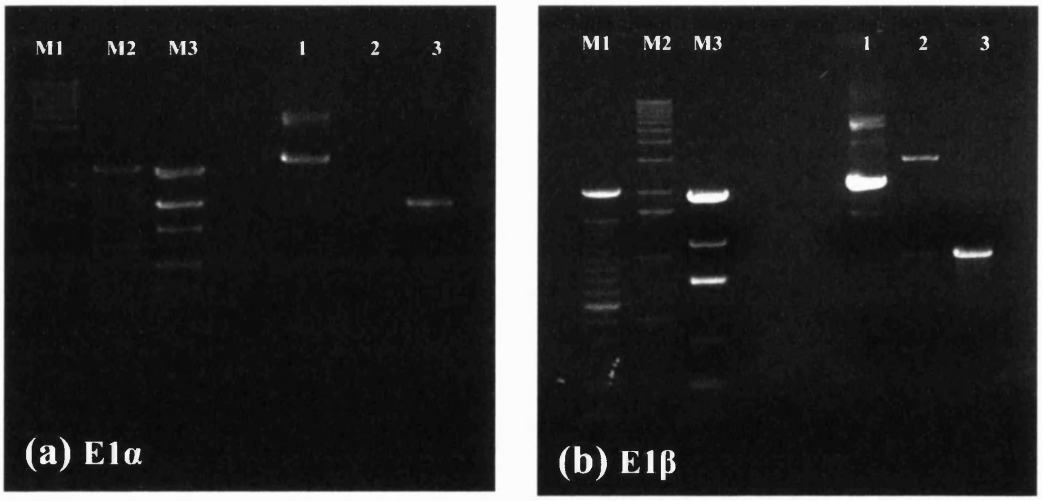

Figure 6.5: Double and single digestion of E1α and E1β out of pGEM-T vector.
Marker lanes M1, M2 and M3 contain 100 bp ladder, 1kb ladder and low DNA mass ladder, respectively. Double digestion was visualized using 0.8% (w/v) agarose gel. Gels (a) and (b) represent respectively, lane 1: miniprep of each gene with pGEM-T. Lane 2: double digest of the genes with *Nde*I and *Bam*HI resulted in two bands, the higher M_r is the pGEM-T vector and the lower one is the insert of interest of correct size. Lane 3: PCR product of E1α and E1β. With the E1α gene the insert resulting from the double digestion was of a low concentration compared to the E1β, but was clear under UV light.

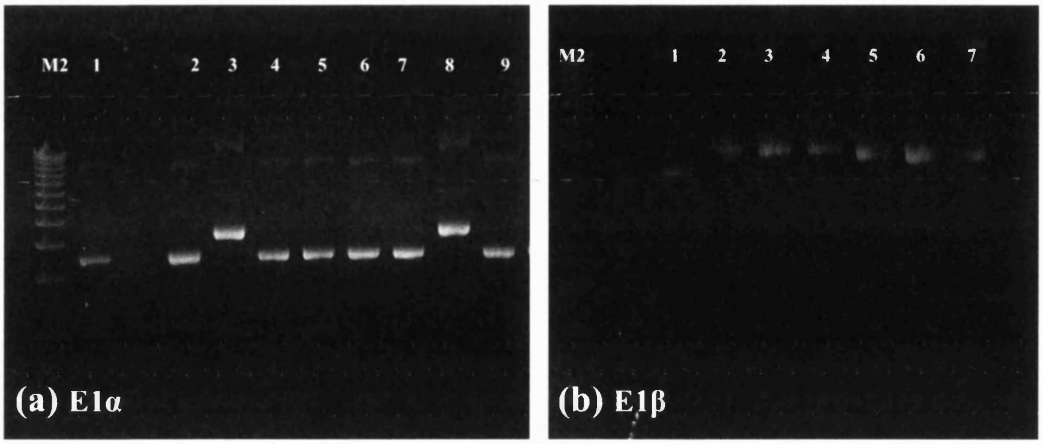

Figure 6.6: Miniprep of E1α and E1β after cloning into pET-19b and pET-28a respectively (after JM109 transformation).
Marker lane M2 contains 1 kbp ladder. Gel (a) shows lane 1: pET-19b vector without insert, and lanes 2-9: miniprep of pET-19b-E1α construct; only the minipreps in lane 3 and 8 show a size shift which indicates successful ligation. Gel (b) represents lane 1: pET-28a vector without insert, and lanes 2-7: miniprep of pET-28a-E1β; all minipreps show a size shift which indicates successful ligation.

6.4.2 Expression of recombinant E1α and E1β

Following the transformation of the constructs, then plating and overnight incubation, a large number of colonies were produced: ~100 colonies with pET-19b-E1α and ~150 with pET-28a-E1β transformed cells. This successful transformation of both E1α and E1β constructs into BL21(DE3)pLysS cells enabled the initiation of E1α and E1β expression.

The expression of the E1α and E1β genes started with a small-scale expression to optimize the level of expression, in terms of duration of induction with IPTG. Samples were taken before induction and after 2 and 4 h of induction. Also, samples of soluble cell extracts and their pellets were analysed by 10% SDS-PAGE to determine the protein content (Figure 6.7 and 6.8). Both gels show that both E1α and E1β had been successfully expressed. However, the level of E1β expression is higher than E1α,

and this may be due to the lower copy number of the plasmid in the BL21(DE3)pLysS cells, lower transcription and translation rates or instability of the expressed protein. Also, the gels indicate that the level of expression was the same or lower after 4 h of induction with IPTG compared with a 2 h induction; therefore, it was decided that for large-scale expression and for further studies cells could be induced for 2 h only before pelleting the cells for further purification. In addition, both proteins were found to be in a higher concentration in the cell pellets (insoluble protein) than in the soluble extracts. The bands of the recombinant proteins in the insoluble fraction of cell extract compose almost 60% of the total cell protein. Thus the majority of the expressed protein was in the form of inclusion bodies, so they need further purification, solubilization and refolding into active native protein in order to be able to measure their activity. The M_r values of the α and β polypeptides were determined by SDS-PAGE to be ~ 50000 and ~ 37000, respectively, compared with predicted values of 40971 and 36020, respectively from the gene sequence. However 50000 vs 40000 is a large difference, but it is known that separation of halophilic proteins by SDS-PAGE gel electrophoresis usually overestimates their molecular weight, as a consequence of excess acidic charge (Bonete *et al.*, 1996; Karadzic and Maupin-Furlow, 2005).

Following expression, the insoluble fractions were purified using Bugbuster to obtain highly enriched inclusion bodies containing the expressed insoluble E1 components. These purified inclusion bodies, together with aliquots of the expression procedure, were analysed by SDS-PAGE to view the extent of E1 enrichment.

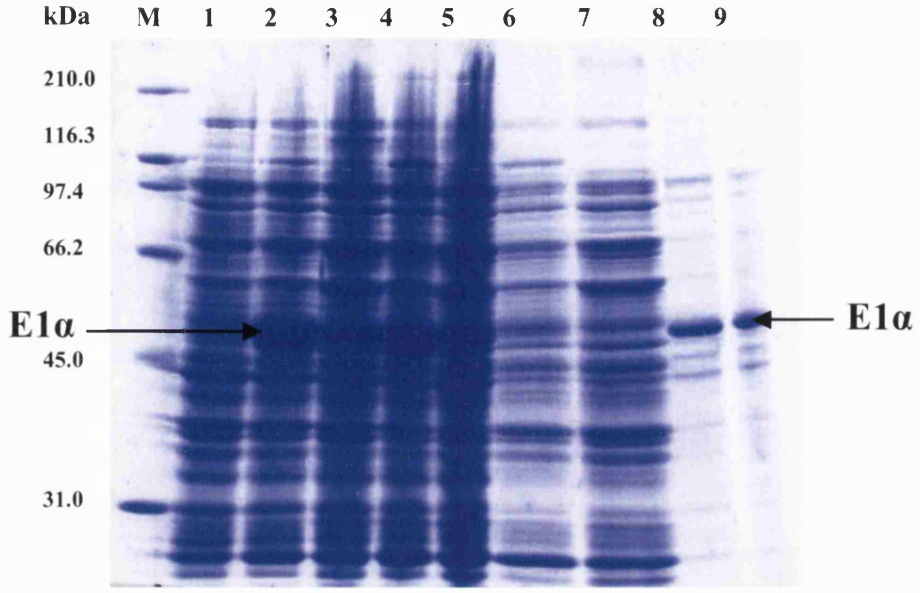

Figure 6.7: SDS-PAGE gel showing samples of E1α small-scale expression.
M: standard protein markers. Lane 1: cell extract prior to IPTG induction. Lanes 3 and 5: whole cell sample with no IPTG induction after 2 and 4 h. Lanes 2 and 4: whole cell sample after IPTG induction after 2 and 4 h. Lanes 6 and 7: whole cell extracts after induction and without induction, respectively. Lanes 8 and 9: pellets (insoluble proteins) after induction using 5 and 2.5µl.

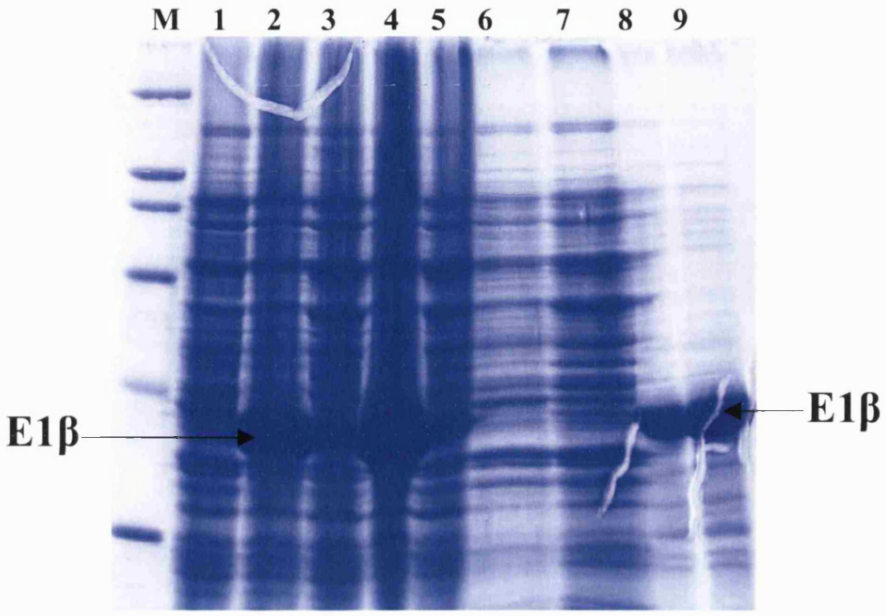

Figure 6.8: SDS-PAGE gel showing samples of E1β small-scale expression.
M: standard protein markers. Lane 1: cell extract prior to IPTG induction. Lanes 3 and 5: whole cell sample with no IPTG induction after 2 and 4 h. Lanes 2 and 4: whole cell sample after IPTG induction after 2 and 4 h. Lanes 6 and 7: whole cell extracts after induction and without induction, respectively. Lanes 8 and 9: pellets (insoluble proteins) after induction using 5 and 2.5µl.

6.4.3 Solubilization and refolding of E1α and E1β

Consequently, after the successful purification of E1α and E1β, the next step was to try to solubilize and refold them hoping to get a catalytically active E1 enzyme, in order to enable us to determine the substrate specificity of the OADHC in *Hfx. volcanii.*

The obtained inclusion bodies were first solubilized in a buffer containing 8 M urea in order to denature all the proteins present in the samples. Surprisingly, upon the addition of the solubilization buffer, some of the insoluble content remained. Then the samples were centrifuged and the pellets were discarded. Nevertheless, even if not all the protein had been solubilized by the exposure to 8 M urea, the procedure would at least have solubilized a proportion of the total protein in the samples.

Moreover, the soluble fractions (presumably containing the E1α and E1β proteins) were slowly diluted in renaturation buffer containing 2 M KCl, the oxido-shuffling reagents GSH and GSSG, and TPP.

In order to obtain a functional E1 enzyme, in addition to being correctly refolded, both subunits would have to be assembled in the correct conformation. To accomplish this, it was decided that E1α and E1β would be assembled in two different stages in order to detect whether this would affect the assembly efficiency of the E1 enzyme. Thus, in one experiment, E1α and E1β were mixed together prior to the refolding step, and in another experiment, each of the E1 subunits was refolded separately and then the two were mixed together just prior to enzyme assay.

Given the difference in the purity of E1α and E1β (Figures 6.7 and 6.8); the subunits were mixed together before refolding in a ratio of 2:1 (α: β) in order to have an equal concentration of E1α and E1β in the mixture. In addition, the two subunits were refolded separately using the same ratio.

During the refolding, some solutions (especially the one containing E1β) became slightly cloudy, indicating that some of the protein was coming out of solution. This could indicate that the E1 subunits were precipitating due to incorrect refolding. On the other hand, it is also possible that *E. coli* proteins were precipitating due to the high salt concentration in the renaturation solution.

Following the refolding step, the samples were then centrifuged to remove any precipitated content. Finally, the protein concentration of the soluble fractions was estimated by Bradford assay as mentioned in Chapter 2 (Section 2.2.3.1), E1α = 0.024 mg/ml, E1β = 0.050 mg/ml and E1α + E1β = 0.010 mg/ml.

6.4.4 Recombinant E1 activity

A fraction of each of the two E1 subunits that had been folded separately, were mixed together in a ratio of 2: 1 (α: β) to achieve an approximately equal proportion of E1α and E1β in the mixture. This solution, together with the sample where E1α and E1β had been mixed prior to the refolding step, was assayed for E1 activity as mentioned in Chapter 2 (Section 2.2.2.7).

Unfortunately, no E1 activity could be detected with any of the known OADHC substrates. The E1 assay depends on measuring the rate of reduction of DCPIP, which acts as an artificial electron acceptor for E1. This reduction is detected spectrophotometrically by a gradual decrease in the A_{595} of the solution where the DCPIP loses its blue colour during reduction. However, in the present assay, the DCPIP was reduced before the substrate had been added to the assay mixture. It was then noticed that there was a reagent present in the refolding buffer, GSH, that reduced the DCPIP.

To overcome this problem, the enzyme samples were concentrated using Vivaspin 10000 MW (Hannover, Germany) with a Tris-KCl neutral salt buffer in order to remove the entire GSH contaminant present in the assay mixture. At the end, highly enriched samples were obtained (0.122 mg/ml for E1α, 0.352 mg/ml for E1β, and 0.117 mg/ml for E1α + E1β) devoid of GSH.

However, even after the removal of most of the GSH from the E1α/E1β mixtures, the DCPIP was still being reduced prior to the addition of the substrate.

6.5 Discussion

The main objective of this chapter was to express the halophilic E1 enzyme in *E. coli*, hoping to end with a high concentration of recombinant proteins enabling us to detect enzyme activity and substrate specificity, since the homologous expression resulted in a very low concentration of protein to be measured.

Only a few cases have been reported of heterologous expression of halophilic enzymes, such as malate dehydrogenase from *Haloarcula marismortui* (Cendrin *et al.*, 1993), dihydrofolate reductase from *Hfx. volcanii* (Blecher *et al.*, 1993), Hmg-CoA reductase from *Hfx. volcanii* (Bischoff and Rodwell, 1996) and citrate synthase and DHlipDH from *Hfx. volcanii* (Connaris *et al.*, 1999). In these cases, either soluble inactive enzymes or insoluble inclusion bodies were produced which required salt-activation or refolding treatments respectively. However, the yields of *E. coli* expressed enzyme in most cases were greater than those obtained by purification of the enzymes from the native organism (Connaris *et al.*, 1999).

Therefore, the experiments were started by designing primers for the E1α and E1β genes, and these were then PCR amplified and cloned into the intermediate vector pGEM-T to facilitate their sequencing. Then clones with the correct sequence were excised and cloned into pET-19b (Amp^r) and pET-28a (Kan^r), generating the recombinant expression vectors pET-19b-E1α and pET-28a-E1β. This was followed by the separate transformation of each construct into JM109 to produce enough DNA to be transformed in the expression *E.coli* BL21(DE3)pLysS cells. All the previous cloning and expression steps were performed successfully. Finally, the last step was to detect the nature and level of expression, which turned to be that both E1α and E1β were expressed as insoluble inclusion bodies. As a consequence, the inclusion bodies needed to be purified, solubilized and renatured in suitable buffers with a high salt concentration to ensure the correct folding as in the native environment. In the end, recombinant proteins were highly purified but no enzyme activity was detected, although the presence of GSH in the refolding buffers made the accurate assay of enzyme activity almost impossible.

Following the previous successful expression trials of halophilic proteins in *E. coli* using the pET system, we have successfully expressed E1 from *Hfx. volcanii* in *E.*

coli. The pET expression system is under the control of the strong bacteriophage T7 transcription and translation signals (Studier, 1991). The *E. coli* BL21(DE3)pLysS was selected as a host cell due to its T7 RNA polymerase gene that is under the control of lacUV5 promoter. This promoter is induced by IPTG, which stimulates the production of T7 RNA polymerase, which in turn induces the expression of the target gene that is located downstream of the T7 promoter in the pET vectors. High levels of expressed protein were produced compared with the levels in the native organism or in homologous expression system. As a result of this expression, E1α and E1β accumulated as insoluble aggregates; it is possible that the low the ionic strength in the *E. coli* cytoplasm prevents correct folding of the halophilic enzymes.

Formation of inclusion bodies, a problem encountered during heterlogous expression of many proteins, has been related to the kinetics of translation (De Bernardez-Clark and Georgiou, 1991), when the rate of translation exceeds the rate of folding of the protein, resulting in the formation of inclusion bodies. However, the formation of inclusion bodies can be useful, in the sense of protecting the expressed proteins from cytoplasmic proteases and they can be easily purified from the cell lysate. This facilitates the removal of soluble host enzymes prior to purification and solubilization of the expressed protein. Also, the halophilic proteins can be selectively purified from contaminating non-halophilic ones due to the high salt concentration in the purifying buffer that retains the near native environment of the archaeal proteins. The presence of the oxido-shuffling reagents GSH and GSSG, 2M KCl and the coenzyme TPP were included for the attempted recovery of refolded, active E1 enzyme.

SDS-PAGE shows the highly purified and concentrated expressed protein of the two subunits of E1 that indicates successful expression. This differs from the SDS-PAGE of the homologous expression experiments where no bands of expressed protein could be detected. Also, SDS-PAGE analysis of the purified, renatured recombinant E1α and E1β displayed a band of each subunit with an M_r value similar to the predicted value of the gene sequence of *Hfx. volcanii*. However, the E1α protein ran at a higher M_r than expected, and this may be due to the high acidity of the halophilic proteins (Danson and Hough, 1997) that behave differently on SDS-PAGE from normal ones

(Bonete *et al.*, 1996; Karadzic and Maupin-Furlow, 2005). So in the future it is recommended to run halophilic proteins using CTAB-cationic electrophoresis which has been suggested as a method especially applicable for estimation of the moleculr weight of acidic proteins (Eley *et al.*, 1979)

Although all the results seem to be promising and protein expression is confirmed by SDS-PAGE, unfortunately no E1 activity could be detected. This is not necessarily due to inactive recombinant protein, as the presence of GSH in the refolding buffer reduced the artificial electron acceptor DCPIP before the addition of the substrate; therefore, no activity could be measured.

The overall lack of success in measuring the activity of recombinant E1 was disappointing, but due to the promising results the expression of E1 should be repeated. Firstly the use of GSH should be avoided. Also, since the two subunits have been cloned into two vectors with different antibiotics resistant, the co-expression of the two subunits is possible and may simplify the purification and refolding of the expressed protein.

General Discussion

In this Ph.D. project, the main objective was to detect the function of the putative multienzyme complex in the halophilic archaeon, *Hfx. volcanii.* This objective was approached by trying different logical steps that may lead to an answer or logical explanation to this obstacle.

7.1 *In vivo* transcription

The reverse transcription-polymerase chain reaction (RT-PCR) was used to determine whether the OADHC was transcribed in *Hfx. volcanii. Hfx. volcanii* is an excellent model for molecular biological studies, due to its simple growth requirements and storage in the laboratory in hypersaline medium, and its genome is relatively stable compared to other halophiles. These properties permitted the use of *Hfx. volcanii* as a representative archaeal model on which to use the highly sensitive RT-PCR technique. However, although there are many commercial kits available that facilitate the isolation of highly-purified mRNA, most of them are more applicable to eukaryotes than to prokaryote genetic systems. It was concluded that RT-PCR is not an easy reaction to be performed in *Hfx. volcanii* and it took quite a long time to establish a working protocol, owing to the difficulty in isolating prokaryotic mRNA due to its instability and lack of a poly (A) sequence (Cao and Sarkar, 1992). Moreover, the high GC content of the halophilic genome requires a higher denaturation temperature compared to other organisms, and this can be incompatible with some kits.

Due to the above reasons, in the present study, total RNA was isolated and a two-step RT-PCR was used to detect the level of transcription of the putative OADHC operon. The results confirmed the transcription of the complex as a complete message.

7.2 Expression of OADHC genes

According to the *in vivo* transcriptional studies, the genes of OADHC are transcribed as an operon. This raises questions such as if the genes are transcribed are they translated into an active enzyme, and what is their substrate specificity if they are active. The

answers to these questions were investigated in two ways: firstly, by growth studies of *Hfx. volcanii* under different metabolic conditions and secondly, by homologous expression of the OADHC genes in *Hfx. volcanii* and heterologous expression in *E. coli*.

7.2.1 Growth studies

Firstly, the growth of *Hfx. volcanii* was investigated under different nutrient conditions that may lead to an increase in the expression of DHlipDH, which in turn could reflect the expression of the complex. The activity of DHlipDH was detected in all carbon sources under aerobic and anaerobic conditions, with no significant increase in the level of the enzyme except with branched-chain amino acids, especially isoleucine. However, no whole complex activity could be detected in any growth condition. Although previously *Hfx. volcanii* had failed to grow on branched-chain amino acids (Jolley *et al.*, 1996b), in this study growth was achieved.

Similarly, anaerobic growth of *Hfx. volcanii* revealed no significant increase in growth or enzymic levels, except with the addition of sodium nitrate to MGM2 that lead to an increase in DHlipDH activity, although again no OADHC activity could be detected.

Cell extracts were also passed through an analytical gel filtration column to detect the nature of the expressed DHlipDH. Only free DHlipDH could be identified, unlike with an *E. coli* extract where free and complexed enzyme was observed.

Since only free DHlipDH activity could be detected with no OADHC activity, it seems likely that the enzyme exists solely in an unassociated form in these organisms. Unassociated DHlipDH may play role in the oxidative repair mechanisms (Suzuki *et al.*, 1994; Zimmer *et al.*, 1991) or in sugar transport (Richarme, 1989; Richarme and Heine, 1986) although the growth studies seems to rule out the latter. Additionally, it could be that the complex is transcribed but only E3 is expressed, or the level of expression is too low to be detected or that whole complex is produced but it is unstable due to the conditions used to lyse the *Hfx. volcanii* cells. So, we cannot rule out that the genes do code for an active complex whose expression is highly regulated and thus it is only detected under specific assay conditions. Also, it may be that the

true 2-oxoacid substrate has not yet been found and thus no activity is being detected; clearly there are several potential substrates to test.

7.2.2 Homologous expression

The homologous expression of halophilic protein was chosen to facilitate the expression in their native environment that would help the protein to fold into its correct conformation and to undergo any post-translational modifications. On the other hand, slow growth of halophilic archaea compared to *E. coli*, lack of inducible promoters, a limited number of available expression vectors and incomplete knowledge of intracellular biochemistry and genetic system of these organisms may reduce the chances of success and level of expression.

In this study an E1α-β construct of the *Hfx. volcanii* OADHC was homologously expressed using two intermediate vectors, pGEM-T and pIL11, where the later was used to recover the *fdx* promoter prior to its cloning in the expression vector pTA233. Non-methylated constructs were generated by their transformation into the non-methylating *E. coli* strain GM121 just before the transformation of the expression *Haloferax* strain H98. The expression resulted with in a very low and indefinite E1 activity; this is may be due to the low copy number of the expression vector in comparison to other expression vectors.

7.2.3 Heterologous Expression

Another approach was heterologous expression of E1 performed in parallel with homologous expression. The advantages of heterologous expression of halophilic proteins in *E. coli* often overcome the potential disadvantages. These advantages comprise rapid growth, high cell densities and its well-known and developed genetics; also transformation and other expression techniques are common. Moreover, there is the availability of a large number of commercial expression vectors with inducible promoters that offer high levels of control over expression. These include the IPTG-inducible T7 promoter that was used in this study. Previous studies had found that the yield of heterologous expression was greater than those obtained from expression in the native halophilic organism (Connaris *et al.*, 1999; Jolley *et al.*, 1996b). The

disadvantages of expressing halophilic protein in a low salt concentration environment may include incorrect post-translational changes, misfolding of the protein resulting in inactive enzyme or the formation of insoluble inclusion bodies that requires either reactivation or refolding.

In the current study, due to the time limit, only E1α and E1β genes of the OADHC were heterologously expressed in *E. coli* using the well-developed pET vector system. Although initially the expressed proteins were insoluble, solubilization in 8 M urea, followed by refolding in a specific buffer, resulted in purified proteins. Unfortunately, no E1 activity could be detected due the presence of a component (GSH) in the refolding buffer that interfered with the assay component by reducing the DCPIP (artificial electron acceptor) before the addition of the substrate. Attempts to remove the GSH to non-interfering levels were unsuccessful.

7.3 Future work

There are obvious extensions to this Ph.D. project. From the findings in this study, it is recommended to measure the level of transcription in *Haloferax* by using real time RT-PCR, and to perform this with total RNA isolated from *Haloferax* grown on branched-chain 2-oxoacids and on branched-chain amino acids. This suggestion is based on the 4-fold increase in gene expression of BCOADHC in *Enterococcus faecalis* when grown on branched-chain 2-oxoacids compared with branched-chain amino acids (Ward *et al.*, 1999; Ward *et al.*, 2000).

Additionally, the time constraints in this project did not leave enough time to repeat the homologous expression of E1α-β construct by trying to express the gene using a large-scale expression that may lead to higher levels of E1 activity. Also, as previously mentioned, heterologous expression of co-expressed E1α and E1β of *Thermoplasma acidophilum* in *E. coli* revealed a high level of active E1 expression (Heath *et al.*, 2004). Moreover, it is worth repeating the heterologous expression of E1 in *E. coli* since using pET vectors with two different antibiotic resistant facilitates co-expression of the two constructs together and this may lead to a decrease in the level of insolubility and facilitate the refolding process. Furthermore, expression of the two

genes, E1α and E1β, as one construct may further help to increase the level of expression to a measurable standard.

Also, due to the recent improvement in two-dimensional (2-D) gel electrophoresis proteome maps of halophiles and *Hfx. volcanii* this provides tremendous opportunities to identify the nature and function of OADHC proteins and analyze any change that may occur in the protein expression profile between growth conditions (Joo and Kim, 2005; Karadzic and Maupin-Furlow, 2005). Comparison of 2-D proteome maps from *Hfx. volcanii* grown on different substrates, for example branched-chain amino acids and glucose, would permit the identification of proteins that are induced in response to the presence of a particular nutrient. This approach could provide evidence for the expression of the component enzymes of the OADHC under specific growth conditions.

To conclude, further investigation of the recombinant E1 is the first issue followed by the generation of recombinant E2 and E3 components of *Hfx. volcanii* with the main goal being the achievement of whole complex assembly.

References

Allers, T. & Mevarech, M. (2005) Archaeal genetics - The third way. *Nat. Rev. Genet.*, **6,** 58-73.

Allers, T., Ngo, H. P., Mevarech, M. & Lloyd, R. G. (2004) Development of additional selectable markers for the halophilic archaeon *Haloferax volcanii* based on the leuB and trpA genes. *Appl. Environ. Microbiol.*, **70,** 943-953.

Altekar, W. & Rangaswamy, V. (1990) Indication of A modified EMP pathway for fructose breakdown in a halophilic archaebacterium. *FEMS Microbiol. Lett.*, **69,** 139-143.

Altekar, W. & Rangaswamy, V. (1991) Ketohexokinase (ATP-D-fructose 1-phosphotransferase) initiates fructose breakdown via the modified EMP pathway in halophilic archaebacteria. *FEMS Microbiol. Lett.*, **83,** 241-246.

Barns, S. M., Delwiche, C. F., Palmer, J. D. & Pace, N. R. (1996) Perspectives on archaeal diversity, thermophily and monophyly from environmental rRNA sequences. *Proc. Natl. Acad. Sci. U. S. A.*, **93,** 9188-9193.

Bischoff, K. M. & Rodwell, V. W. (1996) 3-hydroxy-3-methylglutaryl-coenzyme A reductase from *Haloferax volcanii*:purification, characterization, and expression in *Escherichia coli*. *J. Bacteriol.*, **178,** 19-23.

Bitan-Banin, G., Ortenberg, R. & Mevarech, M. (2003) Development of a gene knockout system for the halophilic archaeon *Haloferax volcanii* by use of the pyrE gene. *J. Bacteriol.*, **185,** 772-778.

Blaschkowski, H. P., Neuer, G., Ludwigfestl, M. & Knappe, J. (1982) Routes of flavodoxin and ferredoxin reduction in *Escherichia coli* - CoA-acylating pyruvate - flavodoxin and NADPH - flavodoxin oxidoreductases participating in the activation of pyruvate formate-lyase. *Eur. J. Biochem.*, **123,** 563-569.

Blecher, O., Goldman, S. & Mevarech, M. (1993) High expression in *Escherichia coli* of the gene coding for dihydrofolate-reductase of the extremely halophilic archaebacterium *Haloferax volcanii* - reconstitution of the active enzyme and mutation studies. *Eur. J. Biochem.*, **216,** 199-203.

Blochl, E., Rachel, R., Burggraf, S., Hafenbradl, D., Jannasch, H. W. & Stetter, K. O. (1997) *Pyrolobus fumarii,* gen. and sp. nov., represents a novel group of archaea, extending the upper temperature limit for life to 113 degrees C. *Extremophiles,* **1,** 14-21.

Bock, A. K., Schonheit, P. & Teixeira, M. (1997) The iron-sulfur centers of the pyruvate:ferredoxin oxidoreductase from *Methanosarcina barkeri* (Fusaro). *FEBS Lett.*, **414,** 209-212.

Bolhuis, H., Poele, E. M. T. & Rodriguez-Valera, F. (2004) Isolation and cultivation of Walsby's square archaeon. *Environ. Microbiol.*, **6,** 1287-1291.

Bonete, M. J., Pire, C., Llorca, F. I. & Camacho, M. L. (1996) Glucose dehydrogenase from the halophilic archaeon *Haloferax mediterranei*: enzyme purification, characterisation and N-terminal sequence. *FEBS Lett.*, **383,** 227-229.

Borowitzka, L. J. (1981) The microflora-adaptations to life in extremely saline lakes. *Hydrobiologia,* **81-2,** 33-46.

Bradford, M. M. (1976) Rapid and sensitive method for quantitation of microgram quantities of protein utilizing principle of protein-dye binding. *Anal. Biochem.*, **72,** 248-254.

Brasen, C. & Schonheit, P. (2004) Regulation of acetate and acetyl-CoA converting enzymes during growth on acetate and/or glucose in the halophilic archaeon *Haloarcula marismortui*. *FEMS Microbiol. Lett.*, **241,** 21-26.

Brown, J. P. & Perham, R. N. (1976) Selective inactivation of transacylase components of 2-oxo acid dehydrogenase multienzyme complexes of *Escherichia coli*. *Biochem. J.*, **155,** 419-&.

Burns, D. G., Camakaris, H. M., Janssen, P. H. & Dyall-Smith, M. L. (2004) Cultivation of Walsby's square haloarchaeon. *FEMS Microbiol. Lett.*, **238,** 469-473.

Burns, G., Brown, T., Hatter, K., Idriss, J. M. & Sokatch, J. R. (1988) Similarity of the E1 subunits of branched-chain 2-oxoacid dehydrogenase from *Pseudomonas putida* to the corresponding subunits of mammalian branched-chain 2-oxoacid and pyruvate dehydrogenases. *Eur. J. Biochem.*, **176,** 311-317.

Butinar, L., Sonjak, S., Zalar, P., Plemenitas, A. & Gunde-Cimerman, N. (2005) Melanized halophilic fungi are eukaryotic members of microbial communities in hypersaline waters of solar salterns. *Bot. Mar.*, **48,** 73-79.

Cabrera, J. A., Bolds, J., Shields, P. E., Havel, C. M. & Watson, J. A. (1986) Isoprenoid synthesis in *Halobacterium halobium* - modulation of 3-hydroxy-3-methylglutaryl coenzyme-A concentration in response to mevalonate availability. *J. Biol. Chem.*, **261,** 3578-3583.

Cao, G. J. & Sarkar, N. (1992) Poly(A) RNA in *Escherichia coli* - nucleotide-sequence at the junction of the Lpp transcript and the polyadenylate moiety. *Proc. Natl. Acad. Sci. USA.*, **89,** 7546-7550.

Cavicchioli, R., Curmi, P. M. G., Saunders, N. & Thomas, T. (2003) Pathogenic archaea: do they exist? *Bioessays,* **25,** 1119-1128.

Cendrin, F., Chroboczek, J., Zaccai, G., Eisenberg, H. & Mevarech, M. (1993) Cloning, sequencing, and expression in *Escherichia coli* of the gene coding for malate-dehydrogenase of the extremely halophilic archaebacterium *Haloarcula marismortui. Biochemistry,* **32,** 4308-4313.

Chant, J., Hui, I., Dejongwong, D., Shimmin, L. & Dennis, P. P. (1986) The protein synthesizing machinery of the archaebacterium *Halobacterium cutirubrum* - molecular characterization. *Syst. Appl. Microbiol.,* **7,** 106-114.

Charlebois, R. L., Lam, W. L., Cline, S. W. & Doolittle, W. F. (1987) Characterization of Phv2 from *Halobacterium volcanii* and its use in demonstrating transformation of an archaebacterium. *Proc. Natl. Acad. Sci. U. S. A.,* **84,** 8530-8534.

Cline, S. W., Lam, W. L., Charlebois, R. L., Schalkwyk, L. C. & Doolittle, W. F. (1989) Transformation-methods for halophilic archaebacteria. *Can. J. Microbiol.,* **35,** 148-152.

Connaris, H., Chaudhuri, J. B., Danson, M. J. & Hough, D. W. (1999) Expression, reactivation, and purification of enzymes from *Haloferax volcanii* in *Escherichia coli. Biotechnol. Bioeng.,* **64,** 38-45.

Danner, S. & Soppa, J. (1996) Characterization of the distal promoter element of halobacteria *in vivo* using saturation mutagenesis and selection. *Mol. Microbiol.,* **19,** 1265-1276.

Danson, M. J. (1988) Dihydrolipoamide dehydrogenase - a new function for an old enzyme. *Biochem. Soc. T.,* **16,** 87-89.

Danson, M. J. (1989) Central metabolism of the archaebacteria - an overview. *Can. J. Microbiol.,* **35,** 58-64.

Danson, M. J. (1993) Central metabolism of the Archaea. In: *New Comp. Biochemistry [The Biochemistry of Archaea]* (Kates, M., Kushner, D. & Matheson, A. T. Eds.). 1-24. Amsterdam.: Elsevier/North Holland Biomedical Press.

Danson, M. J., Black, S. C., Woodland, D. L. & Wood, P. A. (1985) Citric-acid cycle enzymes of the archaebacteria - citrate synthase and succinate thiokinase. *FEBS Lett.,* **179,** 120-124.

Danson, M. J., Conroy, K., Mcquattie, A. & Stevenson, K. J. (1987) Dihydrolipoamide dehydrogenase from *Trypanosoma brucei* - characterization and cellular location. *Biochem. J.,* **243,** 661-665.

Danson, M. J., Eisenthal, R., Hall, S., Kessell, S. R. & Williams, D. L. (1984) Dihydrolipoamide dehydrogenase from halophilic archaebacteria. *Biochem. J.,* **218,** 811-818.

Danson, M. J. & Hough, D. W. (1992) The enzymology of Archaebacterial pathways of central metabolism. *Biochem. Soc. Symp.*, 7-21.

Danson, M. J. & Hough, D. W. (1997) The structural basis of protein halophilicity. *Comp. Biochem. Phys. A,* **117,** 307-312.

Danson, M. J. & Hough, D. W. (1998) Structure, function and stability of enzymes from the Archaea. *Trends Microbiol.,* **6,** 307-314.

Danson, M. J., Mcquattie, A. & Stevenson, K. J. (1986) Dihydrolipoamide dehydrogenase from halophilic archaebacteria-purification and properties of the enzyme from *Halobacterium halobium. Biochemistry,* **25,** 3880-3884.

Danson, M. J., Morgan, D. J., Jeffries, A. C., Hough, D. W. & Dyall- Smith, M. L. (2004) Multienzyme complexes in the Archaea: predictions from genome sequences. In: *In Halophilic Microorganisms* (Ventosa, A. (Ed.). Berlin: Springer-Verlag.

Dassarma, M. & Fleischmann, E. M. (Eds.) (1995) *Archaea (halophiles) a laboratory manual.* New York: CSHL Press.

Davie, J. R., Wynn, R. M., Meng, M. S., Huang, Y. S., Aahund, G., Chuang, D. T. & Lau, K. S. (1995) Expression and characterization of branched-chain alpha-ketoacid dehydrogenase kinase from the rat -is it a histidine-protein kinase. *J. Biol. Chem.,* **270,** 19861-19867.

De Bernardez-Clark, E. & Georgiou, G. (1991) Inclusion-bodies and recovery of proteins from the aggregated state. *Acs Symposium Series,* **470,** 1-20.

De Kok, A., Hengeveld, A. F., Martin, A. & Westphal, A. H. (1998) The pyruvate dehydrogenase multi-enzyme complex from Gram-negative bacteria. *BBA-Protein Struct. M.,* **1385,** 353-366.

Delille, D., Basseres, A. & Dessommes, A. (1998) Effectiveness of bioremediation for oil-polluted Antarctic seawater. *Polar Biol.,* **19,** 237-241.

Delong, E. F. (2002) Microbial population genomics and ecology. *Curr. Opin. Microbiol,* **5,** 520-524.

Delsuc, F., Brinkmann, H. & Philippe, H. (2005) Phylogenomics and the reconstruction of the tree of life. *Nat. Rev. Genet.,* **6,** 361-375.

Doolittle, W. F. & Brown, J. R. (1994) Tempo, mode, the progenote, and the universal root. *Proc. Natl. Acad. Sci. U. S. A.,* **91,** 6721-6728.

Dyall-Smith, M., Tang, S. L. & Bath, C. (2003) Haloarchaeal viruses: how diverse are they? *Res. Microbiol.,* **154,** 309-313.

Dyall-Smith, M. L. (2004) *The halohandbook: protocols for halobacterial genetics.* [Online]http://test.microbiol.unimelb.edu.au/staff/mds//HaloHandbook/Halohandbook 4.9wd_print.pdf.

Eisenberg, H. & Wachtel, E. J. (1987) Structural studies of halophilic proteins, ribosomes, and organelles of Bacteria adapted to extreme salt concentrations. *Annu. Rev. Biophys. Bio.,* **16,** 69-92.

Eisenthal, R. & Cornish-Bowden, A. (1974) The direct linear plot. A new graphical procedure for estimating enzyme kinetic parameters. *Biochem. J.,* **139,** 715-720.

Elazari-Volcani, B. (1957) Genus XII. Halobacterium Elazari-volcani,1940. In: *Bergey's manual of determinative bacteriology* (Breed, R. S., Murray, E. G. D. & N.R., S. Eds.). 7th ed.pp.207-212. Baltimore: The Williams and Wilkins Company.

Eley, M. H., Burns, P. C., Kannapell, C. C. & Campbell, P. S. (1979) Cetyltrimethylammonium bromide polyacrylamide-gel electrophoresis - estimation of protein subunit molecular-weights using cationic detergents. *Anal. Biochem.,* **92,** 411-419.

Else, A. J., Danson, M. J. & Weitzman, P. D. J. (1988) Models of proteolysis of oligomeric enzymes and their applications to the trypsinolysis of citrate synthases. *Biochem. J.,* **254,** 437-442.

Forterre, P., Brochier, C. & Philippe, H. (2002) Evolution of the archaea. *Theor. Popul. Biol.,* **61,** 409-422.

Franzetti, B., Schoehn, G., Ebel, C., Gagnon, J., Ruigrok, R. W. H. & Zaccai, G. (2001) Characterization of a novel complex from halophilic archaebacteria, which displays chaperone-like activities in vitro. *J. Biol. Chem.,* **276,** 29906-29914.

Fries, M., Chauhan, H. J., Domingo, G. J., Jung, H. I. & Perham, R. N. (2003a) Site-directed mutagenesis of a loop at the active site of E1 ($\alpha_2\beta_2$) of the pyruvate dehydrogenase complex - A possible common sequence motif. *Eur. J. Biochem.,* **270,** 861-870.

Fries, M., Jung, H. I. & Perham, R. N. (2003b) Reaction mechanism of the heterotetrameric ($\alpha_2\beta_2$) E1 component of 2-oxo acid dehydrogenase multienzyme complexes. *Biochemistry,* **42,** 6996-7002.

Frolow, F., Harel, M., Sussman, J. L., Mevarech, M. & Shoham, M. (1996) Insights into protein adaptation to a saturated salt environment from the crystal structure of a halophilic 2Fe-2S ferredoxin. *Nat. Struct. Biol.,* **3,** 1055-1055.

Fukuchi, S., Yoshimune, K., Wakayama, M., Moriguchi, M. & Nishikawa, K. (2003) Unique amino acid composition of proteins in halophilic bacteria. *J. Mol. Biol.,* **327,** 347-357.

Fukuda, E., Kino, H., Matsuzawa, H. & Wakagi, T. (2001) Role of a highly conserved YPITP motif in 2-oxoacid: ferredoxin oxidoreductase - Heterologous expression of the gene from *Sulfolobus* sp. strain 7, and characterization of the recombinant and variant enzymes. *Eur. J. Biochem.*, **268,** 5639-5646.

Fukuda, E. & Wakagi, T. (2002) Substrate recognition by 2-oxoacid: ferredoxin oxidoreductase from *Sulfolobus* sp. strain 7. *BBA-Protein Struct. M.*, **1597,** 74-80.

Gambacorta, A., Gliozzi, A. & Derosa, M. (1995) Archaeal lipids and their biotechnological applications. *World J. Microbiol. Biotechnol.*, **11,** 115-131.

Gochnaue, M. B., Kates, M., Kushner, D. J. & Kushwaha, S. C. (1972) Nutritional control of pigment and isoprenoid compound formation in extremely halophilic bacteria. *Archiv Fur Mikrobiologie,* **84,** 339-&.

Gomes, J. & Steiner, W. (2004) The biocatalytic potential of extremophiles and extremozymes. *Food Technol. Biotech.*, **42,** 223-235.

Grant, W. D., Kamekura, M., Mcgenity, T. J. & Ventosa, A. (2001) Class III Halobacteria class. nov. In: *Bergey's Manual of Systematic Bacteriolgy.* Boone, D. R. & Calstenholz, R. W. Eds.. 2nd ed. pp.294-334. New york: Springer-Verlag.

Gregor, D. & Pfeifer, F. (2005) In vivo analyses of constitutive and regulated promoters in halophilic archaea. *Microbiology-(UK),* **151,** 25-33.

Gustafsson, C., Govindarajan, S. & Minshull, J. (2004) Codon bias and heterologous protein expression. *Trends Biotechnol.*, **22,** 346-353.

Handelsman, J. (2005) Metagenomics: application of genomics to uncultured microorganisms (vol 68, pg 669, 2004). *Microbiol. Mol. Biol. Rev.*, **69,** 195-195.

Hawkins, C. F., Borges, A. & Perham, R. N. (1990) Cloning and sequence-analysis of the genes encoding the alpha-subunit and beta-subunit of the E1 component of the pyruvate-dehydrogenase multienzyme complex of *Bacillus stearothermophilus. Eur. J. Biochem.*, **191,** 337-346.

Heath, C., Jeffries, A. C., Hough, D. W. & Danson, M. J. (2004) Discovery of the catalytic function of a putative 2-oxoacid dehydrogenase multienzyme complex in the thermophilic archaeon *Thermoplasma acidophilum. FEBS Lett.*, **577,** 523-527.

Hester, K., Luo, J., Burns, G., Braswell, E. H. & Sokatch, J. R. (1995) Purification Of active E1$\alpha_2\beta_2$ Of *Pseudomonas putida* branched-chain-oxoacid dehydrogenase. *Eur. J. Biochem.*, **233,** 828-836.

Hofacker, A., Schmitz, K. M., Cichonczyk, A., Sartorius-Neef, S. & Pfeifer, F. (2004) GvpE- and GvpD-mediated transcription regulation of the p-gvp genes encoding gas vesicles in *Halobacterium salinarum. Microbiology-(UK),* **150,** 1829-1838.

Holmes, M. L. & Dyall-Smith, M. L. (2000) Sequence and expression of a halobacterial beta-galactosidase gene. *Mol. Microbiol.*, **36,** 114-122.

Holmes, M. L. & Dyallsmith, M. L. (1990) A plasmid vector with a selectable marker for halophilic archaebacteria. *J. Bacteriol.*, **172,** 756-761.

Holmes, M. L., Nuttall, S. D. & Dyall-Smith, M. L. (1991) Construction and use of *Halobacterial* shuttle vectors and further-studies on *Haloferax* DNA gyrase. *J. Bacteriol.*, **173,** 3807-3813.

Holmes, M. L., Pfeifer, F. & Dyall-Smith, M. L. (1994) Improved shuttle vectors for *Haloferax volcanii* including a dual-resistance plasmid. *Gene,* **146,** 117-121.

Huang, Y. S. & Chuang, D. T. (1996) Structural organization of the rat branched-chain 2-oxo-acid dehydrogenase kinase gene and partial characterization of the promoter-regulatory region. *Biochem. J.*, **313,** 603-609.

Huber, H., Hohn, M. J., Rachel, R., Fuchs, T., Wimmer, V. C. & Stetter, K. O. (2002) A new phylum of Archaea represented by a nanosized hyperthermophilic symbiont. *Nature,* **417,** 63-67.

Huber, H., Hohn, M. J., Stetter, K. O. & Rachel, R. (2003) The phylum nanoarchaeota: present knowledge and future perspectives of a unique form of life. *Res. Microbiol.*, **154,** 165-171.

Izard, T., Aevarsson, A., Allen, M. D., Westphal, A. H., Perham, R. N., De Kok, A. & Hol, W. G. J. (1999) Principles of quasi-equivalence and euclidean geometry govern the assembly of cubic and dodecahedral cores of pyruvate dehydrogenase complexes. *Proc. Natl. Acad. Sci. U. S. A.*, **96,** 1240-1245.

James, K. D., Russell, R. J. M., Parker, L., Daniel, R. M., Hough, D. W. & Danson, M. J. (1994) Citrate synthases from the Archaea - development of a bio- specific, affinity-chromatography purification procedure. *FEMS Microbiol. Lett.*, **119,** 181-185.

Javor, B., Requadt, C. & Stoeckenius, W. (1982) Box-shaped halophilic bacteria. *J. Bacteriol.*, **151,** 1532-1542.

Jolley, K. A. (1996a) *Studies of dihydrolipoamide dehydrogenase from the halophilic archaeon Haloferax volcanii.* Ph.D.thesis, University of Bath.

Jolley, K. A., Maddocks, D. G., Gyles, S. L., Mullan, Z., Tang, S. L., Dyall-Smith, M. L., Hough, D. W. & Danson, M. J. (2000) 2-Oxoacid dehydrogenase multienzyme complexes in the halophilic Archaea? Gene sequences and protein structural predictions. *Microbiology-UK,* **146,** 1061-1069.

Jolley, K. A., Rapaport, E., Hough, D. W., Danson, M. J., Woods, W. G. & Dyallsmith, M. L. (1996b) Dihydrolipoamide dehydrogenase from the halophilic archaeon *Haloferax volcanii*: homologous overexpression of the cloned gene. *J. Bacteriol.*, **178,** 3044-3048.

Jones, W. J., Nagle, D. P. & Whitman, W. B. (1987) Methanogens and the diversity of archaebacteria. *Microbiol. Rev.*, **51,** 135-177.

Joo, W. A. & Kim, C. W. (2005) Proteomics of halophilic archaea. *J. Chromatogr. B.*, **815,** 237-250.

Jordan, S. W. & Cronan, J. E. (1997) A new metabolic link - the acyl carrier protein of lipid synthesis donates lipoic acid to the pyruvate dehydrogenase complex in *Escherichia coli* and mitochondria. *J. Biol. Chem.*, **272,** 17903-17906.

Jordan, S. W. & Cronan, J. E. (2003) The *Escherichia coli* lipB gene encodes lipoyl (octanoyl)-acyl carrier protein: protein transferase. *J. Bacteriol.*, **185,** 1582-1589.

Karadzic, I. M. & Maupin-Furlow, J. A. (2005) Improvement of two-dimensional gel electrophoresis proteome maps of the haloarchaeon *Haloferax volcanii*. *Proteomics,* **5,** 354-359.

Karunakaran, T. & Kuramitsu, H. (1996) Simple and rapid method for isolation of RNA from Gram-negative bacteria. *Biotechniques,* **20,** 546-547.

Kashefi, K. & Lovley, D. R. (2003) Extending the upper temperature limit for life. *Science,* **301,** 934-934.

Kauri, T., Wallace, R. & Kushner, D. J. (1990) Nutrition of the halophilic archaebacterium, *Haloferax volcanii*. *Syst. Appl. Microbiol.*, **13,** 14-18.

Keays, M. (2005) *Cloning of E1α and E1β subunits of the 2-oxoacidd dehydrogenase complex from the halophilic archaeon, Hfx. volcanii.* Final year project report, University of Bath.

Keeling, P. J. & Doolittle, W. F. (1995) Archaea - narrowing the gap between Prokaryotes and Eukaryotes. *Proc. Natl. Acad. Sci. U. S. A.*, **92,** 5761-5764.

Kerscher, L. & Oesterhelt, D. (1981a) Purification and properties of 2 2-oxoacid-ferredoxin oxidoreductases from *Halobacterium halobium*. *Eur. J. Biochem.*, **116,** 587-594.

Kerscher, L. & Oesterhelt, D. (1981b) The catalytic mechanism of 2-oxoacid-ferredoxin oxidoreductases from *Halobacterium halobium* - one-electron transfer at 2 distinct steps of the catalytic cycle. *Eur. J. Biochem.*, **116,** 595-600.

Kerscher, L. & Oesterhelt, D. (1982) Pyruvate - ferredoxin oxidoreductase new findings on an ancient enzyme. *Trends In Biochemical Sciences,* **7,** 371-374.

Kevil, C. G., Walsh, L., Laroux, F. S., Kalogeris, T., Grisham, M. B. & Alexander, J. S. (1997) An improved, rapid Northern protocol. *Biochem. Bioph. Res. Co.,* **238,** 277-279.

Klein, R., Greineder, B., Baranyi, U. & Witte, A. (2000) The structural protein E of the archaeal virus phi Ch1: evidence for processing in *Natrialba magadii* during virus maturation. *Virology,* **276,** 376-387.

Kottemann, M., Kish, A., Iloanusi, C., Bjork, S. & Diruggiero, J. (2005) Physiological responses of the halophilic archaeon *Halobacterium* sp strain NRC1 to desiccation and gamma irradiation. *Extremophiles,* **9,** 219-227.

Krebs, M. P. & Khorana, H. G. (1993) Mechanism of light-dependent proton translocation by bacteriorhodopsin. *J. Bacteriol.,* **175,** 1555-1560.

Kushner, D. J. (1966) Mass-culture of red halophilic bacteria. *Biotechnol. Bioeng.,* **8,** 237-245.

Kushner, D. J. (1988) What is the true internal environment of halophilic and other bacteria. *Can. J. Microbiol.,* **34,** 482-486.

Kushwaha, S. C., Kates, M., Juez, G., Rodriguez-Valera, F. & Kushner, D. J. (1982) Polar lipids of an extremely halophilic bacterial strain (R-4) isolated from salt ponds in Spain. *Biochim Biophys Acta,* **711,** 19-25.

Laemmli, U. K. (1970) Cleavage of structural proteins during assembly of head of bacteriophage-T4. *Nature,* **227,** 680-685.

Lam, W. L. & Doolittle, W. F. (1989) Shuttle vectors for the archaebacterium *Halobacterium volcanii. Proc. Natl. Acad. Sci. U. S. A.,* **86,** 5478-5482.

Lamosa, P., Burke, A., Peist, R., Huber, R., Liu, M. Y., Silva, G., Rodrigues-Pousada, C., Legall, J., Maycock, C. & Santos, H. (2000) Thermostabilization of proteins by diglycerol phosphate, a new compatible solute from the hyperthermophile *Archaeoglobus fulgidus. Appl. Environ. Microbiol.,* **66,** 1974-1979.

Lange, M., Westermann, P. & Ahring, B. K. (2005) Archaea in protozoa and metazoa. *Appl. Microbiol. Biot.,* **66,** 465-474.

Langer, D., Hain, J., Thuriaux, P. & Zillig, W. (1995) Transcription in Archaea – similarity to that in Eucarya. *Proc. Natl. Acad. Sci. U. S. A.,* **92,** 5768-5772.

Lessard, I. A. D. & Perham, R. N. (1994) Expression in *Escherichia coli* of genes encoding the E1α and E1β subunits of the pyruvate-dehydrogenase complex of *Bacillus stearothermophilus* and assembly of a functional E1 Component ($\alpha_2\beta_2$) in-vitro. *J. Biol. Chem.,* **269,** 10378-10383.

Ma, J., Campbell, A. & Karlin, S. (2002) Correlations between Shine-Dalgarno sequences and gene features such as predicted expression levels and operon structures. *J. Bacteriol.,* **184,** 5733-5745.

MacElroy, R. D. (1974) Some comments on evolution of extremophiles. *Biosystems,* **6,** 74-75.

Madern, D., Ebel, C. & Zaccai, G. (2000) Halophilic adaptation of enzymes. *Extremophiles,* **4,** 91-98.

Madigan, M. T. & Marrs, B. L. (1997) Extremophiles. *Sci. Am.,* **276,** 82-87.

Makarova, K. S. & Koonin, E. V. (2003) Comparative genomics of archaea: how much have we learned in six years, and what's next? *Genome Biol.,* **4.**

Margesin, R. & Schinner, F. (1999) Biological decontamination of oil spills in cold environments. *J. Chem. Technol. Biot,* **74,** 381-389.

Marinus, M. G. (1987) DNA methylation in *Escherichia coli. Annu. Rev. Genet.,* **21,** 113-131.

Matzke, M. A. & Birchler, J. A. (2005) RNAi-mediated pathways in the nucleus. *Nat. Rev. Genet.,* **6,** 24-35.

Mevarech, M., Frolow, F. & Gloss, L. M. (2000) Halophilic enzymes: proteins with a grain of salt. *Biophys. Chem.,* **86,** 155-164.

Mevarech, M. & Werczberger, R. (1985) Genetic transfer in *Halobacterium volcanii. J. Bacteriol.,* **162,** 461-462.

Mijts, B. N. & Patel, B. K. C. (2002) Cloning, sequencing and expression of an alpha-amylase gene, amyA, from the thermophilic halophile *Halothermothrix orenii* and purification and biochemical characterization of the recombinant enzyme. *Microbiology-(UK),* **148,** 2343-2349.

Miller, J. R., Busby, R. W., Jordan, S. W., Cheek, J., Henshaw, T. F., Ashley, G. W., Broderick, J. B., Cronan, J. E. & Marletta, M. A. (2000) *Escherichia coli* LipA is a lipoyl synthase: In vitro biosynthesis of lipoylated pyruvate dehydrogenase complex from octanoyl-acyl carrier protein. *Biochemistry,* **39,** 15166-15178.

Morris, T. W., Reed, K. E. & Cronan, J. E. (1994) Identification of the gene encoding lipoate-protein ligase-A of *Escherichia coli* - molecular-cloning and characterization of the LplA gene and gene-product. *J. Biol. Chem.,* **269,** 16091-16100.

Morris, T. W., Reed, K. E. & Cronan, J. E. (1995) Lipoic acid metabolism in *Escherichia coli* - the LplA and LipB genes define redundant pathways for ligation of lipoyl groups to apoprotein. *J. Bacteriol.,* **177,** 1-10.

Mullakhanbhai, M. F. & Larsen, H. (1975) *Halobacterium volcanii* spec. nov., a dead sea halobacterium with a moderate salt requirement. *Arch. Microbiol.*, **104,** 207-214.

Nicholson, D. J. (2005) *Cloning and expression of the E1 components of the 2-oxoacid dehydrogenase complex from Hfx. volcanii in E. coli.* Final year project report, University of Bath.

Nishizawa, Y., Yabuki, T., Fukuda, E. & Wakagi, T. (2005) Gene expression and characterization of two 2-oxoacid:ferredoxin oxidoreductases from *Aeropyrum pernix* K1. *FEBS Lett.*, **579,** 2319-2322.

Nuttall, S. D. & Dyall-Smith, M. L. (1993) Hf1 and Hf2 - novel bacteriophages of halophilic archaea. *Virology,* **197,** 678-684.

Oesterhelt, D. & Stoeckenius, W. (1973) Functions of a new photoreceptor membrane. *Proc. Natl. Acad. Sci. U. S. A.*, **70,** 2853-2857.

Oesterhelt, D. & Stoeckenius, W. (1974) Isolation of the cell membrane of *Halobacterium halobium* and its fractionation into red and purple membrane. *Methods Enzymol.*, **31,** 667-668.

Ogram, A., Sayler, G. S. & Barkay, T. (1987) The extraction and purification of microbial DNA from sediments. *J. Microbiol. Methods,* **7,** 57-66.

Ogram, A., Sun, W. H., Brockman, F. J. & Fredrickson, J. K. (1995) Isolation and characterization of RNA from low-biomass deep-subsurface sediments. *Appl. Environ. Microbiol.*, **61,** 763-768.

Oren, A. & Gurevich, P. (1994) Production of D-lactate, acetate, and pyruvate from glycerol in communities of halophilic archaea in the Dead Sea and in saltern crystallizer ponds. *FEMS Microbiol. Ecol.*, **14,** 147-155.

Oren, A. & Gurevich, P. (1995) Isocitrate lyase activity in halophilic archaea. *FEMS Microbiol. Lett.*, **130,** 91-95.

Oren, A., Lau, P. P. & Fox, G. E. (1988) The taxonomic status of *Halobacterium marismortui* from the Dead Sea - a comparison with *Halobacterium vallismortis*. *Syst. Appl. Microbiol.*, **10,** 251-258.

Ortenberg, R., Rozenblatt-Rosen, O. & Mevarech, M. (2000) The extremely halophilic archaeon *Haloferax volcanii* has two very different dihydrofolate reductases. *Mol. Microbiol.*, **35,** 1493-1505.

Ozawa, Y., Nakamura, T., Kamata, N., Yasujima, D., Urushiyama, A., Yamakura, F., Ohmori, D. & Imai, T. (2005) *Thermococcus profundus* 2-ketoisovalerate ferredoxin oxidoreductase, a key enzyme in the archaeal energy-producing amino acid metabolic pathway. *J. Biochem.*, **137,** 101-107.

Patel, M. S. & Roche, T. E. (1990) Molecular-biology and biochemistry of pyruvate-dehydrogenase complexes. *Faseb J.*, **4,** 3224-3233.

Patenge, N., Haase, A., Bolhuis, H. & Oesterhelt, D. (2000) The gene for a halophilic beta-galactosidase (bgaH) of *Haloferax alicantei* as a reporter gene for promoter analyses in *Halobacterium salinarum. Mol. Microbiol.*, **36,** 105-113.

Perham, R. N. (1991) Domains, motifs, and linkers in 2-oxoacid dehydrogenase multienzyme complexes - a paradigm in the design of a multifunctional protein. *Biochemistry,* **30,** 8501-8512.

Perham, R. N. (2000) Swinging arms and swinging domains in multifunctional enzymes: Catalytic machines for multistep reactions. *Annu. Rev. Biochem.*, **69,** 961-1004.

Perham, R. N., Jones, D. D., Chauhan, H. J. & Howard, M. J. (2002) Substrate channelling in 2-oxo acid dehydrogenase multienzyme complexes. *Biochem. Soc. T.*, **30,** 47-51.

Pettit, F. H., Yeaman, S. J. & Reed, L. J. (1978) Purification and characterization of branched-chain alpha-keto acid dehydrogenase complex of bovine kidney. *Proc. Natl. Acad. Sci. U. S. A.*, **75,** 4881-4885.

Pfeifer, F., Griffig, J. & Oesterhelt, D. (1993) The *fdx* gene gncoding the [2Fe-2S] ferredoxin of *Halobacterium salinarium* (*Hbt. Halobium*). *Mol. Gen. Genet.*, **239,** 66-71.

Pfeifer, F., Zotzel, J., Kurenbach, B., Roder, R. & Zimmermann, P. (2001) A p-loop motif and two basic regions in the regulatory protein GvpD are important for the repression of gas vesicle formation in the archaeon *Haloferax mediterranei. Microbiology-(UK),* **147,** 63-73.

Pimenov, N. V., Severina, L. O. & Plakunov, V. K. (1987) Some characteristics of glucose-transport in the extreme halophilic bacterium *Halobacterium mediterranei. Microbiology,* **56,** 571-575.

Plaga, W., Lottspeich, F. & Oesterhelt, D. (1992) Improved purification, crystallization and primary structure of pyruvate-ferredoxin oxidoreductase from *Halobacterium halobium. Eur. J. Biochem.*, **205,** 391-397.

Porter, K., Kukkaro, P., Bamford, J. K. H., Bath, C., Kivela, H. M., Dyall-Smith, M. L. & Bamford, D. H. (2005) SHI: a novel, spherical halovirus isolated from an Australian hypersaline lake. *Virology,* **335,** 22-33.

Prangishvili, D. (2003) Evolutionary insights from studies on viruses of hyperthermophilic archaea. *Res. Microbiol.*, **154,** 289-294.

Prangishvili, D., Stedman, K. & Zillig, W. (2001) Viruses of the extremely thermophilic archaeon *Sulfolobus*. *Trends Microbiol.*, **9,** 39-43.

Pratt, K. J., Carles, C., Carne, T. J., Danson, M. J. & Stevenson, K. J. (1989) Detection of bacterial lipoic acid - a modified gas-chromatographic-mass-spectrometric procedure. *Biochem. J.*, **258,** 749-754.

Prediger, E. & Chacko, S. (Eds.) (2003) *TechNotes.[Online] http://www.ambion.com/techlib/tn.* **11** Ed, USA: Ambion.

Preston, C. M., Wu, K. Y., Molinski, T. F. & Delong, E. F. (1996) A psychrophilic crenarchaeon inhabits a marine sponge: *Cenarchaeum symbiosum* gen-nov, sp, nov. *Proc. Natl. Acad. Sci. U. S. A.*, **93,** 6241-6246.

Puhler, G., Leffers, H., Gropp, F., Palm, P., Klenk, H. P., Lottspeich, F., Garrett, R. A. & Zillig, W. (1989) Archaebacterial DNA-dependent RNA-polymerases testify to the evolution of the Eukaryotic nuclear genome. *Proc. Natl. Acad. Sci. U. S. A.*, **86,** 4569-4573.

Purdy, K. J., Cresswell-Maynard, T. D., Nedwell, D. B., Mcgenity, T. J., Grant, W. D., Timmis, K. N. & Embley, T. M. (2004) Isolation of haloarchaea that grow at low salinities. *Environ. Microbiol.*, **6,** 591-595.

Rawal, N., Kelkar, S. M. & Altekar, W. (1988) Ribulose 1,5-bisphosphate dependent CO_2 fixation in the halophilic archaebacterium, *Halobacterium mediterranei*. *Biochem. Bioph. Res. Co.*, **156,** 451-456.

Reed, L. J. (1974) Multienzyme complexes. *Accounts Chem. Res.*, **7,** 40-46.

Reed, L. J. & Hackert, M. L. (1990) Structure-function-relationships in dihydrolipoamide acyltransferases. *J. Biol. Chem.*, **265,** 8971-8974.

Reed, L. J., Koike, M., Levitch, M. E. & Leach, F. R. (1958) Studies on the nature and reaction of protein-bound lipoic acid. *J. Biol. Chem.*, **232,** 143-158.

Reed, L. J. & Mukherjee, B. B. (1969) α-Ketoglutarate dehydrogenase complex from *Escherichia coli*. *Methods Enzymol.*, **13,** 55-61.

Rice, G., Tang, L., Stedman, K., Roberto, F., Spuhler, J., Gillitzer, E., Johnson, J. E., Douglas, T. & Young, M. (2004) The structure of a thermophilic archaeal virus shows a double-stranded DNA viral capsid type that spans all domains of life. *Proc. Natl. Acad. Sci. U. S. A.*, **101,** 7716-7720.

Richarme, G. (1989) Purification of a new dihydrolipoamide dehydrogenase from *Escherichia coli*. *J. Bacteriol.*, **171,** 6580-6585.

Richarme, G. & Heine, H. G. (1986) Galactose-simulated and maltose-stimulated lipoamide dehydrogenase-activities related to the binding-protein-dependent transport of galactose and maltose in toluenized cells of *Escherichia coli*. *Eur. J. Biochem.*, **156,** 399-405.

Ringquist, S., Shinedling, S., Barrick, D., Green, L., Binkley, J., Stormo, G. D. & Gold, L. (1992) Translation initiation in *Escherichia coli* - sequences within the ribosome-binding site. *Mol. Microbiol.*, **6,** 1219-1229.

Rodriguez-Valera, F. (1988) Characteristics and microbial ecology of hypersaline environments. In: *Halophilic bacteria* (Rodriguez-Valera, F. (Ed.). 3-30. Florida: CRC Press Inc.

Rodriguez-Valera, F., Juez, G. & Kushner, D. J. (1983) *Halobacterium-mediterranei* spec-nov, a new carbohydrate-utilizing extreme halophile. *Syst. Appl. Microbiol.*, **4,** 369-381.

Ross, H. N. M., Collins, M. D., Tindall, B. J. & Grant, W. D. (1981) A rapid procedure for the detection of archaeobacterial lipids in halophilic bacteria. *J. Gen. Microbiol.*, **123,** 75-80.

Rothschild, L. J. & Mancinelli, R. L. (2001) Life in extreme environments. *Nature,* **409,** 1092-1101.

Ruepp, A. & Soppa, J. (1996) Fermentative arginine degradation in *Halobacterium salinarium* (formerly *Halobacterium halobium*): Genes, gene products, and transcripts of the arcRACB gene cluster. *J. Bacteriol.*, **178,** 4942-4947.

Sambrook, J. & Russel, D. W. (2001) *Molecular cloning: a labratory manual.* New York: CSHL Press.

Sauer, T. & Galinski, E. A. (1998) Bacterial milking: a novel bioprocess for production of compatible solutes. *Biotechnol. Bioeng.*, **57,** 306-313.

Scandurra, R., Consalvi, V., Chiaraluce, R., Politi, L. & Engel, P. C. (2000) Protein stability in extremophilic Archaea. *Front. Biosci.*, **5,** D787-D795.

Schleper, C., Jurgens, G. & Jonuscheit, M. (2005) Genomic studies of uncultivated archaea. *Nat. Rev. Microbiol.*, **3,** 479-488.

Schut, G. J., Menon, A. L. & Adams, M. W. W. (2001) 2-keto acid oxidoreductases from *Pyrococcus furiosus* and *Thermococcus litoralis*. *Methods Enzymol.*, **331,** 144-158 part B.

Sensen, C. W., Klenk, H. P., Singh, R. K., Allard, G., Chan, C. C. Y., Liu, Q. Y., Penny, S. L., Young, F., Schenk, M. E., Gaasterland, T., Doolittle, W. F., Ragan, M. A. & Charlebois, R. L. (1996) Organizational characteristics and information content of an archaeal genome: 156 kb of sequence from *Sulfolobus solfataricus* P2. *Mol. Microbiol.*, **22,** 175-191.

Serrano, J. A., Camacho, M. & Bonete, M. J. (1998) Operation of glyoxylate cycle in halophilic archaea: presence of malate synthase and isocitrate lyase in *Haloferax volcanii*. *FEBS Lett.*, **434,** 13-16.

Severina, L. O. & Pimenov, N. V. (1988) Glucose-metabolism in extreme halophilic archaebacteria. *Microbiology,* **57,** 152-156.

Sheridan, G. E. C., Masters, C. I., Shallcross, J. A. & Mackey, B. M. (1998) Detection of mRNA by reverse transcription PCR as an indicator of viability in *Escherichia coli* cells. *Appl. Environ. Microbiol.*, **64,** 1313-1318.

Slupska, M. M., King, A. G., Fitz-Gibbon, S., Besemer, J., Borodovsky, M. & Miller, J. H. (2001) Leaderless transcripts of the crenarchaeal hyperthermophile *Pyrobaculum aerophilum*. *J. Mol. Biol.*, **309,** 347-360.

Smith, L. D., Bungard, S. J., Danson, M. J. & Hough, D. W. (1987) Dihydrolipoamide dehydrogenase from the thermoacidophilic archaebacterium *Thermoplasma acidophilum*. *Biochem. Soc. T.*, **15,** 1097-1097.

Soppa, J. (1998) Optimization of the 5-bromo-2'-deoxyuridine selection and its application for the isolation of nitrate respiration-deficient mutants of *Haloferax volcanii*. *J. Microbiol. Methods,* **34,** 41-48.

Srere, P. A., Brazil, H. & Gonen, L. (1963) The citrate condensing enzyme of pigeon breast muscle and moth flight muscle. *Acta Chem. Scand.*, **17,** S129-S134.

Studier, F. W. (1991) Use of bacteriophage-T7 lysozyme to improve an inducible T7 expression system. *J. Mol. Biol.*, **219,** 37-44.

Su, C. L. & Sordillo, L. M. (1998) A simple method to enrich mRNA from total prokaryotic RNA. *Mol. Biotechnol.*, **10,** 83-85.

Suzuki, Y. J., Tsuchiya, M. & Packer, L. (1994) Determination of structure antioxidant activity relationships of dihydrolipoic acid. *Methods Enzymol.*, **234,** 454-461.

Tindall, B. J. (1991) Cultivation and preservation of members of the family halobacteriaceae. *World J. Microbiol. Biotechnol.*, **7,** 95-98.

Tolstrup, N., Sensen, C. W., Garrett, R. A. & Clausen, I. G. (2000) Two different and highly organized mechanisms of translation initiation in the archaeon *Sulfolobus solfataricus*. *Extremophiles,* **4,** 175-179.

Tomlinson, G. A. & Hochstein, L. I. (1972a) Isolation of carbohydrate-metabolizing, extremely halophilic bacteria. *Can. J. Microbiol.,* **18,** 698-&.

Tomlinson, G. A. & Hochstein, L. I. (1972b) Studies on acid production during carbohydrate metabolism by extremely halophilic bacteria. *Can. J. Microbiol.,* **18,** 1973-1976.

Tomlinson, G. A., Koch, T. K. & Hochstein, L. I. (1974) Metabolism of carbohydrates by extremely halophilic bacteria - glucose-metabolism via a modified Entner-Doudoroff Pathway. *Can. J. Microbiol.,* **20,** 1085-1091.

Torsvik, T. & Dundas, I. D. (1974) Bacteriophage of *Halobacterium salinarium. Nature,* **248,** 680-681.

Vettakkorumakankav, N., Danson, M. J., Hough, D. W., Stevenson, K. J., Davison, M. & Young, J. (1992) Dihydrolipoamide dehydrogenase from the halophilic archaebacterium *Haloferax volcanii* - characterization and N- terminal sequence. *Biochem. Cell Biol.,* **70,** 70-75.

Walsby, A. E. (1980) Square Bacterium. *Nature,* **283,** 69-71.

Walsby, A. E. (2005) Archaea with square cells. *Trends Microbiol.,* **13,** 193-195.

Wang, G. J., Kennedy, S. P., Fasiludeen, S., Rensing, C. & Dassarma, S. (2004) Arsenic resistance in *Halobacterium* sp strain NRC-1 examined by using an improved gene knockout system. *J. Bacteriol.,* **186,** 3187-3194.

Wanner, C. & Soppa, J. (1999) Genetic identification of three ABC transporters as essential elements for nitrate respiration in *Haloferax volcanii. Genetics,* **152,** 1417-1428.

Wanner, C. & Soppa, J. (2002) Functional role for a 2-oxo acid dehydrogenase in the halophilic archaeon *Haloferax volcanii. J. Bacteriol.,* **184,** 3114-3121.

Ward, D. E., Ross, R. P., Van Der Weijden, C. C., Snoep, J. L. & Claiborne, A. (1999) Catabolism of branched-chain alpha-keto acids in *Enterococcus faecalis*: the bkd gene cluster, enzymes, and metabolic route. *J. Bacteriol.,* **181,** 5433-5442.

Ward, D. E., Van Der Weijden, C. C., Van Der Merwe, M. J., Westerhoff, H. V., Claiborne, A. & Snoep, J. L. (2000) Branched-chain alpha-keto acid catabolism via the gene products of the bkd operon in *Enterococcus faecalis*: a new, secreted metabolite serving as a temporary redox sink. *J. Bacteriol.,* **182,** 3239-3246.

Williams, W. D. (1981) Inland salt lakes - an introduction. *Hydrobiologia,* **81-2,** 1-14.

Woese, C. R. & Fox, G. E. (1977) Phylogenetic structure of prokaryotic domain - primary kingdoms. *Proc. Natl. Acad. Sci. U. S. A.,* **74,** 5088-5090.

Woese, C. R., Kandler, O. & Wheelis, M. L. (1990) Towards a natural system of organisms - proposal for the domains Archaea, Bacteria, and Eucarya. *Proc. Natl. Acad. Sci. U. S. A.*, **87,** 4576-4579.

Woese, C. R. & Olsen, G. J. (1986) Archaebacterial phylogeny - perspectives on the urkingdoms. *Syst. Appl. Microbiol.*, **7,** 161-177.

Wu, X. Q., Jornvall, H., Berndt, K. D. & Oppermann, U. (2004) Codon optimization reveals critical factors for high level expression of two rare codon genes in *Escherichia coli*: RNA stability and secondary structure but not tRNA abundance. *Biochem. Bioph. Res. Co.*, **313,** 89-96.

Zaigler, A., Schuster, S. C. & Soppa, J. (2003) Construction and usage of a onefold-coverage shotgun DNA microarray to characterize the metabolism of the archaeon *Haloferax volcanii*. *Mol. Microbiol.*, **48,** 1089-1105.

Zhang, Q., Iwasaki, T., Wakagi, T. & Oshima, T. (1996) 2-oxoacid:ferredoxin oxidoreductase from the thermoacidophilic archaeon, *Sulfolobus* sp. strain 7. *J. Biochem.*, **120,** 587-599.

Zhao, X., Miller, J. R., Jiang, Y. F., Marletta, M. A. & Cronan, J. E. (2003) Assembly of the covalent linkage between lipoic acid and its cognate enzymes. *Chem. Biol.*, **10,** 1293-1302.

Zimmer, G., Mainka, L. & Kruger, E. (1991) Dihydrolipoic acid activates oligomycin-sensitive thiol-groups and increases ATP synthesis in mitochondria. *Arch. Biochem. Biophys.*, **288,** 609-613.

Zimmermann, P. & Pfeifer, F. (2003) Regulation of the expression of gas vesicle genes in *Haloferax mediterranei*: interaction of the two regulatory proteins GvpD and GvpE. *Mol. Microbiol.*, **49,** 783-794.

Zusman, T., Rosenshine, I., Boehm, G., Jaenicke, R., Leskiw, B. & Mevarech, M. (1989) Dihydrofolate-reductase of the extremely halophilic archaebacterium *Halobacterium volcanii* - the enzyme and its coding gene. *J. Biol. Chem.*, **264,** 18878-18883.

The putative OADHC operon sequence of Hfx. volcanii

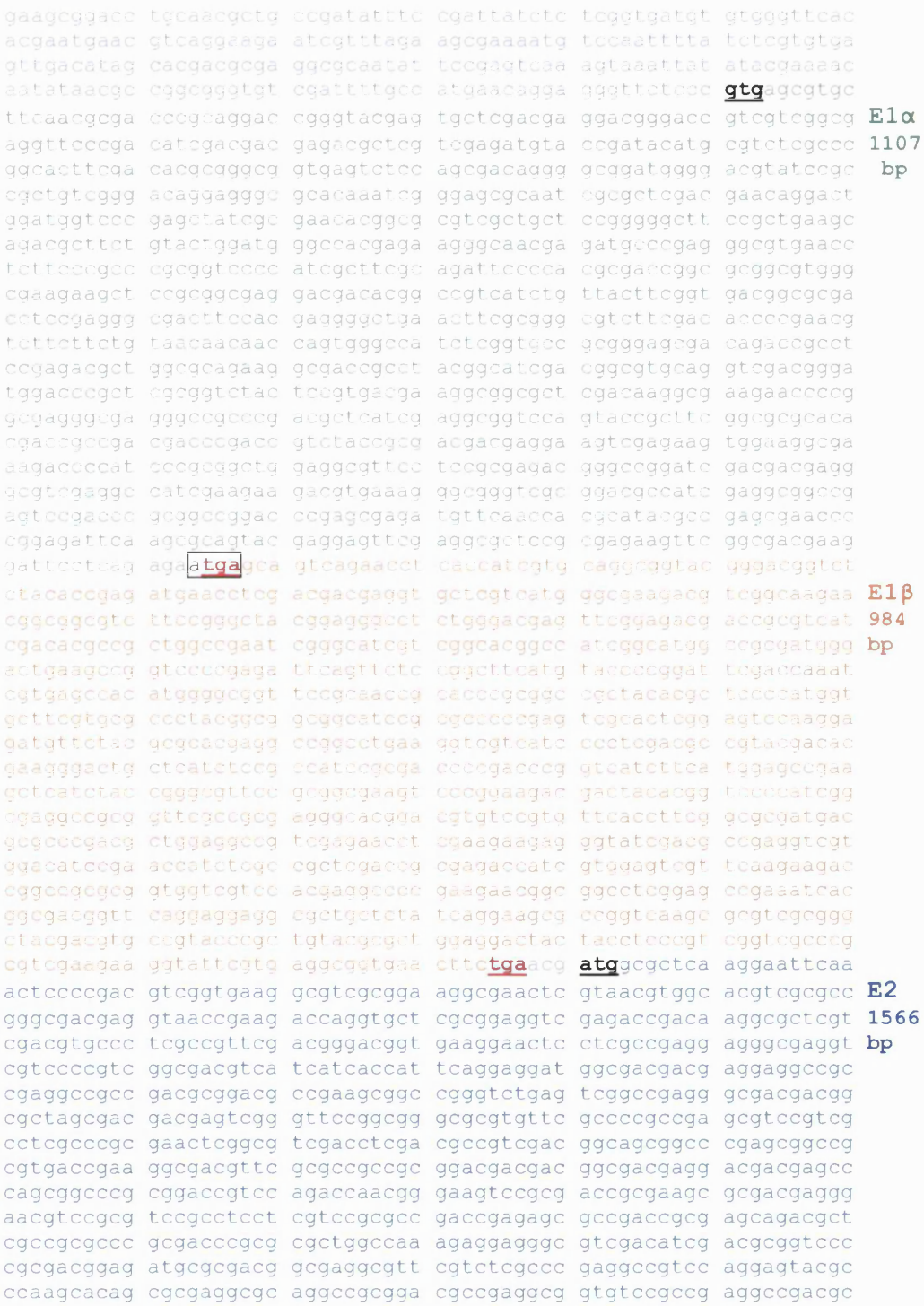

cggaaccgcg accgccgagg cgacggtcga cgcggcgagt gaacccgcac cgcccgaggc
cggccccggt gccggcgagc gcgtccccta caagggcgtc cgcaaggcca tcggcgacca
gatgcagcgg tcgaagtaca ccgcgccgca cgtcacccac cacgacgagg tggacgtgac
ggagctcgtc gaactgcgcg aacagctcaa gcccgtcgcc gaggagcgcg gctcgcggct
gacctacatg ccgttcgtga tgaaggccgt cgtcgcggcg ctgaagggct tcccgtacct
caactcgcag ctcgacgagg aaaacgagga aatcgtcctg cgcgacgagt acaacatcgg
cgtcgcggcc gcgaccgacg ccggtctgct cgtccccgtc gtccacgacg cggaccgcaa
ggggatgctc gaactcgccg acgagatgaa cgagaaggtc gagaaggccc gcaaccgcaa
aatcgcgccc gaggagatgc gcggcggcac cttcaccatc accaacgtcg gcggcatcgg
cggcgagtac gcgacgccga ttatcaacta ccccgaggtg gcgattctcg cgctcggagc
catcaaagaa aagccccggg tcgtcgacgg tgaggtcgtg ccgcgaaacg tcctcaccct
ctcgctgtcg ttcgaccacc gcgtcgtcga cggcgcgcag ggcgctcggttcacgaaccgc
gtgaaggaac tgctcgaaga ccccaaactg ctggtgttag aataatgtc gtcggagaca
tcgcaaccgg aaccgaactg ctcgtcatcg gcgcgggacc cggcggctac gtcgccgcca E3
tccgcgccgc acagaacggc atcgacacga cgctggtcga gaaggacgcc tacgggggca 1428
cctgcctcaa ctacggctgt atcccatcga aggcgctcat cacgggggcg aacctcgccc bp
acgaggcggg caacgccgag gagatgggca tccacgccga ccccgtcgtg gacatgtcgc
aactgcgcga ctggaagagc ggcgtcgtgg accaactcac cggcggcgtc gagaagctct
gtaaggcgaa cggcgtcaac ctcgtcgagg gaaccgcccg cttcaaggac gagaacgccg
tccgcatcgc ccacggcggc gaggggcagg gctcggagac catcgagttc gagcactgca
tcatcgccac cggctcgcgc gtcatccaga ttcccggttt cgacttcggc gacgagccgg
tgtggtcgtc gcgcgacgcc ctcgaggccg acaccgtccc ggagcgactg gtcgtcgtcg
gcggcggcta catcgggatg gagctgtcca cgacgttcgc caagctcggc gcggacgtga
ccgtcgtcga gatgctcgac gacatcctgc cgggctacga gtccgacgtg gcccgcgtcg
tccgcaagcg cgccgaagag ctcggcatcg acatgcacct cggtgagggc gcgacgggct
ggcgcgagga ggacgacggc atcatggtga cgaccgagac cgaagacggc gaggaaaacg
agtaccgcgc cgacaaggtg ctcgtcgccg tcgggcgctc gcccgtcacc gacacgatgg
acatcgagaa cgccggcctc gaagccgacg accgcggctt cctctcggtc gacgaccgcc
gccgcaccga cgtggagcac atctacgccg tcggcgacgt ggtcgaggac acgccgatgc
tcgcccacgt cgcctcgaag gagggcatcg tcgccgccga gcacgtcgcc ggcgaaccgg
tcgccttcga cagtcaggcc gtccccgccg cggtgttcac cgaccccgaa atcggcacgg
tcggcatgac cgaggccgac gccgaggagg ccggcttcac gcccgtcgtc gggcagatgc
ccttccgggc gtccggccgc gcgctgacga cgaaccacgc cgacggcttc gtccgcgtcg
tcgccgacga ggagtccggc ttcgtcctcg gggcgcaaat cgtcggcccc gaggcctccg
aactcatcgc cgaactcgcg ttcgccatcg agatgggcgc gacgctcgaa gacgtggcct
cgaccatcca cacccacccg acgctcgcgg aagcggtcat ggaggccgcc gagaacgcgc
tcggacaggc gattcacacc ctgaatcggt ga ggagcgtc cgaaaaacgg cgagctgacc
ttttttaagc ggtcaggtcg gcatcgagtt gggctgaaga gatc

***Start codon is shown in black underlined.**
***Stop codon is shown in red underlined.**
*** atga: represents an overlap between E1α and E1β –4**
***There is a gap between E1β and E2 +3.**
*** atg: represents an overlap between E2 and E3 -1**